

DISSERTATION

SURVEY ESTIMATORS OF DOMAIN MEANS UNDER SHAPE RESTRICTIONS

Submitted by

Cristian M. Oliva Avilés

Department of Statistics

In partial fulfillment of the requirements

For the Degree of Doctor of Philosophy

Colorado State University

Fort Collins, Colorado

Summer 2018

Doctoral Committee:

Advisor: Mary C. Meyer

Co-Advisor: Jean D. Opsomer

Jay F. Breidt

Haonan Wang

Kenneth R. Wilson

Copyright by Cristian Oliva-Aviles 2018

All Rights Reserved

ABSTRACT

SURVEY ESTIMATORS OF DOMAIN MEANS UNDER SHAPE RESTRICTIONS

Novel methodologies that introduce shape-restricted regression techniques into survey domain estimation and inference are presented in this dissertation. Although population domain means are frequently expected to respect shape constraints that arise naturally on the survey data, their most common direct estimators often violate such restrictions, especially when the variability of these estimators is high. Recently, a monotone estimator that is obtained from adaptively pooling neighboring domains was proposed. When the monotonicity assumption on population domain means is reasonable, the monotone estimator leads to asymptotically valid estimation and inference, and can lead to substantial improvements in efficiency, in comparison with unconstrained estimators. Motivated from these convenient properties adherent to the monotone estimator, the two main questions addressed in this dissertation arise: first, since invalid monotone restrictions may lead to biased estimators, how to create a data-driven decision for whether a restriction violation on the sample occurs due to an actual violation on the population, or simply because of chance; and secondly, how the monotone estimator can be extended to a more general constrained estimator that allows for many other types of shape restrictions beyond monotonicity.

In this dissertation, the Cone Information Criterion for Survey Data (CIC_s) is proposed to detect monotonicity departures on population domain means. The CIC_s is shown to lead to a consistent methodology that makes an asymptotically correct decision when choosing between unconstrained and constrained domain mean estimators. In addition, a design-based estimator of domain means that respect inequality constraints represented through irreducible matrices is presented. This constrained estimator is shown to be consistent and asymptotically normally distributed under mild conditions, given that the assumed restrictions are reasonable for the population. Further, simulation experiments demonstrate that both estimation and variability of domain means are improved

by constrained estimates, in comparison with unconstrained estimates, mainly on domains with small sample sizes. These proposed methodologies are applied to analyze data from the 2011-2012 U.S. National Health and Nutrition Examination Survey and the 2015 U.S. National Survey of College Graduates.

In terms of software development and outside of the survey context, the package `bcgam` is developed in R to fit constrained generalised additive models using a Bayesian approach. The main routines of `bcgam` allow users to easily specify their model of interest, and to produce numerical and graphical output. The package `bcgam` is now available from the Comprehensive R Archive Network.

ACKNOWLEDGEMENTS

As I firmly believe that the journey is more important than the destination, there are many valuable people to whom I will be forever grateful for being part of my PhD journey.

First, I would like to thank my wonderful advisors, Mary Meyer and Jean Opsomer, who initially invited me to do research with them. Through their support in all existing ways, they made me grow as a proper professional and as a human being. Also, they taught me many things not only about Statistics, but also about how to be an ethical researcher. If I were to choose my PhD advisors again, I will undoubtedly choose them. In addition, I would like to thank Jay Breidt, Haonan Wang and Kenneth Wilson, who helped me improve this dissertation through their insightful feedback, which was often based on a different perspective than mine.

Thanks to my beloved wife Debbie, who has been a cornerstone in my life. I could not imagine this challenging journey without her love, patience, empowerment and laughs. Not only her support has been important for me, but also her daily example. She helped me to understand that distance is only a state of mind, not a state of heart. This is not only my achievement, but ours.

Thanks to my parents, Iván and Landy, who have always supported me no matter how complicated my ideas sound. I simply could not ask God for better parents, and I will not be standing where I am now without all sacrifices they have done for me. They will always be my motivation to help others, and to contribute through my knowledge and actions to build a better world.

Thanks to my big siblings, Evelyn and Andrés, who are my greatest examples of human beings. They have unconditionally been there for me, and have believed on me even when I have not. In addition, I would also like to thank their partners, Milagros and Víctor, for giving me 'little' extra motivations who call me uncle.

Thanks to the members of the Latin American Students and Scholars Organization who were, and will always be, my family from Colorado. Sharing similar goals, values and traditions made me always feel that I never left home.

Thanks to Andrés Aluja, who has been one of my greatest influences in life. He was the main responsible for my decision to study my graduate education abroad, as he saw something in me before I did. No matter what I decide to do in the future, it will be inspired on his example. In addition, I would like to thank Luz María Can and Shauna DeLuca, who have always put me on their shoulders to see further. I have an unpayable debt with life for putting incredibly kind human beings like them in my path.

Thanks to the amazing staff of the statistics department, who have been always ready to help me with a smile drawn in their faces. A special mention to Kristin Stephens, who has been infinitely helpful and pleasant with me since my first day as a graduate student.

Thanks to Ann Magennis, Jenifer Thomas, Jennifer Hoeting, Mark Dahlke and Phil Turk, who have been professional role models for me.

Thanks to my fellow graduate students in statistics Soo-Young Kim, Ben Zheng, Henry Scharf, Charlie Vollmer, Aaron Nielsen and Zach Weller, who have been kind enough to share their knowledge and experiences with me. They have taught me much more things than they can imagine.

Last but not least, I would like to thank my lifelong friends Herbert Oliva, Ángel Uc, Marissa Pintor, Patricia Canto, Juan Ríos, Irving Chan, José Carlos Contreras and Alam Cardeña, who have demonstrated me that real friendship does not have neither borders nor expiration date. They will always be in my heart.

This research was supported by National Science Foundation under grant No. MMS-1533804 and Consejo Nacional de Ciencia y Tecnología (CONACYT) under fellowship No. 314583.

DEDICATION

To my wife Debbie, with all my love. Because love is all we need.

TABLE OF CONTENTS

ABSTRACT	ii
ACKNOWLEDGEMENTS	iv
DEDICATION	vi
LIST OF TABLES	ix
LIST OF FIGURES	x
Chapter 1 Introduction	1
1.1 Motivation: small domain estimation	1
1.2 Shape-constrained regression	4
1.3 Overview	10
Chapter 2 Validation of Monotone Domain Mean Estimators	12
2.1 Introduction	12
2.2 Constrained Domain Mean Estimator for Survey Data	13
2.3 Main results	16
2.3.1 Cone Information Criterion for Survey Data (CIC_s)	16
2.3.2 Assumptions	18
2.3.3 Properties of CIC_s	19
2.4 Simulations	23
2.5 Application of the CIC_s to the NHANES data	34
Chapter 3 Estimation and inference of domain means subject to shape constraints	36
3.1 Introduction	36
3.2 Constrained estimator for domain means	39
3.2.1 Notation and preliminaries	39
3.2.2 Proposed estimator	40
3.2.3 Variance estimation of $\tilde{\theta}_{s_d}$	42
3.2.4 Some shape constraints of interest	45
3.3 Properties of the constrained estimator	48
3.3.1 Assumptions	48
3.3.2 Main results	49
3.4 Performance of constrained estimator	52
3.4.1 Simulations	52
3.4.2 Replication methods for variance estimation	59
3.5 Application of constrained estimator to NSCG 2015	65
Chapter 4 <code>bcgam</code> : An R package for Bayesian Constrained Generalised Additive Models	72
4.1 Introduction	72
4.2 Dependencies and main routines	75
4.2.1 <code>NIMBLE</code> dependency	75
4.2.2 The primary function: <code>bcgam</code>	75

4.2.3 Generic functions to summarize results	77
4.3 Application to ‘duncan’ data	79
Chapter 5 Conclusion and Future Work	83
Appendix A Supplemental materials for Chapter 2	90
Appendix B Supplemental materials for Chapter 3	106

LIST OF TABLES

2.1	Simulation results of monotone scenario with $D = 4$.	26
2.2	Simulation results of flat scenario with $D = 4$.	26
2.3	Simulation results of non-monotone scenario with $D = 4$.	27
2.4	Simulation results of the skewed case with $D = 4$.	27
2.5	Simulation results of the correlated case with $D = 4$.	28
2.6	Simulation results of the correlated case when the monotonicity violation is increased, with $D = 4$.	29
2.7	Simulation results when $D = 8$.	30
2.8	Simulation results when $D = 5$ and $\sigma = 0.5$.	31
2.9	Simulation results when $D = 5$ and $\sigma = 1$.	33
2.10	Simulation results when $D = 20$ and $\sigma = 0.5$.	33
2.11	Simulation results when $D = 20$ and $\sigma = 1$.	33
3.1	WMSE values.	59
4.1	Summary of α coefficients for ‘duncan’ data analysis.	82

LIST OF FIGURES

1.1	Unconstrained (a) and constrained (c) estimates of simulated population domain means that are approximately monotone increasing with respect to x_1 and x_2 (b).	4
2.1	GCM example.	20
2.2	One fitted samples for each of four cases obtained using $S_3(\cdot)$. Dots correspond to unconstrained estimates, triangles to constrained estimates.	32
2.3	Proportion of times that the unconstrained estimator is chosen under the 4 scenarios of $S_3(\cdot)$, for several values of δ . Solid lines: CIC _s , dotted lines: Wald test. Dots: $\sigma = 0.5$, triangles: $\sigma = 1$	34
2.4	2011-2012 NHANES laboratory data. Solid lines: constrained and unconstrained estimators. Dotted lines: pointwise 95% Wald confidence intervals. $\text{CIC}_s(\tilde{\boldsymbol{y}}_s) = 23.354$, $\text{CIC}_s(\tilde{\boldsymbol{\theta}}_s) = 18.874$	35
3.1	Population domain means and unconstrained estimator (top). Constrained estimator under three different settings of shape constraints (bottom).	47
3.2	Population domain means for simulations when $\sigma = 1$	53
3.3	Plots of simulation results for the unconstrained and constrained estimators under the double monotone scenario with $\sigma = 1$, based on 10000 replications.	55
3.4	Plots of simulation results for the unconstrained and constrained estimators under the only x_1 monotone scenario with $\sigma = 1$, based on 10000 replications.	56
3.5	Plots of simulation results for the unconstrained and constrained estimators under the double monotone scenario with $\sigma = 2$, based on 10000 replications.	57
3.6	Plots of simulation results for the unconstrained and constrained estimators under the only x_1 monotone scenario with $\sigma = 2$, based on 10000 replications.	58
3.7	Variance estimation (top) and coverage rate (bottom) simulation results based on linearization and DAGJK methods for the unconstrained (left) and constrained (right) estimators, under the double monotone scenario with $n_N = 480$ and $\sigma = 1$	61
3.8	Variance estimation (top) and coverage rate (bottom) simulation results based on linearization and DAGJK methods for the unconstrained (left) and constrained (right) estimators, under the double monotone scenario with $n_N = 480$ and $\sigma = 2$	62
3.9	Variance estimation (top) and coverage rate (bottom) simulation results based on linearization and DAGJK methods for the unconstrained (left) and constrained (right) estimators, under the double monotone scenario with $n_N = 960$ and $\sigma = 1$	63
3.10	Variance estimation (top) and coverage rate (bottom) simulation results based on linearization and DAGJK methods for the unconstrained (left) and constrained (right) estimators, under the double monotone scenario with $n_N = 960$ and $\sigma = 2$	64
3.11	Unconstrained (left) and constrained (right) domain mean estimates for the 2015 NSCG data, given that Postgrad=NO is fixed.	67
3.12	Unconstrained (left) and constrained (right) domain mean estimates for the 2015 NSCG data, given that Postgrad=YES is fixed.	68

3.13	Ratio of the estimated standard errors of unconstrained estimates over those for constrained estimates for the 2015 NSCG data.	70
3.14	Slice plots of: unconstrained and constrained estimates with Wald confidence intervals (top) and sample sizes (bottom) for the 2015 NSCG data, given that Postgrad=YES and Supervise=YES.	71
4.1	Shape-restricted regression splines. Knots are represented by the "X" marks, and dots represent the basis vectors. (a) Quadratic I-spline basis functions. (b) Cubic C-spline basis functions. (c) Spline basis functions for decreasing and concave restrictions. . . .	74
4.2	2D and 3D plots created using the functions <code>plot.bcgam</code> and <code>persp.bcgam</code> with the <code>bcgam.fit</code> object, respectively.	79
4.3	Trace plot of α_{prof} coefficient.	80
4.4	Fitted model and 95% credible bounds for blue-collar occupation.	81
4.5	Fitted models for all types of occupation.	82

Chapter 1

Introduction

1.1 Motivation: small domain estimation

Sample surveys have been widely used to provide timely information about subpopulation (or domain) parameters of a finite population. Some of the most frequent parameters of interest are domain totals and means. *Direct estimators* conform a naive estimation approach of domain parameters, as they depend only on domain-specific sample data. Further, these are typically design-based estimators, meaning that estimation and inference are carried out using certain survey weights that are associated to the known sampling design.

Direct estimators produce reliable estimates only when there is a large enough amount of data available in domains. In certain surveys, although the overall sample size might be very large, there could be domains of interest with samples sizes that are too small to produce estimates with acceptable precision. These domains are known as *small domains*. For instance, large-scale national surveys might produce accurate direct estimates for large geographical areas such as states, or for large subpopulation groups such as sex at the national level, but might not produce estimates that are reliable enough for small subgroups such as race/ethnicity at the county level. In contrast, there is a growing demand from both public and private sectors for accurate estimates of small domains. These increasing demands are due to the growing tendency of formulating data-driven policies, programs, business decisions, regional planning, among others. For example, as discussed in Rao (2008), poverty counts of school-age children at the county level in the United States are used for allocation of federal funds. Thus, the development of appropriate methodologies for small domain estimation has become a demanded area in survey research.

A seemingly straightforward solution for small domain estimation consists on designing the survey sampling in such a way that it generates large samples on small domains. However, not only this is a very unpractical task due to the high cost of human and financial resources, but it

can also lead to oversampling problems. For example, consider the case discussed in Rao (2003, p. 2) about the U.S. Third Health and Nutrition Examination Survey (NHANES III). Here, the sampling fractions for small domains were made larger than the average fraction, so that certain domains in the cross-classification of sex, race/ethnicity, and age allow for direct estimates with adequate precision. However, this oversampling produced a greater sample concentration in certain states, which aggravated the common problem of small sample sizes in some other states. As a consequence of that, many states had to be treated as small domains. In general, even if the ‘best’ sampling design may be created to answer some predetermined questions of interest, unplanned small domains cannot be avoided. As Fuller (1999, p. 344) commented: “the client will always require more than is specified at the design stage”.

Indirect estimators have been developed as an effective alternative to make estimates for small domains with acceptable precision. These estimators allow small domains to ‘borrow strength’ from others with similar characteristics through linking models, which take advantage of auxiliary data sources such as census and administrative records. In that context, borrowing strength can be regarded as an increase in their ‘effective’ sample size. Rao and Molina (2015, p. 4) identified two types of indirect estimators, depending on whether they are based on explicit or implicit linking models. Recently, direct estimators that are based on explicit linking models (known as *small area models*) have received a lot of attention. These estimators are model-based, so they usually require a significant investment in specialized expertise and additional resources. Further, these estimators are prone to model misspecification. Some examples of the models used for these estimators are the Fay-Herriot model (Fay and Herriot, 1979) and spline-based models (Opsomer et al., 2008). In contrast, indirect estimators that are based on implicit linking models are design-based, and their design variances are usually smaller than variances of direct estimators. Although they are typically design-biased, their bias tend to be considerably small when the implicit linking model is approximately true. The classical post-stratified estimator is one significant example of these type of estimators (see Särndal et al. (1992, Chapter 10.7) for details).

Shape or order restrictions, that can arise naturally in the survey context, are often expected to be respected by population domain means. For instance, consider the 2015 U.S. National Survey of College Graduates, which provides data on the characteristics of the U.S. nation’s college graduates, with emphasis on those in the science and engineering workforce. Here, it might be reasonable to assume that, given a job category, wage salaries tend to increase with respect to the time since the highest degree was awarded, at least up until retirement age. In addition, it may be expected that mean salaries are higher for STEM jobs than for non-STEM jobs, without any restriction imposed within STEM jobs or non-STEM jobs. In contrast, direct estimators of domain mean do not necessarily respect such constraints, especially under the presence of small domains. As these are highly variable, violations to the expected restrictions are very likely to occur.

Domain mean estimators that respect reasonable shape constraints have the potential to improve precision and stability of the most regularly used direct estimators. To illustrate that point, consider the simulated scenario shown in Figure 1.1. Population domain means that are approximately monotone with respect to variable x_1 and x_2 are plotted in Figure 1.1b. Further, direct (unconstrained) estimates of these are computed and shown in Figure 1.1a. Two main observations can be easily made from this figure: unconstrained estimates do not seem to estimate appropriately the ‘truth’, and also, they are very ‘spiky’. In contrast, Figure 1.1c shows (constrained) estimates that respect the reasonable monotonicity assumption on both x_1 and x_2 . These estimates are less spiky and look closer to the population domain means, even when the latter are not strictly monotone. Further, note the presence on some flat spots among constrained estimates. These demonstrate that some domains get pooled with their neighbors, allowing small domains to increase their effective sample size. The latter observation suggests that the variability of constrained estimates might potentially improve in comparison with unconstrained estimates. In conclusion, domain estimates that respect assumed shapes are an attractive and intuitive alternative to small domain estimation that is worth to explore.

A first step to introduce shape-constrained regression techniques into survey estimation and inference has been done recently by Wu et al. (2016). They propose a design-weighted isotonic

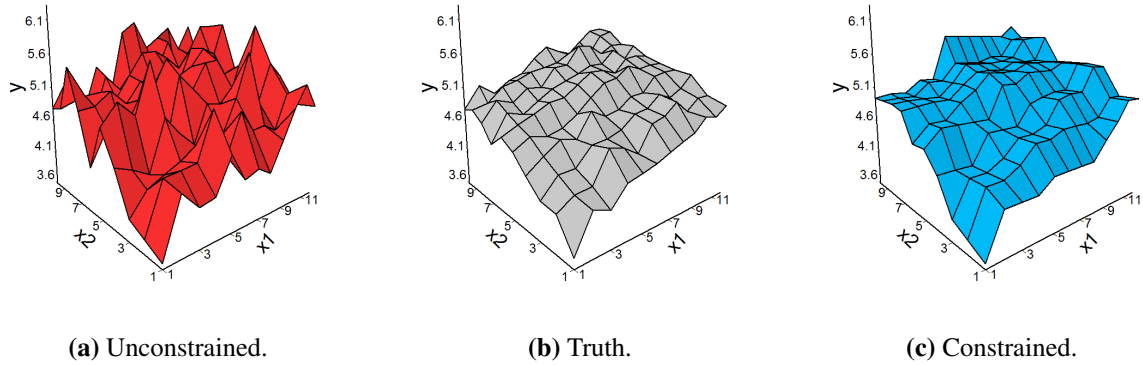


Figure 1.1: Unconstrained (a) and constrained (c) estimates of simulated population domain means that are approximately monotone increasing with respect to x_1 and x_2 (b).

estimator, based on classical design-based domain estimators, that is obtained after adaptively pooling neighboring domains. This estimator was shown to improve both precision and variability of domain means under linearization and replication-based variance estimation, in comparison with unconstrained estimates. Based on these motivating results on the survey context, two questions of interest arise: firstly, given that erroneous shape assumptions lead to biased estimators, what methodology can be used to validate the use of the constrained estimator on top of the unconstrained estimator; and secondly, since their isotonic estimator demonstrated to have convenient properties for estimation and inference, how can it be adapted to allow for many other shape constraints other than univariate monotonicity? These two questions conform the base work of this dissertation.

The following section of this chapter presents the main shape-constrained regression techniques that have been studied outside of the survey context, and constitute an angular stone for the development of the methodologies proposed in this dissertation.

1.2 Shape-constrained regression

Consider the general problem of estimating the function f from n pairs of observations (x_i, y_i) using the following regression model:

$$y_i = f(x_i) + \epsilon_i, \quad (1.1)$$

where $a \leq x_1 < x_2 < \dots < x_n \leq b$, and $\epsilon_1, \dots, \epsilon_n \stackrel{\text{i.i.d.}}{\sim} N(0, \sigma^2)$. Assume that y is assumed to be increasing with respect to f . Defining $\theta_i = f(x_i)$ and following Brunk (1955), consider the isotonic estimator $\hat{\boldsymbol{\theta}} = (\hat{\theta}_1, \dots, \hat{\theta}_n)^\top$ that solves

$$\min_{\theta_1, \dots, \theta_n} \sum_{i=1}^n (y_i - \theta_i)^2, \quad \text{subject to } \theta_1 \leq \dots \leq \theta_n. \quad (1.2)$$

The general solution of this isotonic estimator is given by

$$\hat{\theta}_i = \max_{k \leq i} \min_{l \geq i} \frac{\sum_{j=k}^l y_j}{l - k + 1}. \quad (1.3)$$

In the case when there are repeated x_i values, the least squares formula in Equation 1.2 can be substituted by

$$\min_{\theta_1, \dots, \theta_n} \sum_{j=1}^n n_i (\bar{y}_i - \theta_i)^2, \quad \text{subject to } \theta_1 \leq \dots \leq \theta_n, \quad (1.4)$$

where n_i is the number of repeated x_i values, and \bar{y}_i is the mean of the y_i values that correspond to those repeated x_i . In this case, the general form of the isotonic estimator $\hat{\theta}_i$ is given by

$$\hat{\theta}_i = \max_{k \leq i} \min_{l \geq i} \frac{\sum_{j=k}^l n_j \bar{y}_j}{\sum_{j=k}^l n_j}. \quad (1.5)$$

It can be noted that the isotonic estimator $\hat{\theta}_i$ is simply an average. Further, observe that the monotone increasing constraints can be expressed in matrix form as $\mathbf{A}\boldsymbol{\theta} \geq \mathbf{0}$, where

$$\mathbf{A} = \begin{pmatrix} -1 & 1 & 0 & \dots & 0 & 0 \\ 0 & -1 & 1 & \dots & 0 & 0 \\ \vdots & \vdots & \vdots & \ddots & \vdots & \vdots \\ 0 & 0 & 0 & \dots & -1 & 1 \end{pmatrix}$$

and $\mathbf{0}$ is the zero vector. The matrix \mathbf{A} is known as the constraint matrix, and each row represents a constraint. Here, the constraint matrix is of full-row rank.

Now, consider the following scenario where constraints other than univariate monotonicity arise: f is a bivariate function of the categorical variables x_1 and x_2 , and is assumed to be monotone with respect to each of these variables. For instance, assume that x_1 and x_2 have two and three categories, respectively. Further, assume that f is decreasing with respect to x_1 but increasing with respect to x_2 . Defining $\theta_{ij} = f(x_1 = i, x_2 = j)$ for $i \in \{1, 2\}, j \in \{1, 2, 3\}$ and $\boldsymbol{\theta} = (\theta_{11}, \theta_{12}, \theta_{13}, \theta_{21}, \theta_{22}, \theta_{23})^\top$, the constraint matrix \mathbf{A} can be written as

$$\mathbf{A} = \begin{pmatrix} -1 & 1 & 0 & 0 & 0 & 0 \\ 0 & -1 & 1 & 0 & 0 & 0 \\ 0 & 0 & 0 & -1 & 1 & 0 \\ 0 & 0 & 0 & 0 & -1 & 1 \\ 1 & 0 & 0 & -1 & 0 & 0 \\ 0 & 1 & 0 & 0 & -1 & 0 \\ 0 & 0 & 1 & 0 & 0 & -1 \end{pmatrix}.$$

In this case, \mathbf{A} has more constraints than dimensions, implying that \mathbf{A} is not a full-row rank matrix. However, the matrix \mathbf{A} is an *irreducible* matrix. Meyer (1999) defined a matrix as irreducible where none of its rows is a positive linear combinations of other rows, and the origin is not a positive linear combination of its rows. Intuitively, a constraint matrix is irreducible when there are no redundant constraints. As it can be seen from the previous example, irreducible matrices cover the scenario of having more constraint than dimensions. Also, full-row rank matrices are irreducible matrices by definition, which means that monotone constraints can be represented by these matrices. In practical terms, irreducible matrices have the capability to represent shape assumptions such as monotonicity, convexity, inflection points, among others. See Meyer (1999) for further details.

For the case when \mathbf{A} is an irreducible matrix, Meyer (1999) proposed the constrained estimator $\hat{\boldsymbol{\theta}}$ as the unique vector that solves

$$\min_{\boldsymbol{\theta}} \|\mathbf{y} - \boldsymbol{\theta}\|_w^2, \quad \text{subject to } \mathbf{A}\boldsymbol{\theta} \geq \mathbf{0}, \quad (1.6)$$

where $\|\mathbf{x}\|_w^2 = \langle \mathbf{x}, \mathbf{x} \rangle_w$, and $\langle \mathbf{x}, \mathbf{y} \rangle_w = \sum_{i=1}^n w_i x_i y_i$ is the inner product with weights w_1, \dots, w_n . Since a simple linear transformation converts the weighted problem in Equation 1.6 to an unweighted problem (i.e. $w_1 = \dots = w_n = 1$), then the subscript w might be omitted to simplify the notation.

A set $\mathcal{C} \subseteq \mathbb{R}^n$ is defined as *convex* if for any $\boldsymbol{\theta}_1, \boldsymbol{\theta}_2 \in \mathcal{C}$, then $\alpha\boldsymbol{\theta}_1 + (1 - \alpha)\boldsymbol{\theta}_2 \in \mathcal{C}$ for all $0 \leq \alpha \leq 1$. Further, a set $\mathcal{C} \subseteq \mathbb{R}^n$ is a *cone* if for any $\boldsymbol{\theta} \in \mathcal{C}$, then $\alpha\boldsymbol{\theta} \in \mathcal{C}$ for all $\alpha \geq 0$. The constrained estimator $\hat{\boldsymbol{\theta}}$ obtained from solving the problem in Equation 1.6 is the projection of \mathbf{y} onto the constraint convex cone $\Omega = \{\boldsymbol{\theta} \in \mathbb{R}^n : \mathbf{A}\boldsymbol{\theta} \geq \mathbf{0}\}$, written $\Pi(\mathbf{y}|\Omega)$. Also, Ω is a polyhedral convex cone, i.e., there is a finite number of edges that generate it. Meyer (1999) described the edges of Ω under the assumption that \mathbf{A} is irreducible, and showed that, under certain constraint scenarios, the number of edges may be considerably larger than the number of constraints for large values of n . Therefore, finding the edges of Ω may be a computationally expensive task under certain constraints.

Let Ω^0 be the polar cone, which is defined as the set of vectors $\boldsymbol{\rho} \in \mathbb{R}^n$ that form obtuse angles with every vector in Ω , i.e., $\Omega^0 = \{\boldsymbol{\rho} \in \mathbb{R}^n : \langle \boldsymbol{\theta}, \boldsymbol{\rho} \rangle \leq 0, \forall \boldsymbol{\theta} \in \Omega\}$ (see Rockafellar, 1970). As it is the case with the constraint cone Ω , the polar cone is also a polyhedral convex cone. Further, when \mathbf{A} is irreducible, the edges of Ω are simply the rows of $-\mathbf{A}$. That is, if $-\mathbf{A}$ is a $m \times n$ matrix with rows $\boldsymbol{\gamma}_1, \dots, \boldsymbol{\gamma}_n$, then

$$\Omega^0 = \{\boldsymbol{\rho} \in \mathbb{R}^n : \boldsymbol{\rho} = \sum_{j=1}^n b_j \boldsymbol{\gamma}_j \quad b_j \geq 0, \quad j = 1, \dots, n\}.$$

Further, let $\hat{\boldsymbol{\rho}}$ be the unique projection of \mathbf{y} onto the polar cone Ω^0 , written $\Pi(\mathbf{y}|\Omega^0)$. Meyer (1999) showed that the residual of $\hat{\boldsymbol{\theta}}$ is $\hat{\boldsymbol{\rho}}$, and viceversa. That is, for any $\mathbf{y} \in \mathbb{R}^n$, $\mathbf{y} = \Pi(\mathbf{y}|\Omega) + \Pi(\mathbf{y}|\Omega^0)$.

This result is very useful in practice, as it allows to compute the projection onto Ω by finding first the projection onto the polar cone Ω^0 , which has known edges.

In general, a vector $\hat{\boldsymbol{\theta}} \in \mathbb{R}^n$ solves the problem in Equation 1.6 over Ω (see Robertson et al., 1988, Chapter 1) if and only if

$$\begin{aligned} \langle \mathbf{y} - \hat{\boldsymbol{\theta}}, \hat{\boldsymbol{\theta}} \rangle &= 0, \text{ and} \\ \langle \mathbf{y} - \hat{\boldsymbol{\theta}}, \boldsymbol{\theta} \rangle &\leq 0, \quad \forall \boldsymbol{\theta} \in \Omega. \end{aligned}$$

These necessary and sufficient conditions can be adapted to the polar cone as follows: the vector $\hat{\boldsymbol{\rho}} \in \mathbb{R}^n$ minimizes $\|\mathbf{y} - \boldsymbol{\rho}\|^2$ over Ω^0 if and only if

$$\langle \mathbf{y} - \hat{\boldsymbol{\rho}}, \hat{\boldsymbol{\rho}} \rangle = 0, \text{ and} \tag{1.7}$$

$$\langle \mathbf{y} - \hat{\boldsymbol{\rho}}, \boldsymbol{\gamma}_j \rangle \leq 0, \text{ for } j = 1, \dots, m. \tag{1.8}$$

These conditions suggest that computing $\hat{\boldsymbol{\rho}}$ can be performed by finding a set $J \subseteq \{1, 2, \dots, m\}$ such that the projection of \mathbf{y} onto the linear space generated by the vectors in $\{\boldsymbol{\gamma}_j, j \in J\}$ lands into the polar cone Ω^0 and satisfies the conditions in Equation 1.8 for $j \notin J$. That is, the vector $\hat{\boldsymbol{\rho}}$ is simply the projection of \mathbf{y} onto a linear space induced by certain J , where J might vary as it depends on the vector \mathbf{y} . However, as there are 2^m possible sets J , projecting onto each of these induced linear spaces might be an inefficient task when the number of constraints m is large. Meyer (2013b) developed the Cone Projection Algorithm as a more efficient way to compute $\hat{\boldsymbol{\rho}}$ which avoids projecting onto each of the 2^m linear spaces. This algorithm computes $\hat{\boldsymbol{\rho}}$ by sequentially adding/removing indexes j to an initial set J , based on the values of $\langle \mathbf{y} - \hat{\boldsymbol{\rho}}_J, \boldsymbol{\gamma}_j \rangle$ for $j \notin J$, where $\hat{\boldsymbol{\rho}}_J = \Pi(\mathbf{y} | \boldsymbol{\gamma}_j, j \in J)$. The Cone Projection Algorithm has been implemented in the package `coneproject` in R (Liao and Meyer, 2014), which is compiled in C++ to improve its speed efficiency.

Given $\mathbf{y} \in \mathbb{R}^n$, the projection $\hat{\boldsymbol{\rho}}$ is unique. However, the set J that induces the linear space where such projection lands is not necessarily unique. When \mathbf{A} is full-row rank, the projection $\hat{\boldsymbol{\rho}}$

lands in more than one linear space spanned by $\{\gamma_j; j \in J\}$ only in a set of \mathbf{y} values with Lebesgue measure zero. In contrast, when \mathbf{A} is not a full-row rank matrix, there might exist different sets J_1 and J_2 such that $\{\gamma_j, j \in J_1\}$ and $\{\gamma_j, j \in J_2\}$ span the same linear space and $\hat{\boldsymbol{\rho}}$ lands into it.

Now, consider the additive regression model with n independent observations given by

$$y_i = f_1(x_{1i}) + \cdots + f_L(x_{Li}) + \mathbf{z}_i^\top \boldsymbol{\alpha} + \epsilon_i, \quad (1.9)$$

where the f_l are functions to be modelled nonparametrically, the \mathbf{z}_i are covariates to be modelled parametrically, and $\epsilon_i \stackrel{\text{i.i.d.}}{\sim} N(0, \sigma^2)$. Also, suppose that the f_l functions are assumed to respect shape constraints such as monotonicity and/or convexity. Under these assumptions, Meyer (2013a) estimated $E(\mathbf{y}|\mathbf{x}, \mathbf{z})$ using a single cone projection. Alternatively, the functions f_l can be approximated using shape-restricted splines, which only require that the coefficients on the basis spline vectors are non-negative (Meyer, 2008). This spline regression model can also be estimated using a single cone projection. If a generalised linear additive model is assumed, then estimates can be computed through an iteratively re-weighted cone projection algorithm. The package `cgam` in R (Meyer and Liao, 2017) fits the constrained generalised additive model in Equation 1.9 using the latter algorithm.

Meyer (2013a) proposed the Cone Information Criterion (CIC) to select the best combinations of variables and shapes in a constrained model. That is defined as follows,

$$\text{CIC} = \log(\|\mathbf{y} - \hat{\boldsymbol{\phi}}\|^2) + \log\left(\frac{2(E(D) + d_0)}{n - d_0 - cE(D)} + 1\right), \quad (1.10)$$

where $\hat{\boldsymbol{\phi}}$ is the constrained estimate of $E(\mathbf{y}|\mathbf{x}, \mathbf{z})$, $E(D)$ is the expected degrees of freedom of the constrained estimator $\hat{\boldsymbol{\phi}}$, d_0 is the number of parametrically modelled covariates, and $c \in [1, 2]$ is a fixed constant. Note that the expected degrees of freedom $E(D)$ is preferred to be used instead of the observed degrees of freedom D , since the latter might vary for different realisations of \mathbf{y} . In particular, the use of $E(D)$ aims to avoid the situation in which important variables have large penalties.

The CIC is derived as the log of the estimated Predictive Squared Error (PSE), defined as $\text{PSE} = n^{-1} E \|\mathbf{y}^* - \hat{\phi}\|^2$, where \mathbf{y}^* is another independent realisation of \mathbf{y} generated from the same model. Being similar to the $\text{AIC} = \log(\|\mathbf{y} - \hat{\phi}\|^2) + 2d/n$, the CIC is a measure that balances both the accuracy of the constrained estimator $\hat{\phi}$ and the complexity of the model.

1.3 Overview

In Chapter 2, the Cone Information Criterion for Survey data (CIC_s) is proposed as a consistent criterion that validates the use of the monotone estimator proposed by Wu et al. (2016) to appropriately estimate population domain means. This methodology is based on the Cone Information Criterion (CIC) shown in Equation 1.10, which was originally developed for shape and model selection outside of the survey context. The practical performance of the CIC_s is demonstrated through simulations. Further, an application to the 2011-2012 U.S. National Health and Nutrition Examination Survey data is carried out.

Chapter 3 introduces an extension of the previously discussed monotone estimator to allow for a more general set of restrictions beyond monotonicity. Here, shape constraints that can be expressed using irreducible matrices are considered. Theoretical foundation that supports the use of the proposed constrained estimator for estimation and inference of population domain means is presented. Through a simulation study, the constrained estimator is shown to improve precision and variability of domain mean estimates, in comparison with unconstrained estimates, as long as the assumed constraints hold approximately on population domain means. Further, the proposed estimator is applied to the 2015 U.S. National Survey of College Graduates.

In terms of software development, Chapter 4 describes the package `bccgam` in R (Oliva-Aviles and Meyer, 2018), which implements a Bayesian approach to fit generalised partial additive models with functions that might be modelled nonparametrically using shape-restricted splines. This package is developed outside of the survey context, and aims to the practical implementation of the work in Meyer et al. (2011). To illustrate the usefulness of the `bccgam` package, an analysis of the ‘duncan’ data set, provided within the package, is performed using its main routines.

In Chapter 5, general conclusions about the constrained methodologies introduced in this dissertation are stated. Further, potential research directions related to these methodologies are discussed. The derivation of all theoretical results presented in this dissertation are extensively included in Appendix A and Appendix B.

Chapter 2

Validation of Monotone Domain Mean Estimators

2.1 Introduction

Monotone population characteristics arise naturally in many survey problems. For example, average salary might be increasing in pay grade, average cholesterol level could be decreasing in physical activity time, etc. In large-scale surveys, there is often interest in estimating the characteristics of domains within the overall population, including those of domains with small sample sizes. One possibility to handle small domains is to apply small area estimation methods. However, that requires switching from the design-based to a model-based paradigm, which can be undesirable. An alternative approach is to remain within the design-based paradigm but take advantage of qualitative assumptions about the population structure, when such are available.

Isotonic regression has been widely studied outside of the survey context. Some remarkable works on this topic include Brunk (1955), VanEeden (1956), Brunk (1958), Robertson et al. (1988), and Silvapulle and Sen (2005). In contrast, merging isotonic regression techniques into survey estimation and inference has just been studied recently. Wu et al. (2016) considered the case when both sampling design and monotone restrictions are taken into account on the domain estimation. They proposed a design-weighted constrained estimator by combining domain estimation and the Pooled Adjacent Violators Algorithm (PAVA) (Robertson et al., 1988). Further, they showed that their proposed constrained estimator improved estimation and variability of domain means, under both linearization-based and replication-based variance estimation.

Although the constrained estimator proposed by Wu et al. (2016) improves the precision of the usual survey sampling estimators, it has to be used carefully since invalid population constraint assumptions could lead to biased domain mean estimators. The main objective of this work is to develop diagnostic methods to detect population departures from monotone assumptions. Particularly, we propose the Cone Information Criterion for Survey Data (CIC_s) as a data-driven method

to determine whether or not it is better to use the constrained estimator to estimate the population domain means. The Cone Information Criterion (CIC) was originally developed for the i.i.d. case by Meyer (2013a).

In Section 2.2, we describe the constrained estimator proposed by Wu et al. (2016) and explain some of its properties such as adaptive pooling domain and linearization-based variance estimation. Section 2.3 contains the proposed CIC_s along with some of its theoretical properties. In particular, we show that CIC_s is consistently choosing the correct estimator based on the underlying shape of the population domain means, in the sense that with probability going to 1 as the sample size increases, CIC_s will determine that pooling of domains that violate monotonicity constraints is unwarranted. Section 2.4 demonstrates the performance of the CIC_s under a broad variety of simulation scenarios. In Section 2.5 we apply our CIC_s methodology to the 2011-2012 National Health and Nutrition Examination Survey (NHANES) laboratory data.

2.2 Constrained Domain Mean Estimator for Survey Data

We begin by reviewing the survey setting and the constrained estimator proposed by Wu et al. (2016). Consider a finite population $U_N = \{1, 2, \dots, N\}$, and let $U_{d,N}$ denote a domain for $d = 1, \dots, D$. Assume that $\{U_{d,N} ; d = 1, \dots, D\}$ constitute a partition of the population U_N . Denote N_d as the population size of domain $U_{d,N}$. Given a study variable y , let \bar{y}_{U_d} be the population domain means,

$$\bar{y}_{U_d} = \frac{\sum_{k \in U_{d,N}} y_k}{N_d}, \quad d = 1, \dots, D.$$

Suppose we draw a sample $s_N \subset U_N$ using the probability sampling design $p_N(\cdot)$. Let n_N be the sample size of s_N . We are going to consider the case where the sampling design is measurable, i.e., both first-order $\pi_k = \mathbb{E}(I_k)$ and second-order $\pi_{kl} = \mathbb{E}(I_k I_l)$ inclusion probabilities are strictly positive, where I_k is the indicator variable of whether $k \in s_N$ or not. Denote $s_{d,N}$ as the corresponding sample in domain d obtained from s_N . Further, let $n_{d,N} = |s_{d,N}|$. For simplicity in our notation, we will omit the subscript N from these and related quantities from now on.

Consider the problem of estimating the population domain means \bar{y}_{U_d} . When no qualitative information is assumed on the population domains, we can consider either the Horvitz-Thompson estimator \hat{y}_{s_d} (Horvitz and Thompson, 1952) or the frequently preferred Hájek estimator \tilde{y}_{s_d} (Hájek, 1971), which are given by

$$\hat{y}_{s_d} = \frac{\sum_{k \in s_d} y_k / \pi_k}{N_d}, \quad \tilde{y}_{s_d} = \frac{\sum_{k \in s_d} y_k / \pi_k}{\hat{N}_d}, \quad (2.1)$$

respectively, where $\hat{N}_d = \sum_{k \in s_d} 1/\pi_k$. We will refer to them as unconstrained estimators of \bar{y}_{U_d} . Note that both estimators in Equation 2.1 consider only the information contained in domain d , leading to large standard errors on domains with small sample sizes.

Suppose now that we want to include monotonicity assumptions into the estimation stage of domain means. For instance, assume the population domain means are isotonic over the D domains. That is, $\bar{y}_{U_1} \leq \bar{y}_{U_2} \leq \dots \leq \bar{y}_{U_D}$ (analogously, $\bar{y}_{U_1} \geq \bar{y}_{U_2} \geq \dots \geq \bar{y}_{U_D}$, but which we will not further consider explicitly here). Wu et al. (2016) proposed a domain mean estimator that respect monotone constraints, given by the ordered vector $\tilde{\boldsymbol{\theta}}_s = (\tilde{\theta}_{s_1}, \tilde{\theta}_{s_2}, \dots, \tilde{\theta}_{s_D})^\top$ which optimizes

$$\min_{\theta_1, \theta_2, \dots, \theta_D} \sum_{d=1}^D \hat{N}_d (\tilde{y}_{s_d} - \theta_d)^2, \quad \text{subject to} \quad \theta_1 \leq \theta_2 \leq \dots \leq \theta_D. \quad (2.2)$$

The objective function in Equation 2.2 can be written in matrix terms as $(\tilde{\boldsymbol{y}}_s - \boldsymbol{\theta})^\top \mathbf{W}_s (\tilde{\boldsymbol{y}}_s - \boldsymbol{\theta})$, where $\tilde{\boldsymbol{y}}_s = (\tilde{y}_{s_1}, \tilde{y}_{s_2}, \dots, \tilde{y}_{s_D})^\top$, $\boldsymbol{\theta} = (\theta_1, \theta_2, \dots, \theta_D)^\top$, $\mathbf{W}_s = \text{diag}(\hat{N}_1/\hat{N}, \hat{N}_2/\hat{N}, \dots, \hat{N}_D/\hat{N})$ is a consistent estimator of $\mathbf{W}_U = \text{diag}(N_1/N, N_2/N, \dots, N_D/N)$, and $\hat{N} = \sum_{d=1}^D \hat{N}_d$.

Following Brunk (1955), the general closed form solution for the constrained problem in Equation 2.2 can be expressed as the set of pooled weighted domain means given by

$$\tilde{\theta}_{s_d} = \max_{i \leq d} \min_{d \leq j} \tilde{y}_{s_{i:j}}, \quad \text{where} \quad \tilde{y}_{s_{i:j}} = \frac{\sum_{d=i}^j \hat{N}_d \tilde{y}_{s_d}}{\sum_{d=i}^j \hat{N}_d} = \frac{\sum_{k \in s_{i:j}} y_k / \pi_k}{\sum_{k \in s_{i:j}} 1 / \pi_k}, \quad (2.3)$$

where $s_{i:j} = s_i \cup \dots \cup s_j$ for $1 \leq i \leq j \leq D$. Moreover, we can make use of the Pooled Adjacent Violator Algorithm PAVA (Robertson et al., 1988) along with $\tilde{\boldsymbol{y}}_s$ and the weights $\hat{N}_1, \hat{N}_2, \dots, \hat{N}_D$

to compute efficiently the constrained estimator $\tilde{\theta}_s$. Observe that the constrained estimator in Equation 2.3 consists of adaptively collapsing neighboring domains. Furthermore, the above procedure can be simplified in the obvious way when applied to the Horvitz-Thompson estimator $\hat{\mathbf{y}}_s = (\hat{y}_{s_1}, \hat{y}_{s_2}, \dots, \hat{y}_{s_D})^\top$ with weights N_1, N_2, \dots, N_D , leading to the constrained estimator vector $\hat{\theta}_s$ with entries of the form $\hat{y}_{s_{i:j}}$. We refer to Wu et al. (2016) for a discussion of the properties of these constrained estimators, including design consistency and asymptotic distribution.

We conclude this section by defining some of the quantities we will use in the development of the CIC_s. Note that the estimator $\hat{\theta}_s$ has a random weighted projection matrix $\hat{\mathbf{P}}_s$ associated with it, which is defined by the pooling obtained from the PAVA and the weights N_1, N_2, \dots, N_D . That is, $\hat{\mathbf{P}}_s$ is the matrix such that $\hat{\theta}_s = \hat{\mathbf{P}}_s \hat{\mathbf{y}}_s$. For example, suppose $D = 3$ and that PAVA chooses to pool domains 1 and 2, but not to pool domain 2 and 3. Hence, $\hat{\theta}_{s_1} = \hat{\theta}_{s_2} = (N_1 \hat{y}_{s_1} + N_2 \hat{y}_{s_2}) / (N_1 + N_2)$, and $\hat{\theta}_{s_3} = \hat{y}_{s_3}$. Then,

$$\hat{\mathbf{P}}_s = \begin{pmatrix} \frac{N_1}{N_1+N_2} & \frac{N_2}{N_1+N_2} & 0 \\ \frac{N_1}{N_1+N_2} & \frac{N_2}{N_1+N_2} & 0 \\ 0 & 0 & 1 \end{pmatrix}.$$

Let $\hat{\Sigma} = \{\hat{\Sigma}_{ij}\}$ be the unbiased estimator of the covariance matrix of $\hat{\mathbf{y}}_s$, given by

$$\hat{\Sigma}_{ij} = \frac{1}{N_i N_j} \sum_{k \in s_i} \sum_{l \in s_j} \frac{\Delta_{kl} y_k y_l}{\pi_{kl} \pi_k \pi_l}, \quad i, j = 1, 2, \dots, D,$$

where $\Delta_{kl} = \pi_{kl} - \pi_k \pi_l$. Further, for any $i \leq j$, let $\bar{y}_{U_{i:j}}$ be the pooled population mean of domains i through j . That is,

$$\bar{y}_{U_{i:j}} = \frac{\sum_{k \in U_{i:j}} y_k}{N_{i:j}}, \quad \text{where} \quad N_{i:j} = \sum_{d=i}^j N_d,$$

and $U_{i:j} = U_i \cup \dots \cup U_j$.

For any indexes i_1, i_2, j_1, j_2 such that $i_1 \leq j_1$ and $i_2 \leq j_2$, let $\tilde{y}_{s_{i_1:j_1}}, \tilde{y}_{s_{i_2:j_2}}$ be the Hájek estimators of $\bar{y}_{U_{i_1:j_1}}$ and $\bar{y}_{U_{i_2:j_2}}$, respectively. By standard linearization arguments (Särndal et al., 1992, Chapter 5), the approximated covariance of $\tilde{y}_{s_{i_1:j_1}}$ and $\tilde{y}_{s_{i_2:j_2}}$ is given by

$$AC(\tilde{y}_{s_{i_1:j_1}}, \tilde{y}_{s_{i_2:j_2}}) = \frac{1}{N_{i_1:j_1} N_{i_2:j_2}} \sum_{k \in U_{i_1:j_1}} \sum_{l \in U_{i_2:j_2}} \Delta_{kl} \left(\frac{y_k - \bar{y}_{U_{i_1:j_1}}}{\pi_k} \right) \left(\frac{y_l - \bar{y}_{U_{i_2:j_2}}}{\pi_l} \right). \quad (2.4)$$

Moreover, given that $\pi_{kl} > 0$ for all $k, l \in U$, a design consistent estimator of the approximate covariance in Equation 2.4 is

$$\widehat{AC}(\tilde{y}_{s_{i_1:j_1}}, \tilde{y}_{s_{i_2:j_2}}) = \frac{1}{\widehat{N}_{i_1:j_1} \widehat{N}_{i_2:j_2}} \sum_{k \in s_{i_1:j_1}} \sum_{l \in s_{i_2:j_2}} \frac{\Delta_{kl}}{\pi_{kl}} \left(\frac{y_k - \tilde{y}_{s_{i_1:j_1}}}{\pi_k} \right) \left(\frac{y_l - \tilde{y}_{s_{i_2:j_2}}}{\pi_l} \right), \quad (2.5)$$

where $\widehat{N}_{i:j} = \sum_{d=i}^j \widehat{N}_d$.

2.3 Main results

In this section, we present the Cone Information Criterion for Survey Data (CIC_s). The CIC_s is a tool that may be used to validate the monotone estimator in Equation 2.2 as an appropriate estimator of population domain means. In what follows, we define the CIC_s for the Horvitz-Thompson estimator and propose a natural extension that applies to the Hájek setting. Further, main properties of the CIC_s are shown along with their theoretical foundation.

2.3.1 Cone Information Criterion for Survey Data (CIC_s)

For the Horvitz-Thompson estimator, we define the CIC_s as

$$CIC_s(\widehat{\boldsymbol{\theta}}_s) = (\widehat{\boldsymbol{y}}_s - \widehat{\boldsymbol{\theta}}_s)^\top \mathbf{W}_U (\widehat{\boldsymbol{y}}_s - \widehat{\boldsymbol{\theta}}_s) + 2 \text{Tr} \left(\mathbf{W}_U \widehat{\mathbf{P}}_s \widehat{\boldsymbol{\Sigma}} \right), \quad (2.6)$$

where $\widehat{\mathbf{P}}_s$ is the projection matrix associated with $\widehat{\boldsymbol{\theta}}_s$.

The proposed CIC_s has similar features as the Akaike Information Criterion (AIC) (Akaike, 1973) and the Bayesian Information Criterion (BIC) (Schwarz, 1978), which have been broadly used for model selection. The first term measures the deviation between the constrained estimator $\widehat{\boldsymbol{\theta}}_s$ and the unconstrained estimator $\bar{\boldsymbol{y}}_s$, while the second term can be seen as a penalty for the complexity of the constrained estimator. The penalty term is large when the number of different

groups chosen by the constrained estimator is also large, meaning that the number of different parameters to estimate (or effective degrees of freedom) of the constrained estimator is high.

The development of CIC_s proceeds similarly as for the Cone Information Criterion (CIC) proposed by Meyer (2013a). Its motivation comes from properties of the Predictive Squared Error (PSE) under the Horvitz-Thompson setting, which is defined as

$$\text{PSE}(\widehat{\boldsymbol{\theta}}_s) = \mathbb{E} \left[(\widehat{\boldsymbol{y}}_{s^*} - \widehat{\boldsymbol{\theta}}_s)^\top \mathbf{W}_U (\widehat{\boldsymbol{y}}_{s^*} - \widehat{\boldsymbol{\theta}}_s) \right] \quad (2.7)$$

where $\widehat{\boldsymbol{y}}_{s^*}$ is the vector of Horvitz-Thompson domain mean estimators obtained from a sample s^* that is independent to s , where s^* is drawn using the same probability sampling design as s . Furthermore, define the Sum of Squared Errors (SSE) as

$$\text{SSE}(\widehat{\boldsymbol{\theta}}_s) = (\widehat{\boldsymbol{y}}_s - \widehat{\boldsymbol{\theta}}_s)^\top \mathbf{W}_U (\widehat{\boldsymbol{y}}_s - \widehat{\boldsymbol{\theta}}_s).$$

We define $\text{CIC}_s(\widehat{\boldsymbol{\theta}}_s)$ as an estimator of $\text{PSE}(\widehat{\boldsymbol{\theta}}_s)$ that involves $\text{SSE}(\widehat{\boldsymbol{\theta}}_s)$. Proposition 2.1 establishes a relationship between $\text{PSE}(\widehat{\boldsymbol{\theta}}_s)$ and $\text{SSE}(\widehat{\boldsymbol{\theta}}_s)$; its proof and all subsequent ones are included in Appendix A.

Proposition 2.1. $\text{PSE}(\widehat{\boldsymbol{\theta}}_s) = \mathbb{E} \left[\text{SSE}(\widehat{\boldsymbol{\theta}}_s) \right] + 2 \text{Tr} \left[\mathbf{W}_U \text{cov}(\widehat{\boldsymbol{\theta}}_s, \widehat{\boldsymbol{y}}_s) \right]$.

Motivated by Proposition 2.1, an estimate of $\text{PSE}(\widehat{\boldsymbol{\theta}}_s)$ can be derived by estimating both $\mathbb{E} \left[\text{SSE}(\widehat{\boldsymbol{\theta}}_s) \right]$ and $\text{cov}(\widehat{\boldsymbol{\theta}}_s, \widehat{\boldsymbol{y}}_s)$. The first term has a straightforward unbiased estimator $\text{SSE}(\widehat{\boldsymbol{\theta}}_s)$, and an estimator for the covariance term can be obtained using the observed pooling on $\widehat{\boldsymbol{\theta}}_s$. As we will show later, the latter term can be estimated by the asymptotically unbiased estimator $\widehat{\mathbf{P}}_s \widehat{\boldsymbol{\Sigma}}$ under certain assumptions. That produces the proposed CIC_s in Equation 2.6.

However, recall that the use of the Horvitz-Thompson estimator requires information about the population domain sizes N_d , which is not frequently the case in many practical survey applications. Therefore, analogously to Equation 2.6, we extend the CIC_s to the Hájek setting by using the estimator $(\tilde{\boldsymbol{y}}_s - \tilde{\boldsymbol{\theta}}_s)^\top \mathbf{W}_s (\tilde{\boldsymbol{y}}_s - \tilde{\boldsymbol{\theta}}_s)$ instead of $\text{SSE}(\widehat{\boldsymbol{\theta}}_s)$, and $\mathbf{W}_s \widehat{\text{cov}}(\tilde{\boldsymbol{\theta}}_s, \tilde{\boldsymbol{y}}_s)$ instead of $\mathbf{W}_U \widehat{\mathbf{P}}_s \widehat{\boldsymbol{\Sigma}}$;

where $\widehat{\text{cov}}(\tilde{\boldsymbol{\theta}}_s, \tilde{\boldsymbol{y}}_s)$ denotes the estimator of the covariance matrix of $\tilde{\boldsymbol{\theta}}_s$ and $\tilde{\boldsymbol{y}}_s$, which is based on the observed pooling of $\tilde{\boldsymbol{\theta}}_s$ and is defined element-wise as

$$\widehat{\text{cov}}(\tilde{\boldsymbol{\theta}}_s, \tilde{\boldsymbol{y}}_s)_{ij} = \widehat{AC}(\tilde{\theta}_{s_i}, \tilde{y}_{s_j}), \quad \text{for } i, j = 1, 2, \dots, D.$$

Hence, the proposed CIC_s for the Hájek estimator setting is

$$\text{CIC}_s(\tilde{\boldsymbol{\theta}}_s) = (\tilde{\boldsymbol{y}}_s - \tilde{\boldsymbol{\theta}}_s)^\top \mathbf{W}_s (\tilde{\boldsymbol{y}}_s - \tilde{\boldsymbol{\theta}}_s) + 2 \text{Tr} \left[\mathbf{W}_s \widehat{\text{cov}}(\tilde{\boldsymbol{\theta}}_s, \tilde{\boldsymbol{y}}_s) \right]. \quad (2.8)$$

2.3.2 Assumptions

In order to state properly our theoretical results, we need to consider some required assumptions.

(A1) The number of domains D is a fixed known constant.

(A2) The non-random sample size n_N satisfies $0 < \lim_{N \rightarrow \infty} \frac{n_N}{N} < 1$.

(A3) $\limsup_{N \rightarrow \infty} \frac{1}{N} \sum_{k \in U_N} y_k^4 < \infty$.

(A4) $0 < \gamma_d = \lim_{N \rightarrow \infty} \frac{N_d}{N} < 1$ for $d = 1, 2, \dots, D$. Also, for some constants $\mu_1, \mu_2, \dots, \mu_D$ and any integers i, j such that $1 \leq i \leq j \leq D$, then $\bar{y}_{U_{i:j}} - \mu_{i:j} = O(N^{-1/2})$ with $\mu_{i:j} = \sum_{d=i}^j \gamma_d \mu_d$.

(A5) For all N , $\min_{k \in U_N} \pi_k \geq \lambda > 0$, $\min_{k, l \in U_N} \pi_{kl} \geq \lambda^* > 0$, and $\limsup_{N \rightarrow \infty} n_N \max_{k, l \in U_N: k \neq l} |\Delta_{kl}| < \infty$.

(A6) $\lim_{N \rightarrow \infty} \max_{(k_1, k_2, k_3, k_4) \in D_{4,N}} |\mathbb{E}[(I_{k_1} I_{k_2} - \pi_{k_1 k_2})(I_{k_3} I_{k_4} - \pi_{k_3 k_4})]| = 0$, where $D_{4,N}$ denotes the set of all distinct 4-tuples (k_1, k_2, k_3, k_4) from U_N .

(A7) $\lim_{N \rightarrow \infty} \max_{(k_1, k_2, k_3) \in D_{3,N}} |\mathbb{E}[(I_{k_1} - \pi_{k_1})^2 (I_{k_2} - \pi_{k_2})(I_{k_3} - \pi_{k_3})]| = 0$.

(A8) $\limsup_{N \rightarrow \infty} n_N \max_{(k_1, k_2, k_3, k_4) \in D_{4,N}} |\mathbb{E}[(I_{k_1} - \pi_{k_1})(I_{k_2} - \pi_{k_2})(I_{k_3} - \pi_{k_3})(I_{k_4} - \pi_{k_4})]| = 0$.

Assumption (A1) states that the number of domains D will not change as the population size

changes. Assumption (A2) declares that the sample size is asymptotically strictly less than the population size but greater than zero, which intuitively means that the sample and the population size are of the same order. The boundedness property of the finite population fourth moment in Assumption (A3) is used several times in our proofs to show that the approximated scaled covariances in Equation 2.4 are asymptotically bounded, and also, that their estimators are consistent for them. In addition, Assumption (A4) is used to assure that the population size and the subpopulation size are of the same order. Further, it establishes that the pooled population domain means converge to some constant limiting domain means with rate $N^{-1/2}$. The consistency result of CIC_s is based on whether the constants $\mu_1, \mu_2, \dots, \mu_D$ are strictly monotone or not. Assumption (A5) implies that both first and second-order inclusion probabilities can not tend to zero as N increases. Moreover, this assumption states that the sampling design covariances Δ_{kl} ($k \neq l$) tend to zero, i.e., sampling designs that produces asymptotically highly correlated elements are not allowed. Lastly, Assumptions (A6)-(A8) are similar to the higher order assumptions considered by Breidt and Opsomer (2000). These assumptions involve fourth moment conditions on the sampling design. These assumptions hold for simple random sampling without replacement and for stratified simple random sampling with fixed stratum boundaries (Breidt and Opsomer, 2000).

2.3.3 Properties of CIC_s

Under above assumptions, $\text{CIC}_s(\hat{\theta}_s)$ has the property of being an asymptotically unbiased estimator of $\text{PSE}(\hat{\theta}_s)$ when the pooling obtained from applying the PAVA to the vector $\boldsymbol{\mu} = (\mu_1, \mu_2, \dots, \mu_D)^\top$ with weights $\gamma_1, \gamma_2, \dots, \gamma_D$ is unique. To show that, we first prove that there are certain poolings which are chosen with probability tending to zero as N tends to infinity. This is stated in Theorem 2.1, which makes use of the Greatest Convex Minorant (GCM).

The GCM provides of an illustrative way to express monotone estimators. Figure 2.1 displays an example of sample domain means with their respective monotone estimates (Figure 2.1a), and a plot of their corresponding cumulative sum diagram and GCM (Figure 2.1b). The GCM is conformed by $D + 1$ points, indexed from 0 to D , and their left-hand slopes are the $\hat{\theta}_{s_d}$ values.

The points indexed by 0 and D are the boundaries of the GCM, and the rest are its interior points. Three possible scenarios can be identified for each of the interior points: the slope of the GCM changes (*corner points*); the GCM slope does not change and the cumulative sum coincides with the minorant (*flat spots*); or the GCM slope does not change but the cumulative sum is strictly above the minorant (*points above the GCM*). The example displayed in Figure 2.1b shows that the indexes 1, 2, 5 correspond to corner points, the index 6 to a flat spot, and the indexes 3, 4 to points above the GCM. In particular, note that flat spots correspond to cases where consecutive domain means are equal ($\hat{y}_{s_6} = \hat{y}_{s_7}$).

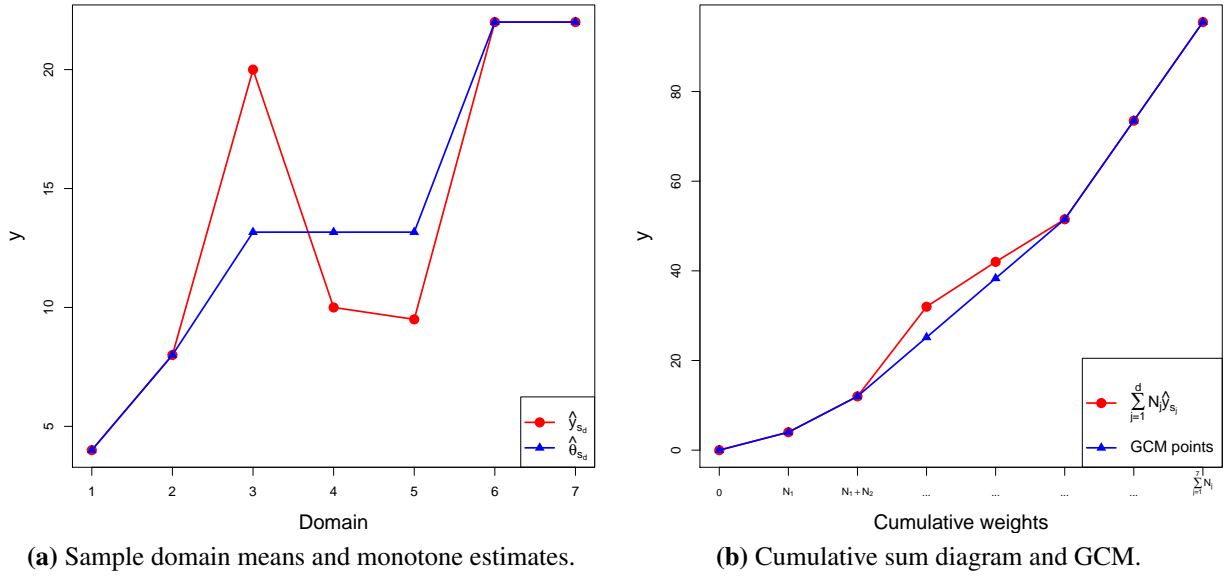


Figure 2.1: GCM example.

Theorem 2.1. Let $t_\mu(d) = \mu_{1:d}$ and $r_\mu(d) = \gamma_{1:d}$, for $d = 1, 2, \dots, D$, where $\mu_{i:j} = \sum_{d=i}^j \gamma_d \mu_d$, $\gamma_{i:j} = \sum_{d=i}^j \gamma_d$ and $t_\mu(0) = r_\mu(0) = 0$. Let $G_\mu(d) = (r_\mu(d), g_\mu(d))$ be the GCM points of the cumulative sum diagram with points $(r_\mu(d), t_\mu(d))$. Define J_μ^0 and J_μ^1 to the indexes of points strictly above G_μ and indexes of its corner points, respectively. Based on the sample s , define $t_s(d) = \hat{y}_{s_{1:d}}$ and $r_s(d) = N_{1:d}$, with $t_s(0) = r_s(0) = 0$, and let $g_s(\cdot)$, G_s , J_s^0 , and J_s^1 be the analogous sample quantities of $g_\mu(\cdot)$, G_μ , J_μ^0 , and J_μ^1 . Denote A_0 and A_1 to be the events where

$J_\mu^0 \subseteq J_s^0$ and $J_\mu^1 \subseteq J_s^1$, respectively. Then, $P(A_0^c) = o(n_N^{-1})$ and $P(A_1^c) = o(n_N^{-1})$.

To have a better understanding of Theorem 2.1, note that for every pair of mutually exclusive sets J_s^0, J_s^1 , there are certain poolings (groupings) allowed by $\hat{\mathbf{y}}_s$ to obtain $\hat{\boldsymbol{\theta}}_s$. In particular, if $J_s^0 \cup J_s^1 = \{1, 2, \dots, D-1\}$ (i.e. no flat spots), then there is a unique pooling allowed by $\hat{\mathbf{y}}_s$. Speaking somewhat loosely and referring to ‘bad poolings’ to those poolings of $\hat{\mathbf{y}}_s$ that are chosen with zero asymptotic probability, Theorem 2.1 states that bad poolings correspond to those pairs of disjoint sets J_s^0, J_s^1 that do not satisfy $J_\mu^0 \subseteq J_s^0$ and $J_\mu^1 \subseteq J_s^1$. One case of particular interest is when there are no flat spots on the GCM corresponding to $\boldsymbol{\mu}$, i.e., $J_\mu^0 \cup J_\mu^1 = \{1, 2, \dots, D-1\}$. Such scenario is equivalent than saying that, asymptotically, there is a unique pooling allowed by $\hat{\mathbf{y}}_s$. Moreover, under this scenario, it can be proved (Theorem 2.2) that the proposed CIC_s in Equation 2.6 is an asymptotic unbiased estimator of the PSE in Equation 2.7.

Theorem 2.2. *If $J_\mu^0 \cup J_\mu^1 = \{1, 2, \dots, D-1\}$, then $\mathbb{E}[\text{CIC}_s(\hat{\boldsymbol{\theta}}_s)] = \text{PSE}(\hat{\boldsymbol{\theta}}_s) + o(n_N^{-1})$.*

In practice, the proposed CIC_s can be used as a decision tool that validates the use of the constrained estimator as an estimate of the population domain means. The decision rule would be to choose the estimator, either the constrained or the unconstrained, that produces the smallest CIC_s value. As we mentioned, CIC_s is an overall measure that balances the deviation of the constrained estimator from the unconstrained, as well as the complexity of such estimator. The fact that CIC_s measures the estimator complexity would avoid the undesired situation of choosing always the unconstrained estimator above the constrained estimator. Although we will focus on the Hájek version of the CIC_s (Equation 2.8) for the rest of this section, it is important to remark that the following properties are also valid under the Horvitz-Thompson setting.

Let $\text{CIC}_s(\tilde{\mathbf{y}}_s)$ and $\text{CIC}_s(\tilde{\boldsymbol{\theta}}_s)$ denote the CIC_s values for the unconstrained and constrained estimators, respectively. From Equation 2.8, that is,

$$\begin{aligned} \text{CIC}_s(\tilde{\mathbf{y}}_s) &= 2 \text{Tr} [\mathbf{W}_s \widehat{\text{cov}}(\tilde{\mathbf{y}}_s, \tilde{\mathbf{y}}_s)], \\ \text{CIC}_s(\tilde{\boldsymbol{\theta}}_s) &= (\tilde{\mathbf{y}}_s - \tilde{\boldsymbol{\theta}}_s)^\top \mathbf{W}_s (\tilde{\mathbf{y}}_s - \tilde{\boldsymbol{\theta}}_s) + 2 \text{Tr} [\mathbf{W}_s \widehat{\text{cov}}(\tilde{\boldsymbol{\theta}}_s, \tilde{\mathbf{y}}_s)], \end{aligned}$$

where $\widehat{\text{cov}}(\tilde{\mathbf{y}}_s, \tilde{\mathbf{y}}_s)_{ij} = \widehat{AC}(\tilde{y}_{s_i}, \tilde{y}_{s_j})$. Similarly as AIC and BIC, we might choose the estimator that produces the smallest CIC_s value. We show that this decision rule is asymptotically correct when choosing the shape based on the limiting domain means $\boldsymbol{\mu}$ (Theorem 2.5), and also, that the decision made from CIC_s is consistent with the decision made from PSE (Theorem 2.6). Theorems 2.3 and 2.4 contain theoretical properties of $AC(\cdot, \cdot)$ that are required to establish Theorem 2.5.

Theorem 2.3. *For any domains i_1, i_2, j_1, j_2 where $i_1 \leq j_1, i_2 \leq j_2$,*

$$\limsup_{N \rightarrow \infty} n_N AC(\tilde{y}_{s_{i_1:j_1}}, \tilde{y}_{s_{i_2:j_2}}) < \infty.$$

Furthermore,

$$n_N \left(\widehat{AC}(\tilde{y}_{s_{i_1:j_1}}, \tilde{y}_{s_{i_2:j_2}}) - AC(\tilde{y}_{s_{i_1:j_1}}, \tilde{y}_{s_{i_2:j_2}}) \right) = o_p(1).$$

Theorem 2.4. *Let $\boldsymbol{\theta}_U = (\theta_{U_1}, \theta_{U_2}, \dots, \theta_{U_D})^\top$ be the weighted isotonic population domain mean vector of $\bar{\mathbf{y}}_U$ with weights N_1, N_2, \dots, N_D . Then,*

$$\tilde{\theta}_{s_d} - \theta_{U_d} = O_p(n_N^{-1/2}), \quad \text{for } d = 1, \dots, D.$$

Theorem 2.5. *As $N \rightarrow \infty$,*

$$P\left(\text{CIC}_s(\tilde{\mathbf{y}}_s) < \text{CIC}_s(\tilde{\boldsymbol{\theta}}_s)\right) \rightarrow \begin{cases} 0, & \text{if } \mu_1 < \mu_2 < \dots < \mu_D; \\ 1, & \text{if } \mu_1, \mu_2, \dots, \mu_D \text{ are not monotone.} \end{cases}$$

Theorem 2.3 states that the scaled $AC(\cdot, \cdot)$ is asymptotically bounded and also, that $\widehat{AC}(\cdot, \cdot)$ is a consistent estimator of $AC(\cdot, \cdot)$ with a rate of n_N^{-1} . Hence, both the covariance between $\tilde{y}_{s_{i_1:j_1}}$ and $\tilde{y}_{s_{i_2:j_2}}$, and its proposed estimate are well defined. Theorem 2.4 establishes that the constrained estimator gets closer to the weighted isotonic population domain mean with a rate of $n_N^{-1/2}$. This theorem generalizes the results in Wu et al. (2016), where it was only considered the case when the limiting domain means are monotone. Recall that $\boldsymbol{\theta}_U = \bar{\mathbf{y}}_U$ if and only if the population domain means are monotone increasing. Theorem 2.5 shows that CIC_s consistently chooses the correct estimator based on the order of the limiting domain means $\mu_1, \mu_2, \dots, \mu_D$.

Finally, Theorem 2.6 establishes that the chosen estimator driven by PSE in Equation 2.7 is analogous to the decision made by CIC_s .

Theorem 2.6. As $N \rightarrow \infty$,

$$n_N[PSE(\hat{\theta}_s) - PSE(\hat{y}_s)] \rightarrow \begin{cases} 0, & \text{if } \mu_1 < \mu_2 < \dots < \mu_D; \\ \infty, & \text{if } \mu_1, \mu_2, \dots, \mu_D \text{ are not monotone.} \end{cases}.$$

Observe that neither Theorem 2.5 nor Theorem 2.6 deal with the case where the vector entries of μ are non-strictly monotone. Although in that case we would like both PSE and CIC_s to choose the constrained estimator, neither of them is able to choose it universally. Nevertheless, we show in the Simulations section that the constrained estimator is chosen with a high frequency under the non-strictly monotone scenario.

2.4 Simulations

We demonstrate the CIC_s performance through simulations under several settings. We consider the set-up in Wu et al. (2016) as a baseline to produce our simulation scenarios. For the first set of simulations, we generate populations of size N using limiting domain means μ_1, \dots, μ_D . Each element y_{d_k} in the population domain d is independently generated from a normal distribution with mean μ_d and standard deviation σ . That is, for a given domain d , $y_{d_k} \stackrel{iid}{\sim} N(\mu_d, \sigma^2)$ for $k = 1, 2, \dots, N_d$. Samples are generated using a stratified simple random sampling design without replacement in all H strata. The strata constitutes a partition of the total population of size N . We make use of an auxiliary random variable z to define the stratum membership of the population elements, with z created by adding random noise $N(0, 1)$ to $\sigma(d/D)$, for $d = 1, 2, \dots, D$. Stratum membership of y is then determined by sorting the vector z , creating H blocks of N/H elements based on their ranks, and assigning these blocks to the strata. Also, we set $\sigma = 3$, $H = 4$, $N_d = N/4$, and $D = 4$. The number of replications per simulation is 10000.

The vector of limiting domain means μ is created using the sigmoid function $S_1(\cdot)$ given by $S_1(d) = 2 \exp(5d/D - 2)/(1 + \exp(5d/D - 2))$ for $d = 1, 2, \dots, D$. We consider three different

scenarios for $\boldsymbol{\mu}$: the *monotone scenario*, where μ_d 's are strictly increasing; the *flat scenario*, where μ_d 's are non-strictly increasing; and the *non-monotone scenario*, where μ_d 's are not monotone increasing. The limiting domain means on the monotone scenario are given by $\mu_d = S_1(d)$ for $d = 1, 2, \dots, D$. The flat scenario is formed by “pulling down” μ_D until it is equal to μ_{D-1} , that is, $\mu_D = S_1(D) - \Delta$ where $\Delta = S_1(D) - S_1(D - 1)$. For the non-monotone scenario, we pull μ_D down until it gets below μ_{D-1} by using $\mu_D = S_1(D) - 2\Delta$. Note that the only difference among these three scenarios relies on the right tail. For each of the above scenarios, the total population size varies from $N = 10000, 20000, 40000$. Further, the total sample size $n_N = 200N/k$ is divided among the 4 strata as $(25N/k, 50N/k, 50N/k, 100N/k)$ for $k = 1000, 2000, 10000$, which makes the sampling design informative. Once the sample is generated, the Hájek domain mean estimators are computed along with the CIC_s in Equation 2.8.

We consider the design Mean Squared Error (MSE) of any estimator $\tilde{\boldsymbol{\phi}}_s$ given by

$$\text{MSE}(\tilde{\boldsymbol{\phi}}_s) = \mathbb{E} \left[(\tilde{\boldsymbol{\phi}}_s - \bar{\boldsymbol{y}}_U)^\top \mathbf{W}_U (\tilde{\boldsymbol{\phi}}_s - \bar{\boldsymbol{y}}_U) \right].$$

For each scenario mentioned above, we compute both the MSE for the unconstrained estimator $\text{MSE}(\tilde{\boldsymbol{y}}_s)$ and for the constrained estimator $\text{MSE}(\tilde{\boldsymbol{\theta}}_s)$ through simulations. In addition, we compute the MSE for the CIC_s -adaptive estimator $\dot{\boldsymbol{\theta}}_s$, given by

$$\dot{\boldsymbol{\theta}}_s = \tilde{\boldsymbol{y}}_s I\{\text{CIC}(\tilde{\boldsymbol{y}}_s) < \text{CIC}(\tilde{\boldsymbol{\theta}}_s)\} + \tilde{\boldsymbol{\theta}}_s I\{\text{CIC}(\tilde{\boldsymbol{y}}_s) \geq \text{CIC}(\tilde{\boldsymbol{\theta}}_s)\}.$$

Although there are no other existing methods that aim to choose between the unconstrained and the constrained estimator for survey data, we compare the performance of CIC_s versus two conditional testing methods that are based on the following hypothesis test under the linear regression model setting,

$$H_0 : \mu_1 \leq \mu_2 \leq \dots \leq \mu_D \quad H_1 : \text{no restrictions on } \mu_d \text{'s.}$$

The first test is a naive Wald test which depends on the sample-observed pooling. For this, we compute the test statistic

$$Q = (\tilde{\mathbf{y}}_s - \tilde{\boldsymbol{\theta}}_s)^\top [\widehat{\text{cov}}(\tilde{\mathbf{y}}_s, \tilde{\mathbf{y}}_s)]^{-1} (\tilde{\mathbf{y}}_s - \tilde{\boldsymbol{\theta}}_s)$$

and then compare it to a $\chi^2(D - k)$, where k is the number of different estimated values on $\tilde{\boldsymbol{\theta}}_s$.

The second test is the conditional test proposed by Wollan and Dykstra (1986). Even though the latter test is established for independent data with known variances, we use instead the estimated design variances of the sample-observed pooling obtained from Equation 2.5. To perform this, we compute the test statistic Q -as in the Wald test- but then we compare it to a $\chi^2(D - k)$ with point mass of p_0 at $Q = 0$, where p_0 is the probability that $Q = 0$ under the hypothesis $\mu_1 = \mu_2 = \dots = \mu_D$. Note that the conditional test might perform similar as the Wald test when the number of domains D is large.

Since both Wald and conditional tests require the variance-covariance matrix of the domain mean estimators to be non-singular, these could be performed only when the variance-covariance matrix formed by the estimates in Equation 2.5 is in fact a valid covariance matrix. We set the significance level of these tests at 0.05.

Tables 2.1, 2.2 and 2.3 contain the proportion of times that the unconstrained estimator is chosen over the constrained estimator under the monotone, flat and non-monotone scenarios, respectively. In cases where the unconstrained and constrained estimators agree (i.e. the unconstrained estimator satisfies the constraint), this is counted as a constrained estimator in the calculation of this proportion. The last two rows of these tables show the MSE of the constrained estimator and the CIC_s -adaptive estimator, relative to the MSE of the unconstrained estimator. The former ratio can be viewed as a measure of how much better (or worse) naively applying the constrained estimator is under the different scenarios, while the latter ratio shows how well the adaptive estimator is in terms of balancing the MSE's of the constrained and unconstrained estimators.

From Table 2.1, we can note that CIC_s tends not to choose the unconstrained estimator under the monotone scenario as N increases. In contrast, the unconstrained estimator is chosen most of

the times under the non-monotone simulation scenario (Table 2.3). Flat scenario results (Table 2.2) show that although the proportion of times the unconstrained estimator is chosen do not tend to zero as N grows, it is fairly small, meaning that CIC_s is choosing the constrained estimator most of the times. From these three tables, we can observe that CIC_s tends to be more conservative when choosing the unconstrained estimator over the constrained, in comparison with both Wald and conditional tests.

Table 2.1: Monotone scenario. $D = 4$. y_{d_k} generated from $N(\mu_d, 3^2)$. Based on 10000 replications. Rows 1-3: Proportion of times that unconstrained estimator is chosen using CIC_s , Wald test, and conditional test. Rows 4-5: MSE ratios.

$y_{d_k} \sim N(\mu_d, 3^2)$	$N = 10000$			$N = 20000$			$N = 40000$		
	$n = 200$	$n = 1000$	$n = 2000$	$n = 400$	$n = 2000$	$n = 4000$	$n = 800$	$n = 4000$	$n = 8000$
CIC_s	0.061	0.016	0.005	0.045	0.014	0.004	0.022	4×10^{-4}	0
Wald	0.018	0.003	0.001	0.012	0.002	0.001	0.005	10^{-4}	0
Conditional	0.020	0.004	0.001	0.013	0.003	0.001	0.005	10^{-4}	0
$\text{MSE}(\tilde{\theta}_s)/\text{MSE}(\tilde{y}_s)$	0.721	0.896	0.962	0.774	0.938	0.968	0.875	0.994	1
$\text{MSE}(\hat{\theta}_s)/\text{MSE}(\hat{y}_s)$	0.796	0.917	0.970	0.831	0.953	0.972	0.902	0.994	1

Table 2.2: Flat scenario. $D = 4$. y_{d_k} generated from $N(\mu_d, 3^2)$. Based on 10000 replications. Rows 1-3: Proportion of times that unconstrained estimator is chosen using CIC_s , Wald test, and conditional test. Rows 4-5: MSE ratios.

$y_{d_k} \sim N(\mu_d, 3^2)$	$N = 10000$			$N = 20000$			$N = 40000$		
	$n = 200$	$n = 1000$	$n = 2000$	$n = 400$	$n = 2000$	$n = 4000$	$n = 800$	$n = 4000$	$n = 8000$
CIC_s	0.098	0.045	0.121	0.102	0.081	0.079	0.073	0.134	0.015
Wald	0.033	0.011	0.044	0.036	0.026	0.024	0.023	0.048	0.003
Conditional	0.038	0.013	0.047	0.040	0.029	0.026	0.025	0.052	0.004
$\text{MSE}(\tilde{\theta}_s)/\text{MSE}(\tilde{y}_s)$	0.720	0.860	0.906	0.789	0.898	0.906	0.844	0.918	0.942
$\text{MSE}(\hat{\theta}_s)/\text{MSE}(\hat{y}_s)$	0.813	0.902	0.972	0.869	0.953	0.959	0.901	0.985	0.959

Table 2.3: Non-monotone scenario. $D = 4$. y_{d_k} generated from $N(\mu_d, 3^2)$. Based on 10000 replications. Rows 1-3: Proportion of times that unconstrained estimator is chosen using CIC_s , Wald test, and conditional test. Rows 4-5: MSE ratios.

$y_{d_k} \sim N(\mu_d, 3^2)$	$N = 10000$			$N = 20000$			$N = 40000$		
	$n = 200$	$n = 1000$	$n = 2000$	$n = 400$	$n = 2000$	$n = 4000$	$n = 800$	$n = 4000$	$n = 8000$
CIC_s	0.118	0.126	0.602	0.126	0.497	0.513	0.172	0.623	0.963
Wald	0.042	0.045	0.386	0.051	0.299	0.302	0.070	0.420	0.894
Conditional	0.048	0.049	0.403	0.056	0.310	0.315	0.073	0.434	0.899
$\text{MSE}(\tilde{\theta}_s)/\text{MSE}(\tilde{y}_s)$	0.712	0.854	1.346	0.695	1.211	1.224	0.860	1.400	2.705
$\text{MSE}(\hat{\theta}_s)/\text{MSE}(\tilde{y}_s)$	0.814	0.928	1.128	0.807	1.115	1.118	0.945	1.137	1.037

On a second set of simulations, we consider the case where the population elements are generated from a skewed distribution. For a given domain d , y_{d_k} is generated from a χ^2 distribution with μ_d degrees of freedom, for $k = 1, 2, \dots, N_d$ and $D = 4$. As in the first set of simulations, we consider the same three scenarios for μ using the $S_1(\cdot)$ sigmoid function. For each of them, we consider the case where $N = 10000$ and $n_N = 200, 1000, 2000$. Table 2.4 contains the results of this skewed case. Again, we can observe that CIC_s behaves as expected despite the skewness of the population generating distribution.

Table 2.4: Skewed case. $D = 4$. y_{d_k} generated from $\chi^2(\mu_d)$. Based on 10000 replications. Rows 1-3: Proportion of times that unconstrained estimator is chosen using CIC_s , Wald test, and conditional test. Rows 4-6: MSE ratios.

$y_{d_k} \sim \chi^2(\mu_d)$	Monotone			Flat			Non-monotone		
	$n = 200$	$n = 1000$	$n = 2000$	$n = 200$	$n = 1000$	$n = 2000$	$n = 200$	$n = 1000$	$n = 2000$
CIC_s	0.029	0.003	0	0.052	0.079	0.138	0.193	0.326	0.693
Wald	0.014	0.001	0	0.024	0.031	0.055	0.114	0.172	0.573
Conditional	0.014	0.001	0	0.025	0.033	0.057	0.117	0.177	0.579
$\text{MSE}(\tilde{\theta}_s)/\text{MSE}(\tilde{y}_s)$	0.808	0.958	1	0.806	0.853	0.886	0.817	1.034	1.890
$\text{MSE}(\hat{\theta}_s)/\text{MSE}(\tilde{y}_s)$	0.855	0.966	1	0.872	0.936	0.982	0.927	1.086	1.230

A third set of simulations considers the case where the domain mean estimators are more correlated in comparison with the stratified simple random sample simulations. The setting for this simulation set is basically equal to the first set, except that we use the auxiliary variable z

to create 100 clusters. Then, we sample r clusters with equal probability. We let $r = 2, 10, 20$. We only consider the case where $N = 10000$ and $n_N = 200, 1000, 2000$ for each of the three scenarios. Table 2.5 contains the simulation results for this correlated case. Note that CIC_s is choosing the unconstrained estimator with a low proportion under the monotone scenario, which is desired. However, the proportion of times that the unconstrained estimator is chosen under the non-monotone scenario is almost half in comparison of its corresponding stratified simple random sample simulation (see Table 2.3). The stars (*) in Table 2.5 mean that results for the Wald and the conditional tests are not available since the estimated variance-covariance matrix of the Hájek domain means is in fact a singular matrix. Recall that both tests need such matrix to be a valid covariance matrix in order to be performed. Note that on those cases with stars, CIC_s continues to be a plausible option to choose between the two estimators.

Table 2.5: Correlated case. $D = 4$. y_{d_k} generated from $N(\mu_d, 3^3)$. Based on 10000 replications. Rows 1-3: Proportion of times that unconstrained estimator is chosen using CIC_s , Wald test, and conditional test. Rows 4-6: MSE ratios.

$y_{d_k} \sim N(\mu_d, 3^2)$	Monotone			Flat			Non-monotone		
	$r = 2$	$r = 10$	$r = 20$	$r = 2$	$r = 10$	$r = 20$	$r = 2$	$r = 10$	$r = 20$
CIC_s	0.194	0.025	0.005	0.245	0.085	0.069	0.284	0.461	0.696
Wald	*	0.011	0.001	*	0.071	0.035	*	0.417	0.574
Conditional	*	0.019	0.002	*	0.072	0.037	*	0.422	0.582
$\text{MSE}(\tilde{\theta}_s)/\text{MSE}(\tilde{y}_s)$	0.717	0.901	0.958	0.690	0.838	0.842	0.694	1.263	1.911
$\text{MSE}(\dot{\theta}_s)/\text{MSE}(\tilde{y}_s)$	0.862	0.937	0.966	0.836	0.930	0.929	0.856	1.178	1.233

Table 2.5 shows that although the CIC_s performs as expected for the correlated case, the unconstrained estimator is being chosen only 69.6% of the times under the non-monotone scenario when the sample size is 20% of the total population. One plausible reason could be the fact that the monotonicity violation on this scenario is weak. Therefore, we would like to analyze the efficacy of the CIC_s as the violation of monotonicity increases. To do that, we consider again the correlated case. To increase the violation on the limiting domain means, we create μ_D from pulling

down $S_1(D)$ by a quantity $t\Delta$, where $t = 3, 4, 5$. That is, $\mu_D = S_1(D) - t\Delta$. The results of this simulation case (Table 2.6) shows that the MSE ratio between the unconstrained and the constrained estimators overpass 1 as the violation increases. Moreover, the proportion of times that the unconstrained estimator is chosen also increases and approaches to 1 as expected.

Table 2.6: Increasing Monotonicity Violation - Correlated case. $D = 4$. y_{d_k} generated from $N(\mu_d, 3^2)$. Based on 10000 replications. Rows 1-3: Proportion of times that unconstrained estimator is chosen using CIC_s , Wald test, and conditional test. Rows 4-6: MSE ratios.

$y_{d_k} \sim N(\mu_d, 3^2)$	$\mu_D = S_1(D) - 3\Delta$			$\mu_D = S_1(D) - 4\Delta$			$\mu_D = S_1(D) - 5\Delta$		
	$r = 2$	$r = 10$	$r = 20$	$r = 2$	$r = 10$	$r = 20$	$r = 2$	$r = 10$	$r = 20$
CIC_s	0.388	0.708	0.934	0.450	0.881	0.936	0.507	0.963	1
Wald	*	0.658	0.882	*	0.852	0.835	*	0.952	1
Conditional	*	0.664	0.885	*	0.854	0.890	*	0.953	1
$\text{MSE}(\tilde{\theta}_s)/\text{MSE}(\tilde{y}_s)$	0.798	1.963	3.554	0.882	2.999	3.617	1.022	4.302	9.037
$\text{MSE}(\dot{\theta}_s)/\text{MSE}(\tilde{y}_s)$	0.962	1.233	1.107	1.002	1.169	1.109	1.059	1.081	1.000

We also perform simulations to study the behavior of CIC_s when the number of domains is larger than 4. We consider the case where $D = 8$. The values of μ are obtained from the sigmoid function $S_2(d) = 4 \exp(5d/D - 2)/(1 + \exp(5d/D - 2))$. The setting in this 8-domain case is basically the same as the first simulation set, but using $S_2(\cdot)$ instead of $S_1(\cdot)$, $N = 20000$, and $n_N = 400, 2000, 40000$. We choose these values for N and n_N in order to have a similar rough average sample size in each domain as it was in simulations where $D = 4$. As shown in Table 2.7, CIC_s follows a similar behavior as in the previous simulations.

Table 2.7: 8-domain case. $D = 8$. y_{d_k} generated from $N(\mu_d, 3^2)$. Based on 10000 replications. Rows 1-3: Proportion of times that unconstrained estimator is chosen using CIC_s , Wald test, and conditional test. Rows 4-5: MSE ratios.

$y_{d_k} \sim N(\mu_d, 3^2)$	Monotone			Flat			Non-monotone		
	$n = 400$	$n = 2000$	$n = 4000$	$n = 400$	$n = 2000$	$n = 4000$	$n = 400$	$n = 2000$	$n = 4000$
CIC_s	0.054	0.042	0.003	0.075	0.127	0.060	0.084	0.287	0.631
Wald	0.021	0.010	4×10^{-4}	0.031	0.048	0.017	0.037	0.158	0.439
Conditional	0.023	0.010	4×10^{-4}	0.034	0.049	0.017	0.041	0.159	0.441
$\text{MSE}(\tilde{\theta}_s)/\text{MSE}(\tilde{y}_s)$	0.666	0.902	0.975	0.648	0.877	0.961	0.666	0.935	1.162
$\text{MSE}(\hat{\theta}_s)/\text{MSE}(\hat{y}_s)$	0.719	0.921	0.978	0.710	0.918	0.978	0.731	0.970	1.047

We end this section by showing simulation results obtained using the exact same set-up as in Wu et al. (2016). To get the μ_d values, we use the sigmoid function $S_3(d) = \exp(20d/D - 10)/(1 + \exp(20d/D - 10))$. We set the population size as $N = 1000$ and the domain size as $N_d = N/D$. We simulate the y_{d_k} values from a normal distribution with mean μ_d and standard deviation σ . As it was done before, samples are generated from a stratified sampling design with simple random sampling without replacement in each of four strata; and the stratum membership was assigned using the auxiliary random variable z .

We study four cases obtained by varying the number of domains $D = 5, 20$; and the standard deviation $\sigma = 0.5, 1$. The sample size is set to $n_N = 200$ when $D = 5$, splitted as 25, 50, 50, 75 samples in each stratum; and $n_N = 800$ when $D = 20$, splitted as 100, 200, 200, 300 samples in each stratum. For each case, we create 7 different cases for μ . These cases are determined by setting $\mu_d = S_3(d)$ for $d = 1, \dots, D - 1$; and $\mu_D = S_3(D - 1) - \delta$ for $\delta = 0, \pm 0.15, \pm 0.3, \pm 0.45$. Note that $\delta = 0$ corresponds to the flat scenario, meanwhile $\delta < 0$ define monotone scenarios and $\delta > 0$ define non-monotone scenarios.

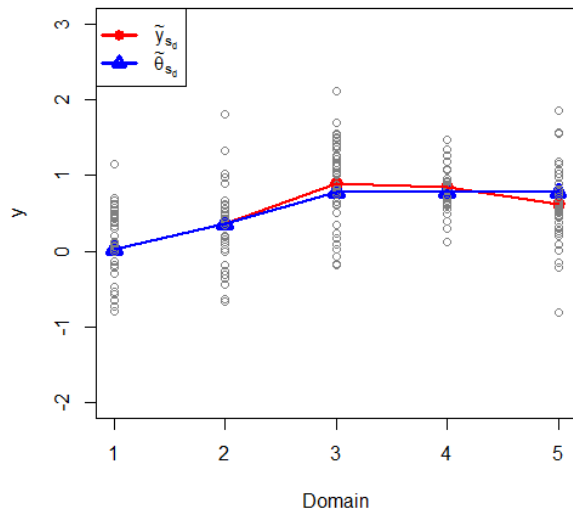
Figure 2.2 contains examples of one fitted samples for each of the four cases mentioned above. Note that the fact that the S_3 sigmoid function is considerably flat at its extremes makes especially complicated to decide whether the population domain means are isotonic or not, when $D = 20$. Tables 2.8-2.11 present the proportion of times that the unconstrained estimator is chosen in each

case, along with MSE ratios. To visualize these results better, we create Figure 2.3 which contains plots of the proportion of times that the unconstrained estimator is chosen under CIC_s and Wald test, for the set values of δ . We ignore the results obtained by the conditional test since these are shown to be practically the same as lead by the Wald test (see Tables 2.8-2.11).

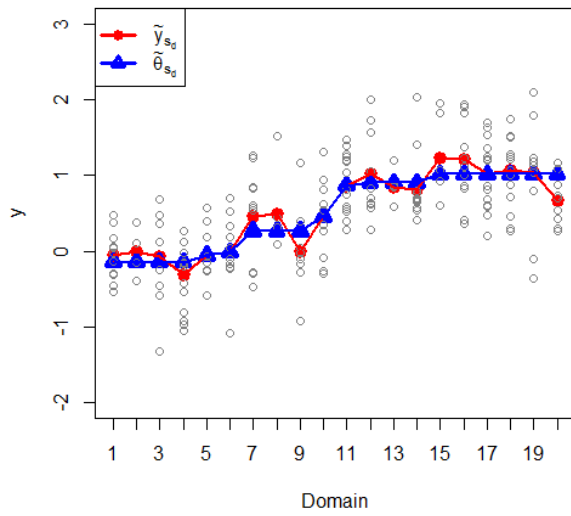
Plots in Figure 2.3 demonstrates that both CIC_s and Wald test perform better when the standard deviation is smaller. Figure 2.3a shows that CIC_s tends to choose more the unconstrained estimator than the Wald test, when $D = 5$. This fact provides evidence that the CIC_s does better than the Wald test under non-monotone scenarios. In contrast, Figure 2.3b shows an opposite behavior between CIC_s and Wald test. The worst performance for both CIC_s and Wald test is shown when $D = 20$ and $\sigma = 1$. In this case, CIC_s chooses the constrained estimator more than 80% of times, meanwhile Wald test choose it a little less than 60% of times, although is desirable to never choose it. However, it can be seen in Table 11 that the MSE ratio of the constrained estimator over the unconstrained estimator does not show neither a clear preference for the latter estimator.

Table 2.8: $S_3(\cdot)$, $D = 5$, $\sigma = 0.5$. $n_N = 200$. Based on 10000 replications. Rows 1-3: Proportion of times that unconstrained estimator is chosen using CIC_s , Wald test, and conditional test. Rows 4-5: MSE ratios.

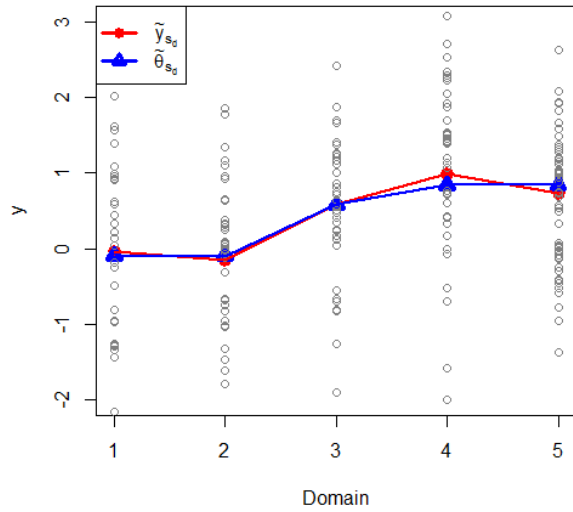
$y_{d_k} \sim N(\mu_d, 0.5^2)$	Monotone			Flat	Non-monotone		
	$\delta = -0.45$	$\delta = -0.30$	$\delta = -0.15$	$\delta = 0$	$\delta = 0.15$	$\delta = 0.30$	$\delta = 0.45$
CIC_s	0.023	0.023	0.024	0.072	0.352	0.787	0.980
Wald	0.006	0.006	0.006	0.026	0.212	0.667	0.958
Conditional	0.006	0.006	0.006	0.026	0.213	0.668	0.959
$MSE(\tilde{\theta}_s)/MSE(\tilde{y}_s)$	0.882	0.880	0.857	0.781	0.957	1.822	3.479
$MSE(\hat{\theta}_s)/MSE(\tilde{y}_s)$	0.911	0.909	0.887	0.849	1.013	1.153	1.036



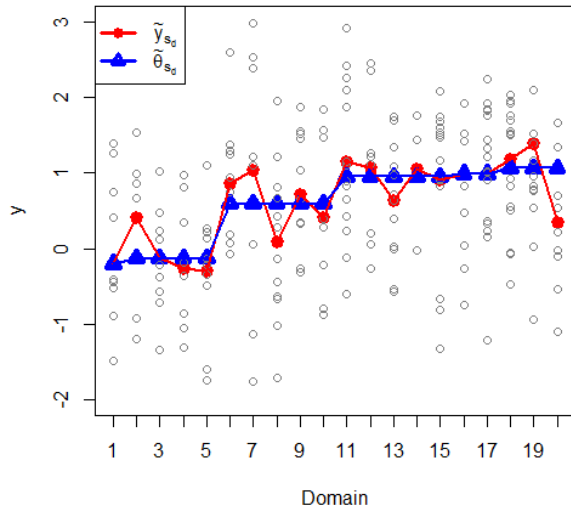
(a) $\sigma = 0.5, D = 5$.



(b) $\sigma = 0.5, D = 20$.



(c) $\sigma = 1, D = 5$.



(d) $\sigma = 1, D = 20$.

Figure 2.2: One fitted samples for each of four cases obtained using $S_3(\cdot)$. Dots correspond to unconstrained estimates, triangles to constrained estimates.

Table 2.9: $S_3(\cdot)$, $D = 5$, $\sigma = 1$. $n_N = 200$. Based on 10000 replications. Rows 1-3: Proportion of times that unconstrained estimator is chosen using CIC_s , Wald test, and conditional test. Rows 4-5: MSE ratios.

$y_{d_k} \sim N(\mu_d, 1^2)$	Monotone			Flat	Non-monotone		
	$\delta = -0.45$	$\delta = -0.30$	$\delta = -0.15$	$\delta = 0$	$\delta = 0.15$	$\delta = 0.30$	$\delta = 0.45$
CIC_s	0.065	0.065	0.070	0.099	0.181	0.358	0.600
Wald	0.021	0.021	0.021	0.036	0.095	0.236	0.473
Conditional	0.022	0.021	0.021	0.036	0.095	0.237	0.474
$MSE(\tilde{\theta}_s)/MSE(\tilde{y}_s)$	0.806	0.788	0.747	0.704	0.732	0.915	1.296
$MSE(\hat{\theta}_s)/MSE(\tilde{y}_s)$	0.875	0.858	0.826	0.807	0.861	1.012	1.145

Table 2.10: $S_3(\cdot)$, $D = 20$, $\sigma = 0.5$. $n_N = 800$. Based on 10000 replications. Rows 1-3: Proportion of times that unconstrained estimator is chosen using CIC_s , Wald test, and conditional test. Rows 4-5: MSE ratios.

$y_{d_k} \sim N(\mu_d, 0.5^2)$	Monotone			Flat	Non-monotone		
	$\delta = -0.45$	$\delta = -0.30$	$\delta = -0.15$	$\delta = 0$	$\delta = 0.15$	$\delta = 0.30$	$\delta = 0.45$
CIC_s	0.037	0.037	0.036	0.034	0.087	0.422	0.881
Wald	0.074	0.074	0.073	0.078	0.229	0.697	0.972
Conditional	0.074	0.074	0.073	0.078	0.229	0.697	0.972
$MSE(\tilde{\theta}_s)/MSE(\tilde{y}_s)$	0.503	0.503	0.495	0.468	0.556	0.905	1.533
$MSE(\hat{\theta}_s)/MSE(\tilde{y}_s)$	0.539	0.539	0.530	0.503	0.625	0.994	1.075

Table 2.11: $S_3(\cdot)$, $D = 20$, $\sigma = 1$. $n_N = 800$. Based on 10000 replications. Rows 1-3: Proportion of times that unconstrained estimator is chosen using CIC_s , Wald test, and conditional test. Rows 4-5: MSE ratios.

$y_{d_k} \sim N(\mu_d, 1^2)$	Monotone			Flat	Non-monotone		
	$\delta = -0.45$	$\delta = -0.30$	$\delta = -0.15$	$\delta = 0$	$\delta = 0.15$	$\delta = 0.30$	$\delta = 0.45$
CIC_s	0.031	0.030	0.028	0.028	0.034	0.067	0.156
Wald	0.081	0.079	0.078	0.084	0.119	0.235	0.466
Conditional	0.081	0.079	0.078	0.084	0.119	0.235	0.466
$MSE(\tilde{\theta}_s)/MSE(\tilde{y}_s)$	0.415	0.410	0.398	0.386	0.402	0.475	0.617
$MSE(\hat{\theta}_s)/MSE(\tilde{y}_s)$	0.451	0.445	0.431	0.420	0.441	0.540	0.723

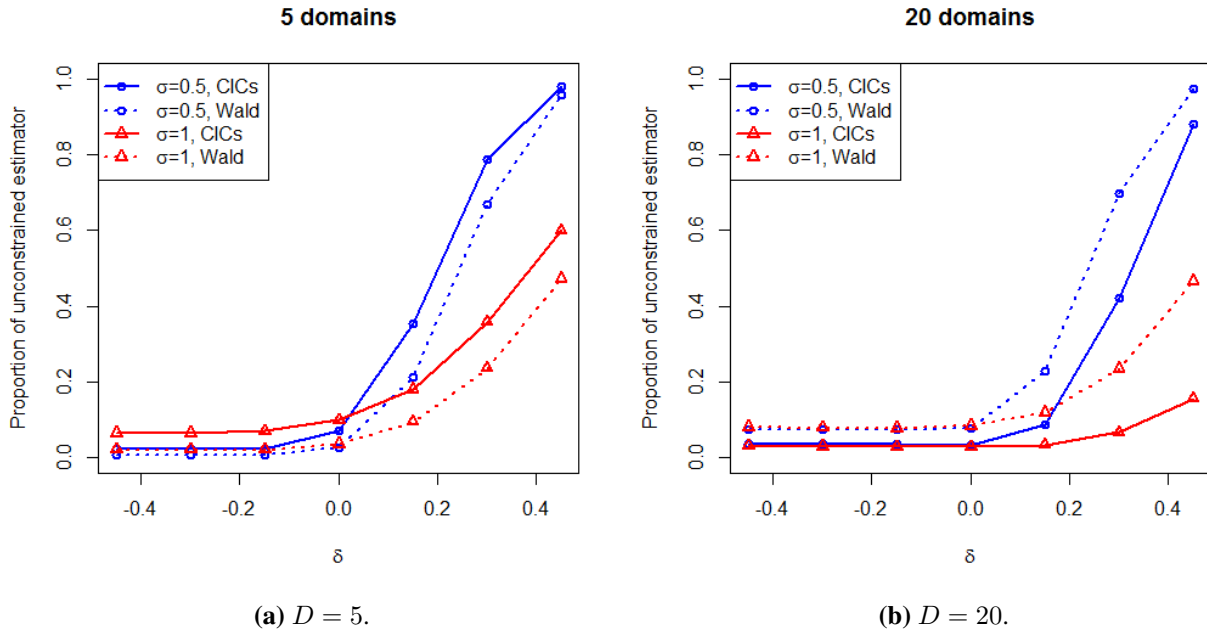


Figure 2.3: Proportion of times that the unconstrained estimator is chosen under the 4 scenarios of $S_3(\cdot)$, for several values of δ . Solid lines: CIC_s , dotted lines: Wald test. Dots: $\sigma = 0.5$, triangles: $\sigma = 1$.

2.5 Application of the CIC_s to the NHANES data

We apply the proposed CIC_s methodology to the 2011-2012 NHANES laboratory data obtained from the Center of Disease Control website. There are $n_N = 1637$ complete observations for variables age and LDL-cholesterol measures (mg/dL), where we only consider observations with age range between 21-60 years old. The LDL-cholesterol measure is the variable of interest y . Under the consideration that LDL-cholesterol measures might increase with age, we intend to use that information on the construction of domain means estimates. We create 10 domains by partitioning the age variable in 10 categories of three years each, i.e., 21-24, 25-28, ..., 57-60.

Since there is no information available regard the population domain sizes N_d , we compute both unconstrained and constrained estimators of the population domain means using the Hájek estimator. The constrained estimator in Equation 2.3 is obtained by using the PAVA. The covariance term in CIC_s for both estimators is estimated using Equation 2.5.

Figure 2.4 contains both unconstrained and constrained estimators along with their pointwise 95% Wald confidence intervals. The variance estimates to construct these intervals are based on

Equation 2.5, and the observed pooling is used to compute the estimated variance of the constrained estimator. Note that there are notable differences between them on the last three domains. Since $CIC_s(\tilde{\mathbf{y}}_s) = 23.354$ and $CIC_s(\tilde{\boldsymbol{\theta}}_s) = 18.874$, then our proposed method chooses the constrained estimator above the unconstrained as an estimate of the population domain means. Moreover, note that the confidence interval is tighter for the constrained estimator than for the unconstrained, which shows the fact that pooling domains decrease the uncertainty of the estimates.

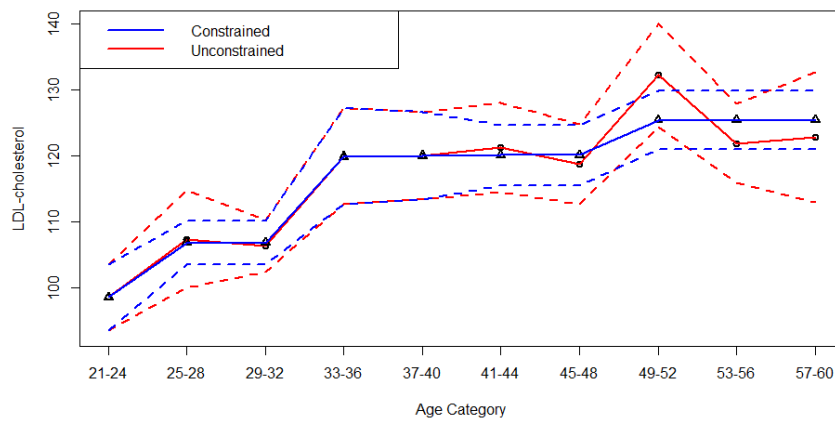


Figure 2.4: 2011-2012 NHANES laboratory data. Solid lines: constrained and unconstrained estimators. Dotted lines: pointwise 95% Wald confidence intervals. $CIC_s(\tilde{\mathbf{y}}_s) = 23.354$, $CIC_s(\tilde{\boldsymbol{\theta}}_s) = 18.874$.

Chapter 3

Estimation and inference of domain means subject to shape constraints

3.1 Introduction

Fine-scale domain estimates are frequently of interest for large-scale surveys, as these are highly useful for many data users in data-producing agencies. Although the overall sample size of such surveys might be very large, samples sizes for numerous domains are often too small for reliable estimates. For instance, the National Compensation Survey (www.bls.gov/ncs), produced by the U.S. Bureau of Labor Statistics, is designed to provide wage and salary estimates by occupation for many metropolitan areas and for the nation. However, for certain cities or regions, the sample sizes might not be large enough to produce estimates with acceptable precision.

Domain estimators that are based only on the domain-specific sample data (*direct estimators*) tend to lack adequate precision for small domains (Rao, 2003). One possible approach to avoid such a problem could be to aggregate small domains into bigger scales so that more reliable direct estimators can be produced for those scales, leading to the generation of more aggregated information than the actual desired scale. An alternative to producing small domain estimates could be changing from a design-based to a model-based estimation methodology such as small area models. In this paper, we present an approach where domains are allowed to borrow information from their neighbors by imposing shape or order assumptions that are reasonable for the population.

Information regarding the *shape* of population domain means arises naturally in surveys. For instance, certain jobs might be expected to receive better salaries than others, or younger people are expected to have, on average, lower glucose level than older people. However, given that small domains tend to produce direct estimates with high variability, such shape constraints are often violated at the sample level. Recently, Wu et al. (2016) proposed a domain mean estimation

methodology that relies on the assumption of monotone population domain means. By combining the monotonicity information of domain means and design-based estimators in the estimation stage, they proposed a *constrained* estimator that respects the monotone assumption. Such an estimator was shown to improve precision and variability of domain mean estimates in comparison with direct estimators, given that the assumption of monotonicity is reasonable.

Many other types of shape constraints beyond monotonicity may also be expected to hold in estimates of population domain means. In general, any set of constraints can be represented through a *constraint matrix*, where each of its rows defines a constraint. Meyer (1999) introduced the concept of *irreducible* matrices to cover the possible case of having more constraints than dimensions. Intuitively, a constraint matrix is called irreducible when it does not contain redundant restrictions. For illustration of a constraint matrix, suppose the variable of interest is the annual average salary of faculty in certain university. Further, consider the 6 domains generated from the cross-classification of the variables job position (x_1 ; 1=Assistant and 2=Associate) and department (x_2 ; 1=Anthropology, 2=English and 3=Engineering). Under the assumptions that, within a discipline, professors with an associate rank have higher salaries than those with an assistant rank; and that, within a rank, Engineering faculty members are expected to have higher salaries than those in either the Anthropology or English departments, then we can express the corresponding restrictions as,

$$\mathbf{A}\boldsymbol{\mu} \geq \mathbf{0}, \quad \text{where } \mathbf{A} = \begin{pmatrix} -1 & 1 & 0 & 0 & 0 & 0 \\ 0 & 0 & -1 & 1 & 0 & 0 \\ 0 & 0 & 0 & 0 & -1 & 1 \\ -1 & 0 & 0 & 0 & 1 & 0 \\ 0 & 0 & -1 & 0 & 1 & 0 \\ 0 & -1 & 0 & 0 & 0 & 1 \\ 0 & 0 & 0 & -1 & 0 & 1 \end{pmatrix}, \quad (3.1)$$

$\boldsymbol{\mu} = (\mu_{11}, \mu_{21}, \mu_{12}, \mu_{22}, \mu_{13}, \mu_{23})^\top$, with μ_{ij} representing the mean of the domain that corresponds to $x_1 = i$ and $x_2 = j$; $\mathbf{0}$ being the zero vector, and the inequality being element-wise. In this example, the constraint matrix \mathbf{A} is irreducible.

This paper contains theoretical properties and applications of a new constrained estimator for population domain means that respect shape constraints that are expressed with irreducible matrices. Through combining design-based domain mean estimators with these shape constraints, we propose a broadly applicable estimator that improves precision and variability of the most common direct estimators. Moreover, we provide a design-based variance estimation method that depends on the sample-determined linear space where the constrained estimator lands. If the constraints correspond to partial orderings, as in Equation 3.1, then the proposed estimator is simply a design-based estimator computed after adaptively pooling domains to respect the imposed restrictions, and the variance estimator depends on the pooling chosen by the constrained estimator. As monotone constraints can be written as one particular case from the broad class of shapes covered by irreducible matrices, our proposed estimator is an extension of the monotone estimator developed by Wu et al. (2016). Constrained estimators that respect constraints driven by irreducible matrices have been already proposed for non-survey data. For instance, Meyer (2013a) made use of them to perform convex regression or isotonic regression on partial orderings. However, this general class of shape constraints have not been considered yet for survey data.

This paper is organized as follows: in Section 3.2 we introduce the constrained estimator and propose a linearization-based method for variance estimation. This section also contains some scenarios of interest where shape constraints can naturally arise for survey data. Section 3.3 states the main theoretical properties of the constrained estimator that guarantee its use for estimation and inference of population domain means. The necessary assumptions used in these theoretical derivations are also stated in this section. Proofs of main theorems and auxiliary lemmas are fully contained in the Appendix. Section 3.4 shows through simulations that the constrained estimator improves domain mean estimation and variability in comparison with the unconstrained estimator, even though the assumed shape holds only approximately at the population level. Section 3.5

demonstrates the advantages of the proposed methodology on real survey data through an application to the 2015 National Survey of College Graduates. The proofs of the theoretical results shown in this paper are included in Appendix B.

3.2 Constrained estimator for domain means

3.2.1 Notation and preliminaries

Let U_N be the set of elements in a population of size N . Consider a sample s_N of size n_N that is drawn from U_N using a probability sampling design $p_N(\cdot)$. Denote $\pi_{k,N} = \Pr(k \in s_N)$ and $\pi_{kl,N} = \Pr(k \in s_N, l \in s_N)$ as the first and second order inclusion probabilities, respectively. Assume that $\pi_{k,N} > 0, \pi_{kl,N} > 0$ for $k, l \in U_N$. Denote $\{U_{d,N}\}_{d=1}^D$ as a domain partition of U_N , where D is the fixed number of domains and each $U_{d,N}$ is of size N_d . Also, let $s_{d,N}$ be the subset of size $n_{d,N}$ of s_N that belongs to $U_{d,N}$.

For any study variable y , denote $\bar{\mathbf{y}}_{U_N} = (\bar{y}_{U_{1,N}}, \dots, \bar{y}_{U_{D,N}})^\top$ to be the vector of population domain means, where

$$\bar{y}_{U_{d,N}} = \frac{\sum_{k \in U_{d,N}} y_k}{N_d}. \quad (3.2)$$

In addition, consider the Horvitz-Thompson (HT) and Hájek estimators of $\bar{y}_{U_{d,N}}$, respectively given by

$$\hat{y}_{s_{d,N}} = \frac{\sum_{k \in s_{d,N}} y_k / \pi_k}{N_d}, \quad \tilde{y}_{s_{d,N}} = \frac{\sum_{k \in s_{d,N}} y_k / \pi_k}{\hat{N}_d}; \quad (3.3)$$

where $\hat{N}_d = \sum_{k \in s_{d,N}} 1 / \pi_k$. Denote $\hat{\mathbf{y}}_{s_N}$ and $\tilde{\mathbf{y}}_{s_N}$ to be the vectors of HT and Hájek estimators, respectively. Taking into consideration that the Hájek estimator is more useful in practice since it does not require information about the population domain sizes N_d , then we exclusively focus this paper on properties based on it. However, all developed results can be adapted to the HT estimator by replacing \hat{N}_d with N_d . For simplicity in our notation, we will avoid using the subscript N for the rest of this paper unless needed for clarification.

3.2.2 Proposed estimator

Assume there is information available regarding the shape of the population domain means that can be expressed with m constraints through a $m \times D$ irreducible constraint matrix \mathbf{A} . A matrix \mathbf{A} is irreducible if none of its rows is a positive linear combination of other rows, and if the origin is also not a positive linear combination of its rows (Meyer, 1999). To take advantage of $\tilde{\mathbf{y}}_s$ to obtain an estimator that respects these shape constraints, we propose the constrained estimator $\tilde{\boldsymbol{\theta}}_s = (\tilde{\theta}_{s_1}, \dots, \tilde{\theta}_{s_D})^\top$ to be the unique vector that solves the following constrained weighted least squares problem,

$$\min_{\boldsymbol{\theta}} (\tilde{\mathbf{y}}_s - \boldsymbol{\theta})^\top \mathbf{W}_s (\tilde{\mathbf{y}}_s - \boldsymbol{\theta}) \quad \text{subject to} \quad \mathbf{A}\boldsymbol{\theta} \geq \mathbf{0}; \quad (3.4)$$

where \mathbf{W}_s is the diagonal matrix with elements $\hat{N}_1/\hat{N}, \hat{N}_2/\hat{N}, \dots, \hat{N}_D/\hat{N}$, and $\hat{N} = \sum_{d=1}^D \hat{N}_d$. The constrained problem in Equation 3.4 can be alternatively written as finding the unique vector $\tilde{\boldsymbol{\phi}}_s$ that solves

$$\min_{\boldsymbol{\phi}} \|\tilde{\mathbf{z}}_s - \boldsymbol{\phi}\|^2 \quad \text{subject to} \quad \mathbf{A}_s \boldsymbol{\phi} \geq \mathbf{0}; \quad (3.5)$$

where $\tilde{\mathbf{z}}_s = \mathbf{W}_s^{1/2} \tilde{\mathbf{y}}_s$, $\boldsymbol{\phi} = \mathbf{W}_s^{1/2} \boldsymbol{\theta}$, and $\mathbf{A}_s = \mathbf{A} \mathbf{W}_s^{-1/2}$. Note that solving the optimization problem in Equation 3.5 allows straightforward computation of the constrained estimator $\tilde{\boldsymbol{\theta}}_s$. Moreover, observe that the transformed constrained matrix \mathbf{A}_s is also irreducible if \mathbf{A} is, and that it depends on the sample although \mathbf{A} does not.

From a geometrical viewpoint, $\tilde{\boldsymbol{\phi}}_s$ can be seen as the projection of the vector $\tilde{\mathbf{z}}_s$ onto the constraint cone Ω_s defined by the irreducible matrix \mathbf{A}_s as

$$\Omega_s = \{\boldsymbol{\phi} \in \mathbb{R}^D : \mathbf{A}_s \boldsymbol{\phi} \geq \mathbf{0}\}. \quad (3.6)$$

That is, $\tilde{\boldsymbol{\phi}}_s = \Pi(\tilde{\mathbf{z}}_s | \Omega_s)$, where $\Pi(\mathbf{u} | V)$ stands for the projection of \mathbf{u} onto the space V . Further, the polar cone Ω_s^0 (Rockafellar, 1970, p. 121), which is the dual vector space of Ω_s , is defined as

$$\Omega_s^0 = \{\boldsymbol{\rho} \in \mathbb{R}^D : \langle \boldsymbol{\rho}, \boldsymbol{\phi} \rangle \leq 0, \quad \forall \boldsymbol{\phi} \in \Omega_s\}, \quad (3.7)$$

where $\langle \mathbf{u}, \mathbf{v} \rangle = \mathbf{u}^\top \mathbf{v}$. Such a definition characterizes the polar cone as the set of vectors that form obtuse angles with all vectors in Ω_s . Meyer (1999) showed that the negative rows of an irreducible matrix are the *edges* (generators) of the polar cone, leading to the following characterization of the polar cone in Equation 3.7:

$$\Omega_s^0 = \left\{ \boldsymbol{\rho} \in \mathbb{R}^D : \boldsymbol{\rho} = \sum_{j=1}^m a_j \boldsymbol{\gamma}_{s_j}, \quad a_j \geq 0, \quad j = 1, 2, \dots, m \right\}, \quad (3.8)$$

where $\boldsymbol{\gamma}_{s_1}, \boldsymbol{\gamma}_{s_2}, \dots, \boldsymbol{\gamma}_{s_m}$ are the rows of $-\mathbf{A}_s$. Equation 3.8 shows that Ω_s^0 is a finitely generated cone, which implies that it is a *polyhedral* cone. Robertson et al. (1988, p. 17) established necessary and sufficient conditions for a vector $\tilde{\boldsymbol{\phi}}_s$ to be the projection of $\tilde{\mathbf{z}}_s$ onto Ω_s . That is, $\tilde{\boldsymbol{\phi}}_s \in \Omega_s$ solves the constrained problem in Equation 3.5 if and only if

$$\langle \tilde{\mathbf{z}}_s - \tilde{\boldsymbol{\phi}}_s, \tilde{\boldsymbol{\phi}}_s \rangle = 0, \quad \text{and} \quad \langle \tilde{\mathbf{z}}_s - \tilde{\boldsymbol{\phi}}_s, \boldsymbol{\phi} \rangle \leq 0, \quad \forall \boldsymbol{\phi} \in \Omega_s.$$

Moreover, the above conditions can be adapted to the polar cone as follows: the vector $\tilde{\boldsymbol{\rho}}_s \in \Omega_s^0$ minimizes $\|\tilde{\mathbf{z}}_s - \boldsymbol{\rho}\|^2$ over Ω_s^0 if and only if

$$\langle \tilde{\mathbf{z}}_s - \tilde{\boldsymbol{\rho}}_s, \tilde{\boldsymbol{\rho}}_s \rangle = 0, \quad \text{and} \quad \langle \tilde{\mathbf{z}}_s - \tilde{\boldsymbol{\rho}}_s, \boldsymbol{\gamma}_{s_j} \rangle \leq 0 \quad \text{for } j = 1, 2, \dots, m. \quad (3.9)$$

Although the constrained problem in Equation 3.5 does not have a general closed form solution, there are some particular cases where this can be explicitly characterized. For instance, Robertson et al. (1988, p. 23) demonstrated that, under partial ordering constraints, the solution $\tilde{\boldsymbol{\theta}}_s$ of the constrained problem in Equation 3.4 takes the form

$$\tilde{\theta}_{s_d} = \max_{U: d \in U} \min_{L: d \in L} \frac{\sum_{d \in L \cap U} \hat{N}_d \tilde{y}_{s_d}}{\sum_{d \in L \cap U} \hat{N}_d}, \quad \text{for } d = 1, \dots, D; \quad (3.10)$$

where L and U are lower and upper sets with respect to the partial ordering, respectively. Equation 3.10 shows that the proposed constrained estimator is simply pooling neighboring domains in such

a way that the imposed constraints are respected. Heuristically, this is an advantageous property for small domains, as it allows them to borrow strength from other domains.

One approach to computing $\tilde{\phi}_s$ is based on the edges of the constraint cone Ω_s . However, the number of edges can be considerably larger than the number of constraints for large values of D , especially for the case when there are more constraints than domains (see Meyer, 1999). Moreover, given the lack of a general closed form solution for the edges of Ω_s (when $m > D$), then the edges need to be computed numerically. This task can be a computationally demanding job, which makes this approach an inefficient way to compute $\tilde{\phi}_s$. Fortunately, a more efficient algorithm based on computing the projection onto the polar cone has been developed: the Cone Projection Algorithm (CPA) (Meyer, 2013b). This alternative approach takes advantage of the easy-to-find edges γ_{s_j} of the polar cone, the conditions in Equation 3.9, and the fact that $\Pi(\tilde{z}_s|\Omega_s) = \tilde{z}_s - \Pi(\tilde{z}_s|\Omega_s^0)$. We remark that the latter fact is a key component on the proofs of the main theoretical results shown in this paper. CPA has been implemented in the software R into the `coneproject` package. See Liao and Meyer (2014) for further details.

3.2.3 Variance estimation of $\tilde{\theta}_{s_d}$

The conditions in Equation 3.9 can be used to show that the projection of \tilde{z}_s onto the polar cone Ω_s^0 coincides with the projection onto the linear space generated by the edges γ_{s_j} such that $\langle \tilde{z}_s - \tilde{\rho}_s, \gamma_{s_j} \rangle = 0$. This set of edges could be empty, meaning that the projection onto Ω_s^0 is equal to the projection onto the zero vector. Moreover, this set of edges might not be unique. To formalize this idea, denote $V_{s,J} = \{\gamma_{s_j} : j \in J\}$ for any $J \subseteq \{1, 2, \dots, m\}$. Define the set $\overline{\mathcal{F}}_{s,J}$ as,

$$\overline{\mathcal{F}}_{s,J} = \{\boldsymbol{\rho} \in \mathbb{R}^D : \boldsymbol{\rho} = \sum_{j \in J} a_j \gamma_{s_j}, \quad a_j \geq 0, \quad j \in J\}, \quad (3.11)$$

where $\overline{\mathcal{F}}_{s,\emptyset} = \mathbf{0}$ by convention. That is, $\overline{\mathcal{F}}_{s,J}$ is the polyhedral sub-cone of Ω_s^0 that starts at the origin and is defined by the edges in $V_{s,J}$. Further, let $\mathcal{L}(V_{s,J})$ be the linear space generated by the vectors in $V_{s,J}$. Hence, projecting onto Ω_s^0 is equivalent to projecting onto $\mathcal{L}(V_{s,J})$, for an appropriate set J .

Estimating appropriately the variance of $\tilde{\theta}_{s_d}$ is a complicated task, derived from the fact that the projection of $\tilde{\mathbf{z}}_s$ onto Ω_s^0 (or onto Ω_s) might not always land on the same linear space $\mathcal{L}(V_{s,J})$ for different samples s . To better understand that, define $\tilde{\mathcal{G}}_s$ to the set of all subsets $J \subseteq \{1, 2, \dots, m\}$ such that $\Pi(\tilde{\mathbf{z}}_s | \Omega_s^0) = \Pi(\tilde{\mathbf{z}}_s | \mathcal{L}(V_{s,J})) \in \overline{\mathcal{F}}_{s,J}$. The latter definition is motivated by the following non-efficient procedure to find $\tilde{\boldsymbol{\rho}}_s$: project $\tilde{\mathbf{z}}_s$ onto each of the 2^m linear spaces generated by the edges in $V_{s,J}$, and then check if such a projection lands inside the portion of the polar cone Ω_s^0 defined by $V_{s,J}$ (that is, $\overline{\mathcal{F}}_{s,J}$) and that satisfies the conditions stated in Equation 3.9. Note that, for different samples s , the sets $\tilde{\mathcal{G}}_s$ might be different. In addition, the cardinality of $\tilde{\mathcal{G}}_s$ can be greater than one. That is, there could be different sets J_1 and J_2 such that the projection onto the polar cone Ω_s^0 is equal to projecting onto either $\mathcal{L}(V_{s,J_1})$ or $\mathcal{L}(V_{s,J_2})$. However, independently of which set is chosen, the projection $\tilde{\boldsymbol{\rho}}_s$ is unique. For instance, consider the case where $m > D$, so the set of all edges γ_{s_j} constitutes a linear dependent set of vectors. Hence, there could exist different subsets J_1, J_2 that induce the same linear space such that $J_1, J_2 \in \tilde{\mathcal{G}}_s$. A different example where the cardinality of $\tilde{\mathcal{G}}_s$ is greater than 1 is based on the drawn sample. For illustration, consider monotone increasing restrictions with $D = 3$. Suppose that $\tilde{y}_{s_1} = \tilde{y}_{s_2} < \tilde{y}_{s_3}$. As there are only 3 domains, the transformed vector $\tilde{\mathbf{z}}_s$ has elements of the form

$$\tilde{z}_{s_1} = \sqrt{\frac{\hat{N}_1}{\hat{N}}} \tilde{y}_{s_1}, \quad \tilde{z}_{s_2} = \sqrt{\frac{\hat{N}_2}{\hat{N}}} \tilde{y}_{s_2}, \quad \tilde{z}_{s_3} = \sqrt{\frac{\hat{N}_3}{\hat{N}}} \tilde{y}_{s_3}.$$

In this setting, it is straightforward to see that $\Pi(\tilde{\mathbf{z}}_s | \Omega_s^0) = \mathbf{0}$. However, to compute it, we project $\tilde{\mathbf{z}}_s$ onto each of the $2^2 = 4$ linear spaces generated by the polar cone edges

$$\gamma_{s_1} = \left(\sqrt{\frac{\hat{N}}{\hat{N}_1}}, -\sqrt{\frac{\hat{N}}{\hat{N}_2}}, 0 \right)^\top, \quad \gamma_{s_2} = \left(0, \sqrt{\frac{\hat{N}}{\hat{N}_2}}, -\sqrt{\frac{\hat{N}}{\hat{N}_3}} \right)^\top.$$

Hence, it can be seen that the conditions $\Pi(\tilde{\mathbf{z}}_s | \Omega_s^0) = \mathbf{0} = \Pi(\tilde{\mathbf{z}}_s | \mathcal{L}(V_{s,J})) \in \overline{\mathcal{F}}_{s,J}$ are satisfied only for $J = \emptyset$ and $J = \{1\}$, which implies that $\tilde{\mathcal{G}}_s = \{\emptyset, \{1\}\}$. Moreover, note that $V_{s,\emptyset}$ and $V_{s,\{1\}}$ do not span the same linear spaces, which is what complicates the variance estimation of $\tilde{\theta}_{s_d}$. In

general, the set of sample vectors where these scenarios occur has measure zero. However, they cannot be excluded at the population level.

We propose a variance estimator for $\tilde{\theta}_{s_d}$ that relies on the sets in $\tilde{\mathcal{G}}_s$ and is based on linearization methods. Consider any $J \in \tilde{\mathcal{G}}_s$, and let $\mathbf{P}_{s,J}$ be the projection matrix corresponding to the linear space $\mathcal{L}(V_{s,J})$, where $\mathbf{P}_{s,\emptyset}$ is the matrix of zeros by convention. By the selection of J , then $\tilde{\rho}_s$ can be expressed as $\mathbf{P}_{s,J}\tilde{\mathbf{z}}_s$, which implies that $\tilde{\theta}_s$ can be written as $\tilde{\theta}_{s,J} = \tilde{\mathbf{y}}_s - \mathbf{W}_s^{-1/2}\mathbf{P}_{s,J}\mathbf{W}_s^{1/2}\tilde{\mathbf{y}}_s$, where we add the subscript J in $\tilde{\theta}_s$ to be aware that the expression depends on the chosen J .

Now, observe that $\tilde{\theta}_{s,J}$ is a smooth non-linear function of the \hat{t}_d 's and the \hat{N}_d 's, where \hat{t}_d is the HT estimator of $t_d = \sum_{k \in U_d} y_k$. Therefore, treating J as fixed, we can approximate the variance of $\tilde{\theta}_{s_d,J}$ via Taylor linearization (Särndal et al., 1992, p. 175) by

$$AV(\tilde{\theta}_{s_d,J}) = \sum_{k \in U} \sum_{l \in U} \Delta_{kl} \frac{u_k}{\pi_k} \frac{u_l}{\pi_l}, \quad (3.12)$$

where $\Delta_{kl} = \pi_{kl} - \pi_k \pi_l$, and

$$u_k = \sum_{i=1}^D \alpha_i y_k 1_{k \in U_i} + \sum_{i=1}^D \beta_i 1_{k \in U_i} \quad \text{for } k = 1, 2, \dots, N,$$

with 1_A being the indicator variable for the event A , and

$$\alpha_i = \left. \frac{\partial \tilde{\theta}_{s_d,J}}{\partial \hat{t}_i} \right|_{(\hat{t}_1, \dots, \hat{t}_D, \hat{N}_1, \dots, \hat{N}_D) = (t_1, \dots, t_D, N_1, \dots, N_D)}; \quad \beta_i = \left. \frac{\partial \tilde{\theta}_{s_d,J}}{\partial \hat{N}_i} \right|_{(\hat{t}_1, \dots, \hat{t}_D, \hat{N}_1, \dots, \hat{N}_D) = (t_1, \dots, t_D, N_1, \dots, N_D)}.$$

In addition, a consistent estimator of the approximated variance in Equation 3.12, is given by

$$\hat{V}(\tilde{\theta}_{s_d,J}) = \sum_{k \in s} \sum_{l \in s} \frac{\Delta_{kl}}{\pi_{kl}} \frac{\hat{u}_k}{\pi_k} \frac{\hat{u}_l}{\pi_l}, \quad (3.13)$$

where

$$\hat{u}_k = \sum_{i=1}^D \hat{\alpha}_i y_k 1_{k \in s_i} + \sum_{i=1}^D \hat{\beta}_i 1_{k \in s_i} \quad \text{for } k = 1, 2, \dots, N,$$

with $\widehat{\alpha}_i, \widehat{\beta}_i$ obtained from α_i, β_i by substituting the appropriate Horvitz-Thompson estimators for each total population. Thus, we propose the estimator in Equation 3.13 as a variance estimator of $\tilde{\theta}_{s_d}$.

3.2.4 Some shape constraints of interest

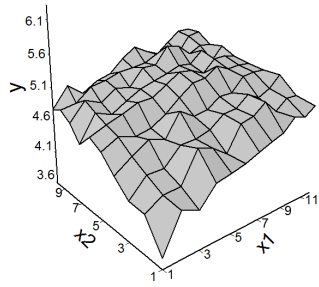
As it was mentioned before, irreducible matrices can be used to express a broad range of shape constraints. We include some scenarios of interest with the sole purpose of highlighting the potential utility of our proposed estimator. Several other restrictions can be also considered by our constrained methodology as long as they conform to an irreducible matrix.

- **Double monotone:** domain means are expected to be monotone with respect to two covariates. For instance, average glucose level may increase with people's age, and decrease with mean weekly exercising time.
- **Tree-ordering:** there is one domain mean that is expected to be smaller (or larger) than the others. For example, a placebo effect could be expected to be smaller than treatment effects.
- **Relaxed monotone:** assuming monotonicity on domain means is a strong restriction which could be relaxed so that better estimates can be potentially obtained. As an example, assume it is known from past records that wage salary jobs have certain increasing trend based on job category, but researchers feel uncomfortable by imposing such a strict order. However, if changes are not too severe, then a relaxed monotone ordering can provide more efficient estimates. One way to relax a monotone order could be through the use of weights. Consider $2D - 1$ weights $\omega_t, t = -(D - 1), \dots, D - 1$, such that $0 \leq \omega_{-(D-1)} \leq \dots \leq \omega_{-1} \leq \omega_0$ and $\omega_0 \geq \omega_1 \geq \dots \geq \omega_{D-1} \geq 0$. For $1 \leq i \leq D - 1$, assume the following constraints:

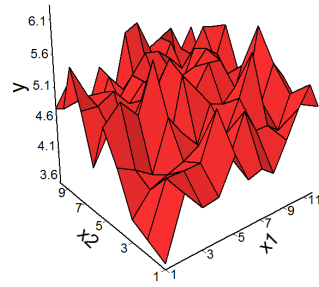
$$\frac{\sum_{d=1}^D \omega_{d-i} \theta_d}{\sum_{d=1}^D \omega_{d-i}} \leq \frac{\sum_{d=1}^D \omega_{d-(i+1)} \theta_d}{\sum_{d=1}^D \omega_{d-(i+1)}}. \quad (3.14)$$

Two estimators of interest arise from the constraints in Equation 3.14: the monotone estimator developed by Wu et al. (2016) is obtained when all weights but ω_0 are equal to zero (i.e. $\theta_1 \leq \dots \leq \theta_D$), meanwhile the unconstrained estimator appears in the particular case when all weights are equal. As these two extreme cases are covered by the relaxed monotone constraints, it is of interest to be able to control the amount of relaxation imposed. This could be done by defining a kernel function $K(\cdot)$ such that $K(0) = 1$, and that decreases away from zero. Now, for any bandwidth $h > 0$, define $\omega_t = K(\frac{t}{h})$. Hence, the constrained estimator is obtained as $h \rightarrow 0$, meanwhile the unconstrained estimator arises as $h \rightarrow \infty$, which implies that h is a tuning parameter that controls the amount of monotone relaxation.

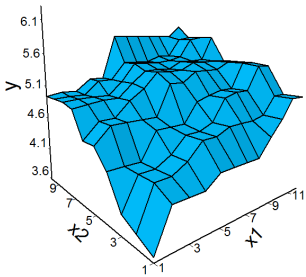
In general, combinations of the above shape scenarios could also be considered. For instance, Figure 3.1 contains four different estimates of the population domains means in Figure 3.1(a): unconstrained estimates are shown in Figure 3.1(b), and three constrained estimates obtained from different shape restrictions on variables x_1 and x_2 are shown in Figure 3.1(c)-(e). Note that unconstrained estimates are wiggly and do not look closer to the population domain means, meanwhile constrained estimates seem to be a more reasonable choice. Further, the relaxed monotone assumption on x_1 appears to be an appropriate option to consider given the non-strict monotonicity on the population domain means.



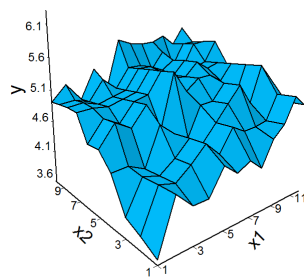
(a) Population domain means.



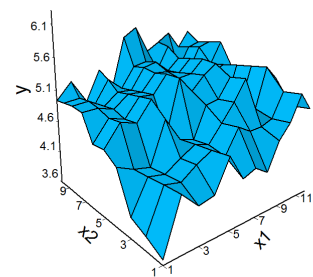
(b) Unconstrained.



(c) x_1 : monotone, x_2 : monotone.



(d) x_1 : relaxed, x_2 : monotone.



(e) x_1 : unconstrained, x_2 : monotone.

Figure 3.1: Population domain means and unconstrained estimator (top). Constrained estimator under three different settings of shape constraints (bottom).

3.3 Properties of the constrained estimator

3.3.1 Assumptions

To derive our theoretical results, we make assumptions on the asymptotic behavior of the population U_N and the sampling design p_N . Such assumptions are:

A1. The number of domains D is fixed.

A2. $\limsup_{N \rightarrow \infty} N^{-1} \sum_{k \in U} y_k^4 < \infty$.

A3. There exist constants μ_d and $r_d > 0$ such that $\bar{y}_{U_d, N} - \mu_d = O(N^{-1/2})$ and $N_{d, N}/N - r_d = O(N^{-1/2})$, for all d .

A4. The sample size n_N is non-random and satisfies $0 < \lim_{N \rightarrow \infty} n_N/N < 1$. In addition, there exists ϵ , $0 < \epsilon < 1$, such that $n_{d, N} \geq \epsilon n_N/D$ for all d and all N .

A5. For all N , $\min_{k \in U_N} \pi_k \geq \lambda > 0$, $\min_{k, l \in U_N} \pi_{kl} \geq \lambda^* > 0$, and

$$\limsup_{N \rightarrow \infty} n_N \max_{k, l \in U_N: k \neq l} |\Delta_{kl}| < \infty$$

where $\Delta_{kl} = \pi_{kl} - \pi_k \pi_l$.

A6. For any vector of q variables \mathbf{x} with finite fourth population moment,

$$\text{var}_{p_N}(\hat{\mathbf{x}}_{s_N})^{-1/2}(\hat{\mathbf{x}}_{s_N} - \bar{\mathbf{x}}_{U_N}) \xrightarrow{d} \mathcal{N}(\mathbf{0}, \mathbf{I}_q),$$

and

$$\widehat{\text{var}}(\hat{\mathbf{x}}_{s_N}) - \text{var}_{p_N}(\hat{\mathbf{x}}_{s_N}) = o_p(n_N^{-1});$$

where $\hat{\mathbf{x}}_{s_N}$ is the HT estimator of $\bar{\mathbf{x}}_{U_N} = N^{-1} \sum_{k \in U_N} \mathbf{x}_k/\pi_k$, \mathbf{I}_q is the identity matrix of dimension q , the design variance-covariance matrix $\text{var}_{p_N}(\hat{\mathbf{x}}_{s_N})$ is positive definite, and $\widehat{\text{var}}(\hat{\mathbf{x}}_{s_N})$ is the HT estimator of $\text{var}(\hat{\mathbf{x}}_{s_N})$.

Assumption A1 establishes that the number of domains remains constant as the population size changes. The condition in Assumption A2 is made to have the property that the difference between design variances and their estimates are on the order of $o_p(n_N^{-1})$. In particular, note that this condition is satisfied when the variable y is bounded, which can be naturally assumed for most types of survey data. Assumption A3 guarantees that the population domain means and sizes converge to the limiting values μ_d and r_d , respectively. Alternatively, the μ values can be thought as superpopulation parameters that generate the population elements y_k . In fact, our theoretical results depend on whether the assumed constraints hold for these superpopulation parameters and not for the population domain means. Although this might seem to be inappropriate given our interest on using constraints at the population level, Assumption A3 ensures that the shape of the domain means would be reasonable close to the shape of the superpopulation means. Assumption A4 states that the sample size in each domain cannot be smaller than a fraction of the ratio n_N/D , which would be obtained by dividing equally the sample size over all domains. This assumption aims to ensure that the moments of smooth functions of the $N^{-1}\widehat{t}_d$ and the $N^{-1}\widehat{N}_d$ are bounded. Also, it assumes that the sample size is non-random. However, this can be adapted to a random sample size by imposing certain conditions on the expected sample size $\mathbb{E}_{p_N}(n_N)$. Assumption A5 establishes non-zero lower bounds for both first and second order inclusion probabilities, and states that the design covariances Δ_{kl} must converge to zero at least as fast as n_N^{-1} . Assumption A6 ensures asymptotic normality for a general finite fourth moment vector of variables \boldsymbol{x} , which is needed to maintain normality properties on non-linear estimators. Moreover, it establishes consistency conditions on the variance-covariance estimator.

3.3.2 Main results

Based on the property that $\Pi(\tilde{\boldsymbol{z}}_s|\Omega_s) = \tilde{\boldsymbol{z}}_s - \Pi(\tilde{\boldsymbol{z}}_s|\Omega_s^0) = \tilde{\boldsymbol{z}}_s - \tilde{\boldsymbol{\rho}}_s$, we derive some theoretical properties of the constrained estimator by focusing on the projection onto Ω_s^0 instead of Ω_s . Recall that the edges of the polar cone Ω_s^0 are simply the m rows of $-\boldsymbol{A}_s$, denoted by $\boldsymbol{\gamma}_{s_j}$; and that $\tilde{\boldsymbol{\rho}}_s$ can be described by the sets $J \in \tilde{\mathcal{G}}_s$. Being able to characterize the property that $J \in \tilde{\mathcal{G}}_s$ in

terms of the vectors in $V_{s,J}$ allow us to obtain theoretical convergence rates, which are used to develop inference properties of the constrained estimator. When the set $J \in \tilde{\mathcal{G}}_s$ produces a set of linear independent vectors $V_{s,J}$, then it is straightforward that $\tilde{\boldsymbol{\rho}}_s$ can be written as $\mathbf{P}_{s,J}\tilde{\mathbf{z}}_s = \mathbf{A}_{s,J}^\top(\mathbf{A}_{s,J}\mathbf{A}_{s,J}^\top)^{-1}\mathbf{A}_{s,J}\tilde{\mathbf{z}}_s$, where $\mathbf{A}_{s,J}$ denotes the matrix formed by the rows of \mathbf{A}_s in positions J . Hence, based on the conditions in Equation 3.9, $J \in \tilde{\mathcal{G}}_s$ if and only if

$$\langle \tilde{\mathbf{z}}_s - \mathbf{P}_{s,J}\tilde{\mathbf{z}}_s, \boldsymbol{\gamma}_{s_j} \rangle \leq 0 \quad \text{for } j \notin J, \quad \text{and } (\mathbf{A}_{s,J}\mathbf{A}_{s,J}^\top)^{-1}\mathbf{A}_{s,J}\tilde{\mathbf{z}}_s \geq \mathbf{0}; \quad (3.15)$$

where the latter condition assures that $\Pi(\tilde{\mathbf{z}}_s|\mathcal{L}(V_{s,J})) \in \overline{\mathcal{F}}_{s,J}$. However, it is possible that the set $J \in \tilde{\mathcal{G}}_s$ produces a set of linearly dependent vectors $V_{s,J}$. In that case, Theorem 3.1 guarantees that it is always possible to find a subset $J^* \subset J$ such that V_{s,J^*} is a linearly independent set that spans the same linear space as $V_{s,J}$, and also, that satisfies $J^* \in \tilde{\mathcal{G}}_s$. Thus, analogous conditions as in Equation 3.15 can be established using J^* instead of J .

Theorem 3.1. *Let \mathbf{A} be a $m \times D$ irreducible matrix with rows $-\boldsymbol{\gamma}_j$. Let Ω^0 be its corresponding polar cone. For any set $J \subseteq \{1, 2, \dots, m\}$, define $V_J = \{\boldsymbol{\gamma}_j : j \in J\}$. Further, denote $\overline{\mathcal{F}}_J$ to be the subcone of Ω^0 generated by the edges given by the set J . For a vector \mathbf{z} , define its set \mathcal{G} to be conformed by all sets $J \subseteq \{1, 2, \dots, m\}$ such that $\Pi(\mathbf{z}|\Omega^0) = \Pi(\mathbf{z}|\mathcal{L}(V_J)) \in \overline{\mathcal{F}}_J$. Suppose J is a non-empty set such that V_J is a linearly dependent set and $J \in \mathcal{G}$. Then, there exists $J^* \subset J$ such that V_{J^*} is a linearly independent set, $\mathcal{L}(V_{J^*}) = \mathcal{L}(V_J)$, and $J^* \in \mathcal{G}$.*

All different concepts that have been defined at the sample level, can be analogously defined at the superpopulation level. For instance, let \mathcal{G}_μ be the set of all subsets $J \subseteq \{1, \dots, m\}$ such that $\Pi(\mathbf{z}_\mu|\Omega_\mu^0) = \Pi(\mathbf{z}_\mu|\mathcal{L}(V_{\mu,J})) \in \overline{\mathcal{F}}_{\mu,J}$, where \mathbf{z}_μ , Ω_μ^0 , $V_{\mu,J}$ and $\overline{\mathcal{F}}_{\mu,J}$ are the analogous versions of $\tilde{\mathbf{z}}_s$, Ω_s^0 , $V_{s,J}$ and $\overline{\mathcal{F}}_{s,J}$ obtained by substituting $\tilde{\mathbf{y}}_s$ and \mathbf{W}_s by $\boldsymbol{\mu} = (\mu_1, \dots, \mu_D)$ and $\mathbf{W}_\mu = \text{diag}(r_1, r_2, \dots, r_D)$. Moreover, necessary and sufficient conditions as in Equation 3.9 can be analogously established to characterize the vector $\boldsymbol{\rho}_\mu$ to be the projection onto Ω_μ^0 .

Recall the set $\tilde{\mathcal{G}}_s$ could vary for different samples. Also, note that highly variable small samples are likely to choose sets $J \in \tilde{\mathcal{G}}_s$ that are not chosen in the ‘asymptotic true’ \mathcal{G}_μ . However, as the

sample size increases, these wrong choices are less likely to occur since the sample domain means get closer to the limiting domain means. This intuitive idea is formalized in Theorem 3.2, which states that sets that are not in \mathcal{G}_μ have an asymptotic zero probability of being chosen by the sample.

Theorem 3.2. *Consider any set $J \subseteq \{1, 2, \dots, m\}$ such that $J \notin \mathcal{G}_\mu$. Then, $P(J \in \tilde{\mathcal{G}}_s) = O(n_N^{-1})$.*

Theorem 3.3 contains the main result of this paper, which permits the use of the constrained estimator $\tilde{\theta}_s$ to make inference of the population domain means. This generalizes Theorem 2 of Wu et al. (2016), where only monotone restrictions were considered. Note the presence of a bias term B on the mean of the asymptotic normal distribution. We conjecture that this term arises as a consequence of using the estimated variance $\hat{V}(\tilde{\theta}_{s_d, J})$, solely based on the J chosen by the observed sample, which does not always converge to the asymptotic variance of $\tilde{\theta}_{s_d}$. This undesirable situation occurs when there is more than one set $J \in \mathcal{G}_\mu$ such that their corresponding edges in $V_{\mu, J}$ span different linear spaces, or equivalently, that the projection onto the polar cone Ω_μ^0 belongs to the intersection of those different linear spaces. In particular, note that the condition $\mathbf{A}\boldsymbol{\mu} > \mathbf{0}$ means that the vector \mathbf{z}_μ is strictly inside the constraint cone Ω_μ , and then, there is no set $J \neq \emptyset$ such that $\Pi(\mathbf{z}_\mu | \mathcal{L}(V_{\mu, J})) = \mathbf{0}$. Thus, in this case, the bias term vanishes.

Theorem 3.3. *Suppose that $\boldsymbol{\mu}$ satisfies $\mathbf{A}\boldsymbol{\mu} \geq \mathbf{0}$. Consider any set J such that $J \in \tilde{\mathcal{G}}_s$. Then*

$$\hat{V}(\tilde{\theta}_{s_d, J})^{-1/2}(\tilde{\theta}_{s_d} - \bar{y}_{U_d}) \xrightarrow{\mathcal{L}} \mathcal{N}(B, 1),$$

for any $d = 1, 2, \dots, D$, where $B = O(\sqrt{\frac{n_N}{N}})$ is a bias term that vanishes when $\mathbf{A}\boldsymbol{\mu} > \mathbf{0}$.

Note that Theorem 3.3 relies on the fact that the assumed shape constraints hold for the vector of limiting domain means $\boldsymbol{\mu}$ instead of for the vector of population domain means $\bar{\mathbf{y}}_U$. Nevertheless, in the next section, we show through simulations that the constrained estimator improves both estimation and variability when the population domains are approximately close to the assumed shape, in comparison with unconstrained estimators.

3.4 Performance of constrained estimator

3.4.1 Simulations

We run simulation experiments to measure the performance of the proposed methodology to carry out estimation and inference of population domain means. Given a pair of natural numbers D_1 and D_2 , we generate the limiting domain means μ_d from the monotone bivariate function $\mu(x_1, x_2)$ given by

$$\mu(x_1, x_2) = \sqrt{1 + 4x_1/D_1} + \frac{4 \exp(0.5 + 2x_2/D_2)}{1 + \exp(0.5 + 2x_2/D_2)}.$$

The μ_d 's are created by evaluating $\mu(x_1, x_2)$ at every combination of $x_1 = 1, 2, \dots, D_1$ and $x_2 = 1, 2, \dots, D_2$, producing a total number of domains equal to $D = D_1 D_2$. We set $D_1 = 6$ and $D_2 = 4$. Note that although the function $\mu(x_1, x_2)$ produces a matrix rather than a vector of domain means, it can be vectorized in order to represent the limiting domain means as the vector $\boldsymbol{\mu}$. For each domain d , we generate its $N_d = N/D = 400$ elements by adding i.i.d. normal distributed noise with mean 0 and variance σ^2 to the μ_d . Once the elements of the population have been simulated, then the population domain means $\bar{\mathbf{y}}_U$ are computed. The population domain means used for simulations when $\sigma = 1$ are displayed in Figure 3.2. Observe that these domain means are reasonably (not strictly) monotone with respect to x_1 and x_2 .

Samples are drawn from a stratified sampling design without replacement, with 4 strata that cut across the D domains. Strata are constructed using an auxiliary variable ν that is correlated with the variable of interest y . The vector ν is created by adding i.i.d. standard normally distributed noise to $\sigma d/D$, for each element in domain d . Then, stratum membership is assigned by ranking the vector ν , and creating 4 blocks of $N/4 = 2400$ elements each based on such ranks. To make the design informative, we sample $n_N = 480$ elements divided across strata in (60, 120, 120, 180). This probability sampling design is similar to the one described in Wu et al. (2016).

We consider 4 different scenarios obtained from the combination of two possible types of shape constraints and $\sigma = 1$ or 2. The first type of constraints assumes the population domain means

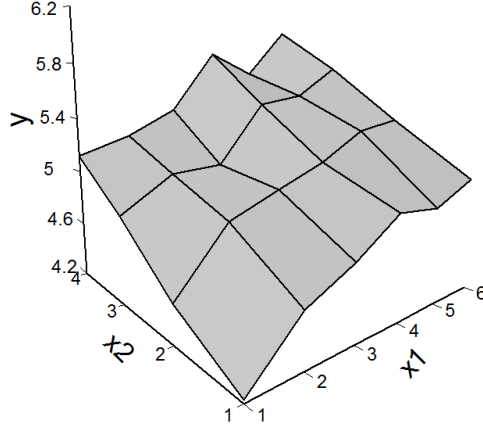


Figure 3.2: Population domain means for simulations when $\sigma = 1$.

are monotone increasing with respect to both x_1 and x_2 (double monotone), while the second type of constraints assumes monotonicity only with respect to x_1 (only x_1 monotone). Moreover, for a fixed σ , the exact same population is considered for the two possible types of constraints. For each scenario, the unconstrained $\tilde{\mathbf{y}}_s$ and constrained $\tilde{\boldsymbol{\theta}}_s$ estimates are computed along with their linearization-based variance estimates (Equation 3.13). Constrained estimates are computed using the CPA, and their variance estimates are computed by relying on the sample-selected set $J \in \tilde{\mathcal{G}}_s$. In addition, 95% Wald confidence intervals based on the normal distribution are constructed for both estimators. The lengths of these confidence intervals are omitted because they have the same behavior (up to the constant 1.96) as the variance estimates.

To measure the precision of $\tilde{\mathbf{y}}_s$ and $\tilde{\boldsymbol{\theta}}_s$ as estimators of the population domain means $\bar{\mathbf{y}}_U$, we consider the Weighted Mean Squared Error (WMSE) given by

$$\text{WMSE}(\tilde{\varphi}_s) = \mathbb{E} [(\tilde{\varphi}_s - \bar{\mathbf{y}}_U)^\top \mathbf{W}_U (\tilde{\varphi}_s - \bar{\mathbf{y}}_U)],$$

where $\tilde{\varphi}_s$ could be either the unconstrained or constrained estimator, \mathbf{W}_U is the diagonal matrix with elements N_d/N , $d = 1, \dots, D$. The WMSE values are approximated by simulations.

Simulation results are summarized in Figures 3.3 - 3.6, and are based on $R = 10000$ replications. These display the 24 domains divided in groups of 6, where each is assumed to be monotone. For the double monotone scenario, similar plots with groups of 4 monotone domains each can be also pictured. From the fitting one sample plots, it can be seen that the constrained estimates can be exactly equal to the unconstrained estimates for some domains. In those cases, their variance estimates are also equal. Also, confidence intervals for the constrained estimator tend to be tighter in comparison with those for the unconstrained estimator. On average, the constrained estimator behaves slightly differently than the population domain means, due to their non-strict monotonicity. As an advantage, the percentiles for the constrained estimator are narrower, demonstrating the distribution of the proposed estimator is tighter than the distribution of the unconstrained estimator. For small values of σ , unconstrained estimates are closer to satisfy the assumed restrictions, which leads to small improvements on the constrained estimator over the unconstrained. In contrast, shape assumptions tend to be more severely violated in unconstrained estimates for larger values of σ , allowing the proposed estimator to gain much more efficiency on these cases. This latter property can be noted by observing that the constrained estimator percentile band gets farther away from the unconstrained estimator band as σ increases.

In terms of variability, the constrained estimator has smaller variance of the two estimators. However, on average, it gets overestimated by its corresponding linearization-based variance estimate. This might be a direct consequence of estimating the variance based only on the set $J \in \tilde{\mathcal{G}}_s$, which is actually a random set that might change from sample to sample. In contrast, the variance estimate of the unconstrained estimator underestimates the true variance, on average. Although it would be ideal to improve both of these variance estimates, we consider it to be less alarming to produce greater variance estimates, at least for inference purposes. In addition, confidence intervals for both estimators demonstrate a similar good coverage rate when $\sigma = 1$, meanwhile such coverage gets slightly improved by the constrained estimator when $\sigma = 2$.

Table 3.1 shows that the constrained estimator is more precise on average than the unconstrained estimator, even though the population domain means are not strictly monotone with re-

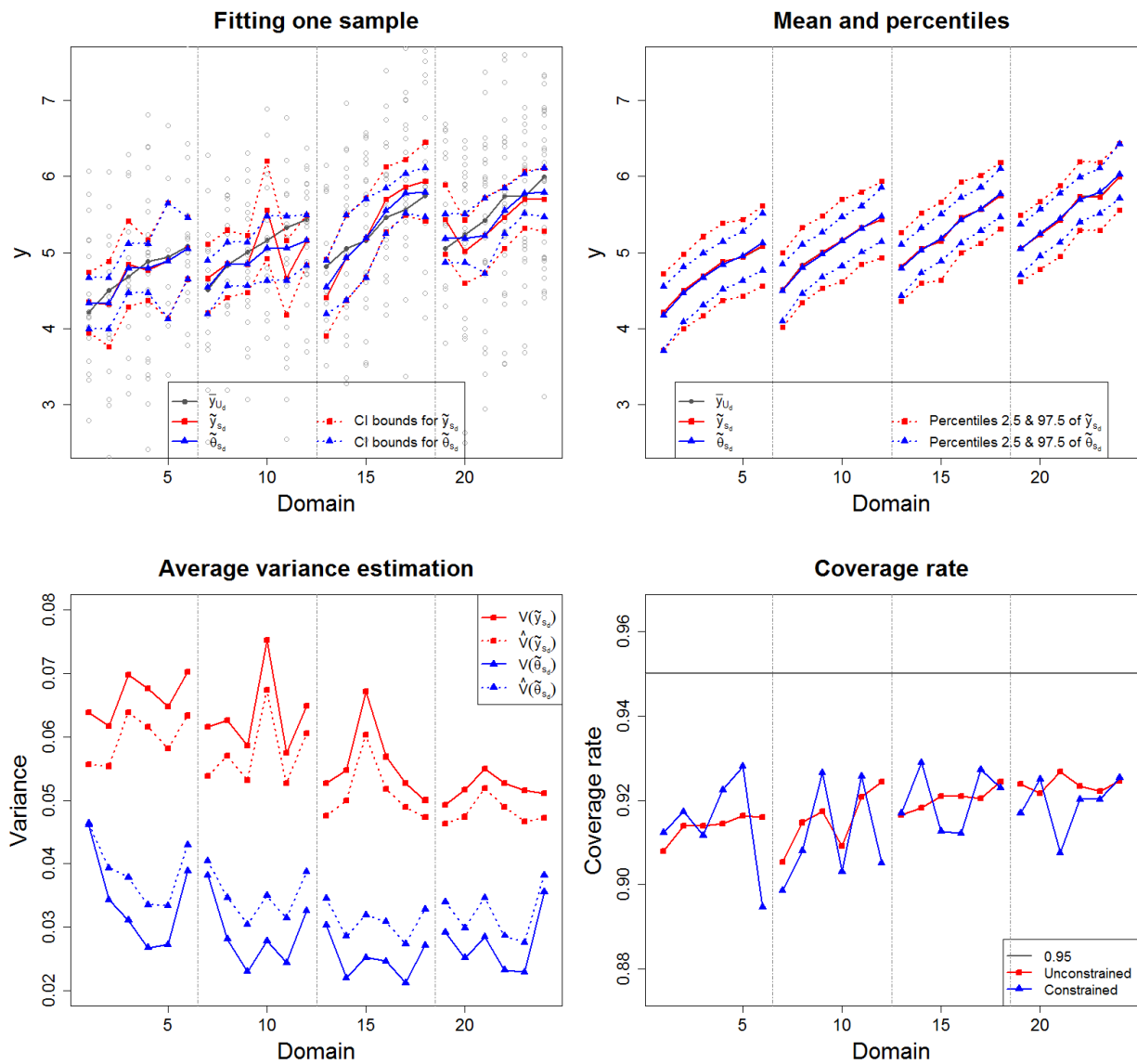


Figure 3.3: Plots of simulation results for the unconstrained and constrained estimators under the double monotone scenario with $\sigma = 1$, based on 10000 replications.

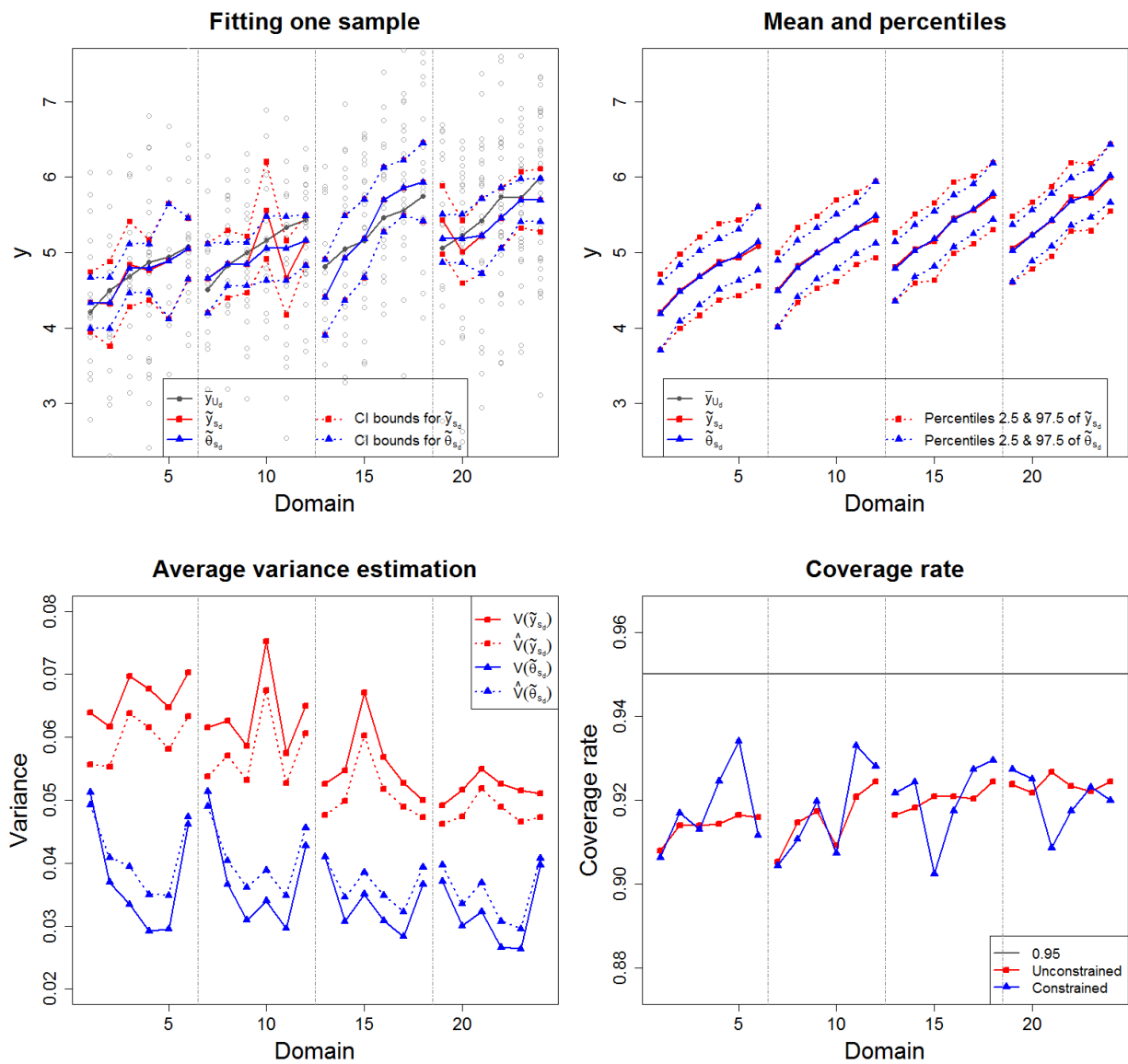


Figure 3.4: Plots of simulation results for the unconstrained and constrained estimators under the only x_1 monotone scenario with $\sigma = 1$, based on 10000 replications.

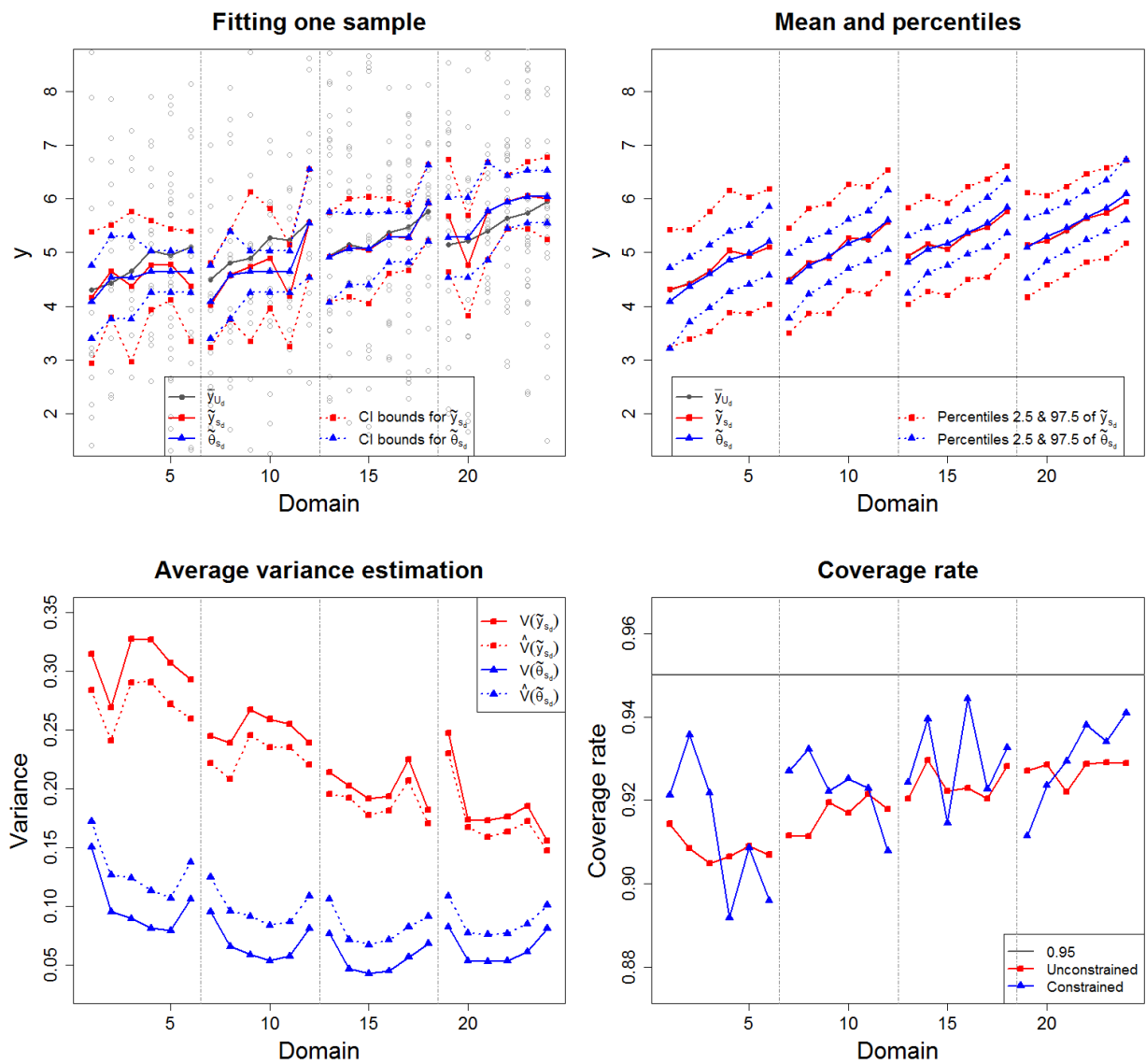


Figure 3.5: Plots of simulation results for the unconstrained and constrained estimators under the double monotone scenario with $\sigma = 2$, based on 10000 replications.

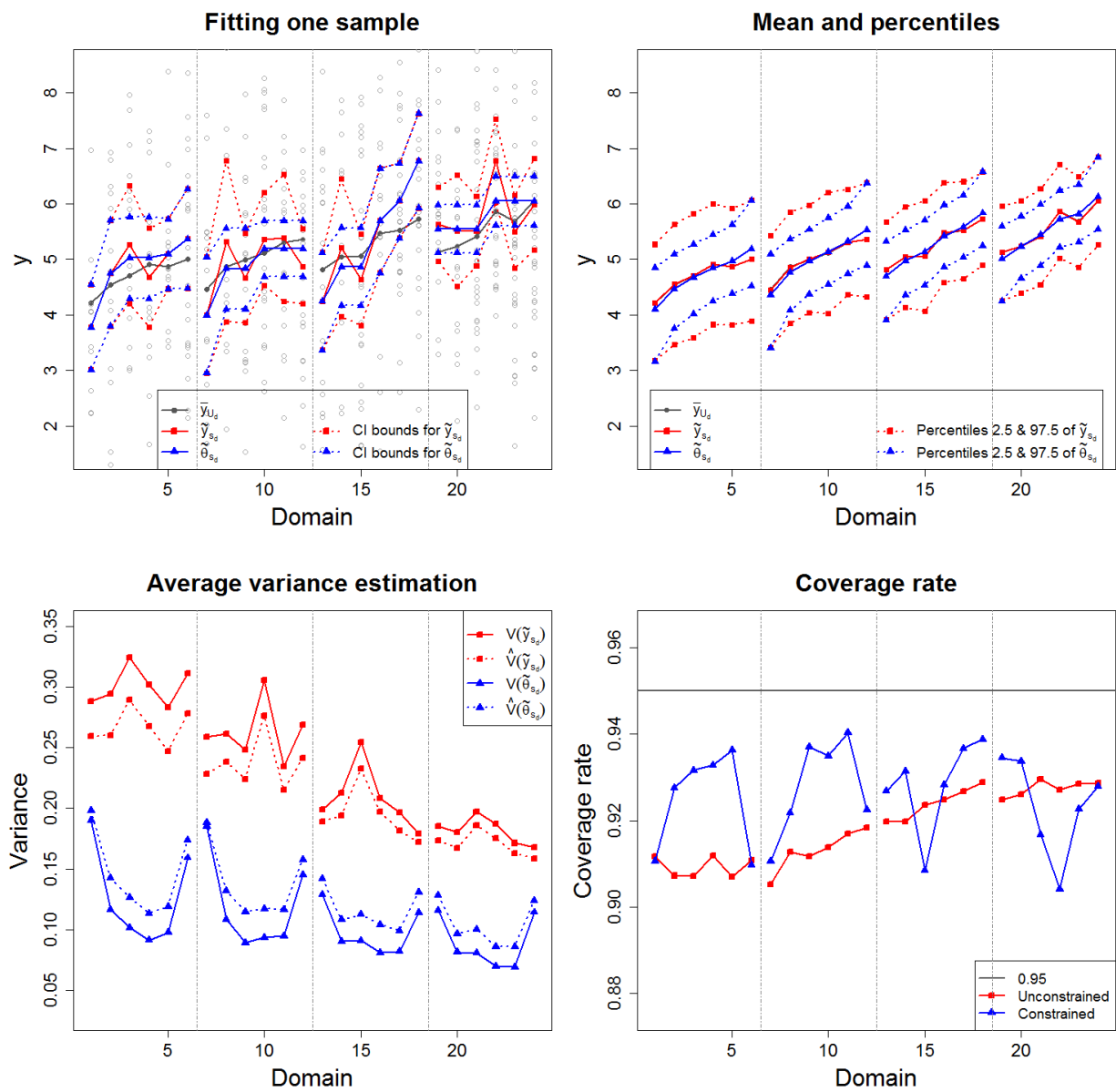


Figure 3.6: Plots of simulation results for the unconstrained and constrained estimators under the only x_1 monotone scenario with $\sigma = 2$, based on 10000 replications.

spect to x_1 and x_2 . Moreover, the precision of the constrained estimator gets improved when the monotonicity with respect to the two variables is assumed, instead of only with respect to x_1 . This can be translated on stating that the precision of the proposed estimator is benefited by taking into account the most appropriate shape assumptions.

Table 3.1: WMSE values.

	Unconstrained	Only x_1 monotone	Double monotone
$\sigma = 1$	0.0593	0.0362	0.0298
$\sigma = 2$	0.2384	0.1175	0.0832

3.4.2 Replication methods for variance estimation

Recently, it is more common that large-scale surveys make use of replication-based methods for variance estimation. Some examples of such surveys are the last editions of the NHANES and the National Survey of College Graduates (NSCG), the latter sponsored by the National Science Foundation (NSF). To study the performance of replication-based variance estimators under the proposed constrained methodology, we carry out simulation studies based on the delete-a-group Jackknife (DAGJK) variance estimator proposed by Kott (2001).

We perform replication-based simulation experiments using the setting described in Section 4.1. To compute the DAGJK variance estimator, we first randomly create G equal-sized groups within each of the 4 strata. Then, for each possible g , we delete the g -th group in each of the strata, adjust the remaining weights by $w_k^{(g)} = (\frac{G}{G-1})w_k$, where $w_k = \pi_k^{-1}$; and compute the replicate constrained estimate $\tilde{\theta}_s^{(g)}$ using the adjusted weights. Hence, the DAGJK variance estimate of $\tilde{\theta}_{s_d}$, $\hat{V}_{JK}(\tilde{\theta}_{s_d})$, is obtained by calculating

$$\hat{V}_{JK}(\tilde{\theta}_{s_d}) = \frac{G-1}{G} \sum_{g=1}^G \left(\tilde{\theta}_{s_d}^{(g)} - \tilde{\theta}_{s_d} \right)^2.$$

Analogously, a replication-based variance estimator of \tilde{y}_{sd} can be derived by substituting the role of $\tilde{\theta}_s$ by \tilde{y}_s .

Our simulations consider only the double monotone scenario, with $\sigma = 1$ or 2 , and $G = 10, 20$ or 30 . Moreover, the sample size is set to either $n_N = 480$ or $n_N = 960$, where the latter case is obtained by doubling the original sample size in each strata. Figures 3.7 - 3.10 contain our replication-based simulation results based on 10000 replications. From these, it can be noted that the DAGJK estimates tend to overestimate the variance of the unconstrained estimator, meanwhile the linearization-based variance estimate has an underestimating behavior. In contrast, both replication-based and linearization-based variance estimates of the constrained estimator overestimate the true variance. Moreover, note that as the number of groups G increases, DAGJK estimates tend to be greater, especially for small values of σ . Such increments on DAGJK estimates have the direct consequence of increasing the coverage rate as G gets larger. In addition, the coverage rate for both estimators is improved (closer to 0.95) when the sample size is increased. As a general conclusion in terms of the constrained estimator, DAGJK variance estimators have a similar behavior than linearization-based estimators. Thus, it seems appropriate to adapt the proposed constrained methodology to allow the use of replication-based variance estimation methods.

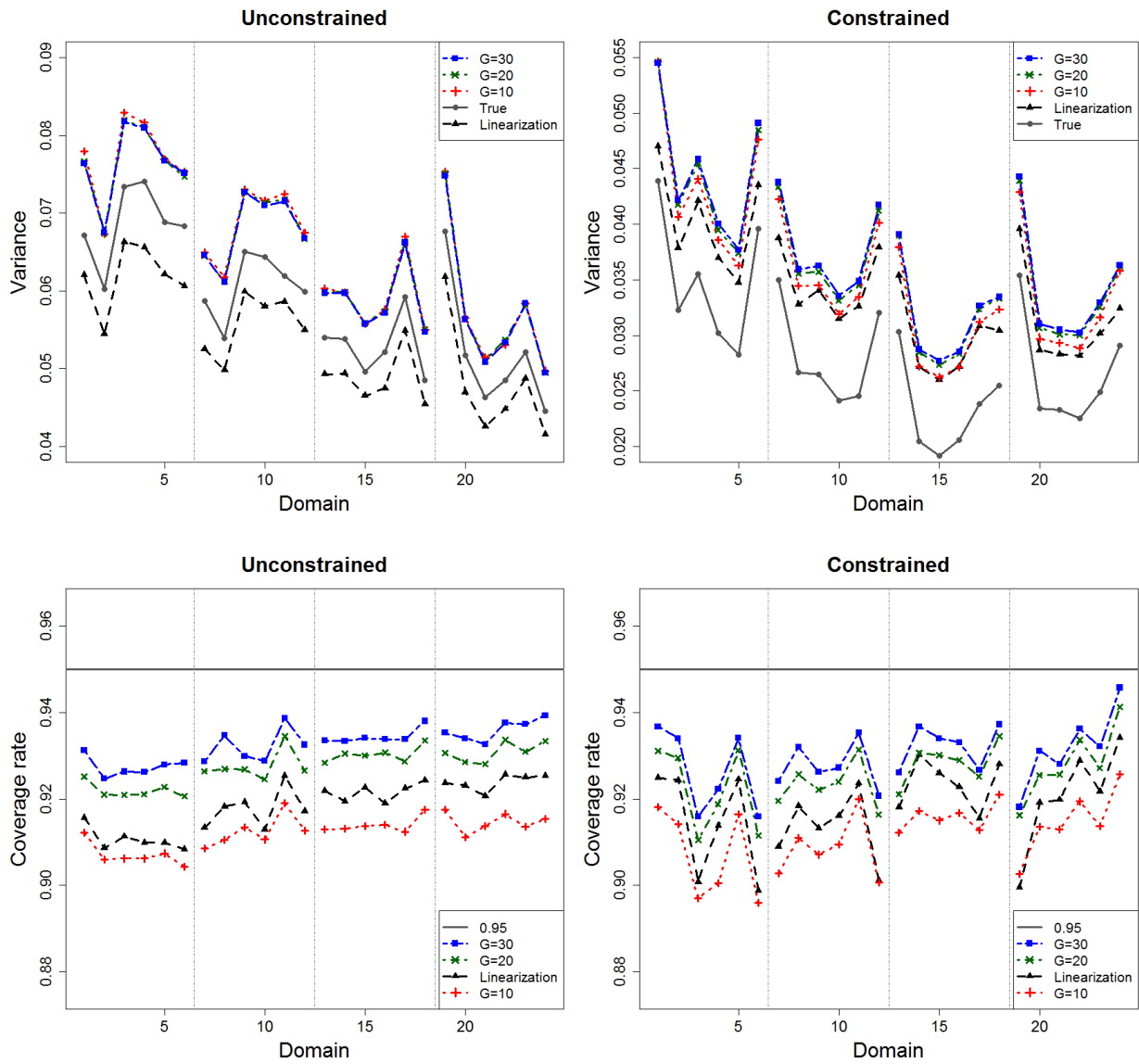


Figure 3.7: Variance estimation (top) and coverage rate (bottom) simulation results based on linearization and DAGJK methods for the unconstrained (left) and constrained (right) estimators, under the double monotone scenario with $n_N = 480$ and $\sigma = 1$.

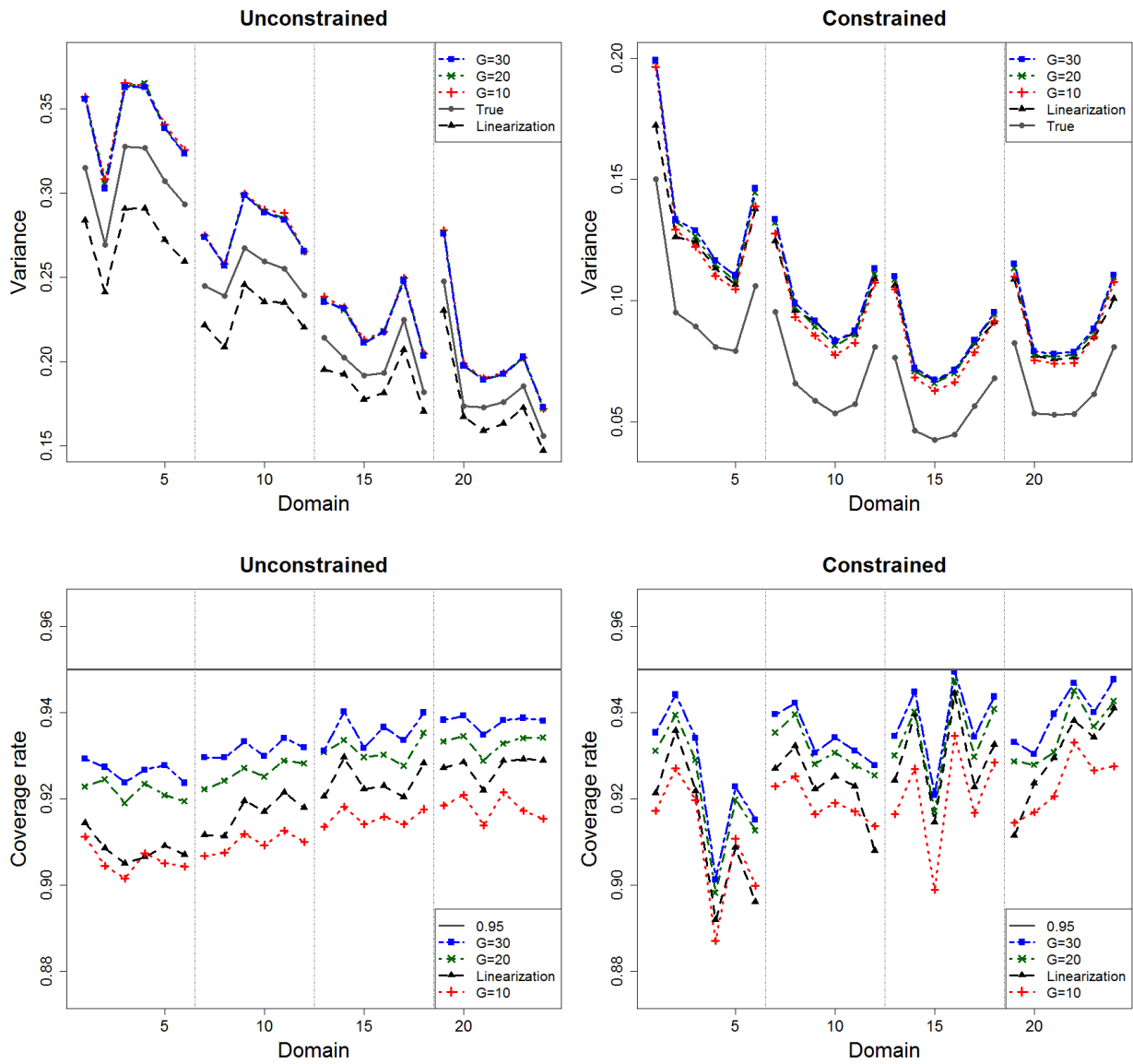


Figure 3.8: Variance estimation (top) and coverage rate (bottom) simulation results based on linearization and DAGJK methods for the unconstrained (left) and constrained (right) estimators, under the double monotone scenario with $n_N = 480$ and $\sigma = 2$.

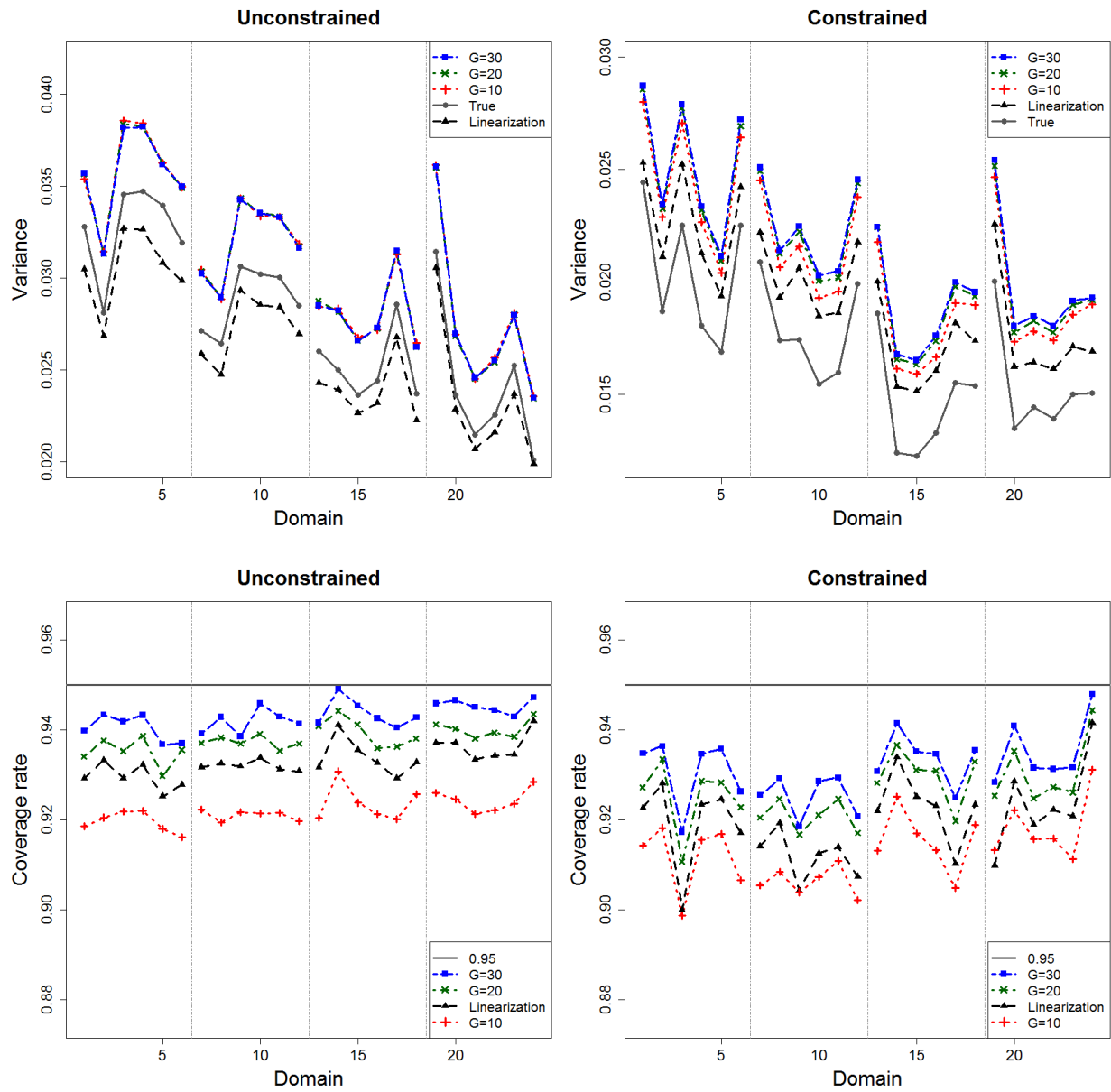


Figure 3.9: Variance estimation (top) and coverage rate (bottom) simulation results based on linearization and DAGJK methods for the unconstrained (left) and constrained (right) estimators, under the double monotone scenario with $n_N = 960$ and $\sigma = 1$.

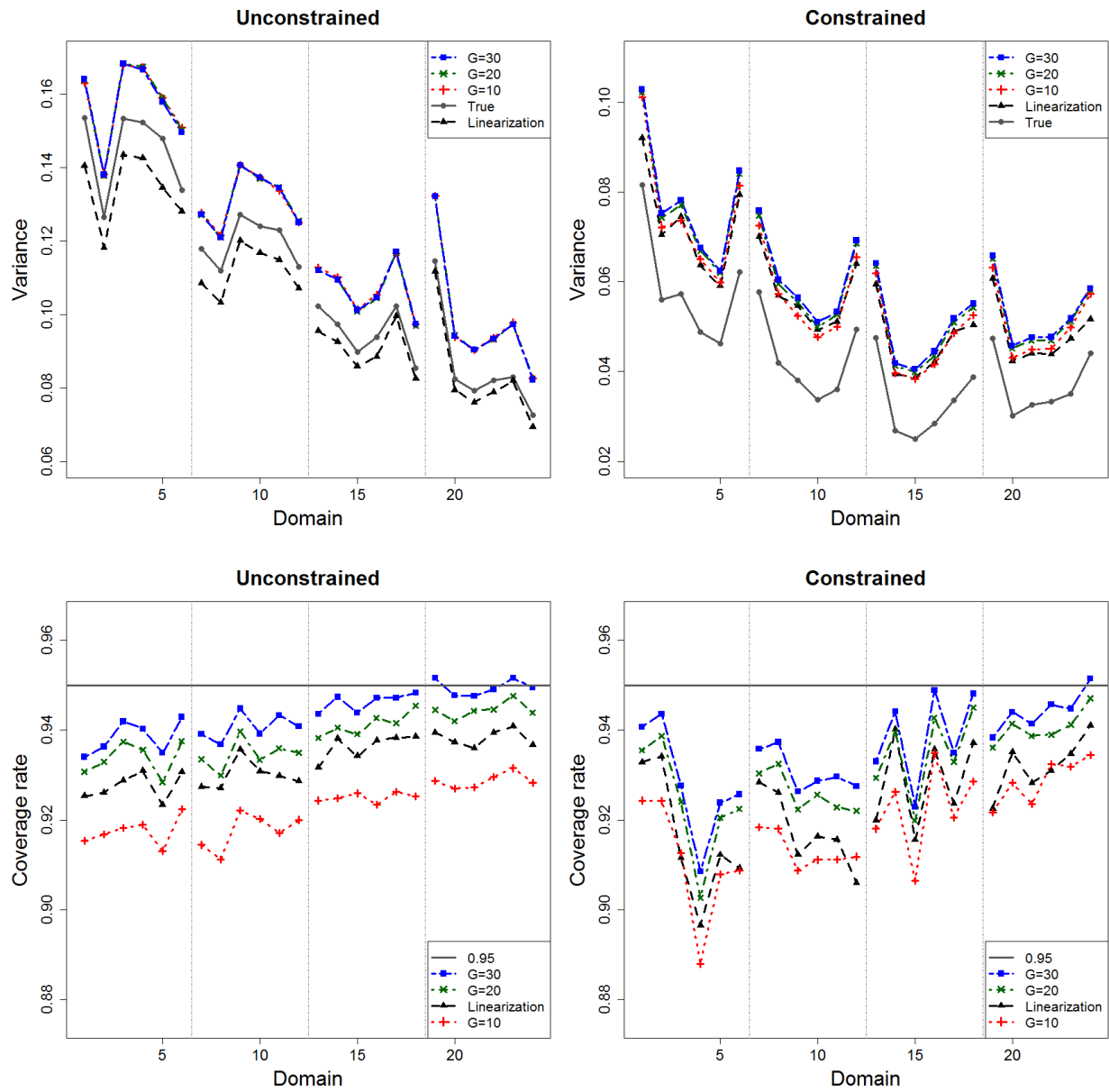


Figure 3.10: Variance estimation (top) and coverage rate (bottom) simulation results based on linearization and DAGJK methods for the unconstrained (left) and constrained (right) estimators, under the double monotone scenario with $n_N = 960$ and $\sigma = 2$.

3.5 Application of constrained estimator to NSCG 2015

To demonstrate the utility of the proposed constrained methodology in real survey data, we consider the 2015 National Survey of College Graduates (NSCG), which is sponsored by the National Center for Science and Engineering Statistics (NCSES) within the National Science Foundation, and is conducted by the U.S. Census Bureau. The 2015 NSCG data and documentation are openly available on the NSF website (www.nsf.gov/statistics/srvygrads). The purpose of the NSCG is to provide data on the characteristics of U.S. college graduates, with particular focus on those in the science and engineering workforce.

We set the total earned income before deductions in previous year (2014) to be the variable of interest (denoted by EARN). To avoid the high skewness of this variable, a log transformation is performed. Moreover, we take into account only those who reported a positive earning amount. A total of 76,389 observations was considered in our analysis. In addition, 252 domains are considered. These are determined by the cross-classification of four predictor variables. Such variables and their assumed constraints are:

- **Time since highest degree.** This ordinal variable defines the year category of award of highest degree. The period from 2015 to 1959 is divided into 9 categories, where the first 8 categories (denoted by 1-8) are of 6 years each, and the last category (denoted by 9) is of 9 years. *Constraint:* given the other predictors, the average total earned income increases with respect to the time since highest degree from year category 1 to 7. No assumption is made with respect to categories 8 and 9, as those people are likely to be retired (at least 42 years since their highest degree).
- **Field category.** This nominal variable defines the field of study for highest degree, based on a major group categorization provided within the 2015 NSCG. The 7 categories for this variable are:
 1. Computer and mathematical sciences,
 2. Biological, agricultural and environmental life sciences,

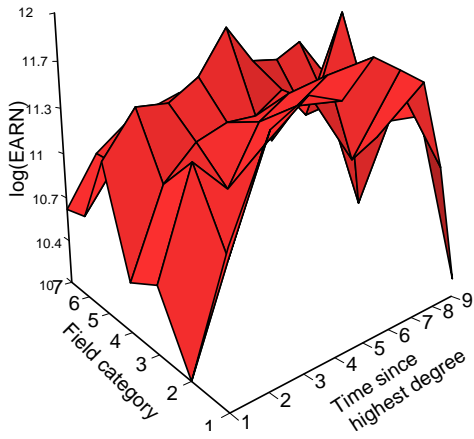
3. Physical and related sciences,
4. Social and related sciences,
5. Engineering,
6. S&E-related fields,
7. Non-S&E fields.

Constraint: given the other predictors, the average total earned income for each of the fields 2 and 4 is less than for the fields 1, 3 and 5. No assumption is made with respect to categories 6 and 7, as they cover many fields for which a reasonable order restriction might be complicated to impose.

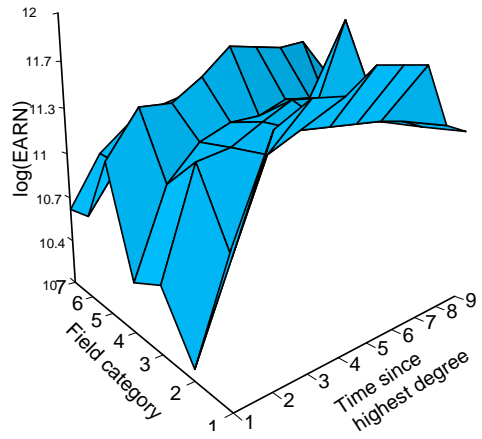
- **Postgrad.** This binary variable defines whether the highest degree is of the postgraduate level (YES) or of the Bachelor's level (NO). *Constraint:* given the other predictors, the average total earned income is higher for those with postgraduate studies.
- **Supervise.** This binary variable defines whether supervising others is a responsibility in the principal job (YES) or not (NO). *Constraint:* given the other predictors, the average total earned income is higher for those who supervise others in their principal job.

Figures 3.11 and 3.12 contain the unconstrained and constrained estimates for each of the four groups obtained from the cross-classification of the Postgrad and Supervise binary variables. Note that since the assumed constraints constitute a partial ordering, then the constrained estimates are obtained by pooling domains. These figures show that the constrained estimator has a smoother behavior than the unconstrained. Moreover, it tends to correct for the large spike domains produced by the unconstrained estimator, which are usually a consequence of a very small sample size.

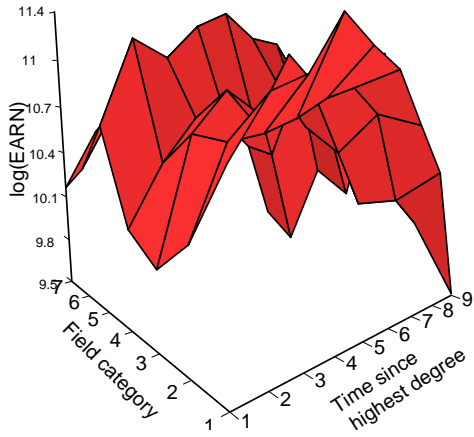
Standard errors for both unconstrained and constrained estimates are computed using the 2015 NSCG replicate weights, which are based on Successive Difference (Opsomer et al., 2016) and Jackknife replication methods. Both the replicate weights and adjustment factors were provided



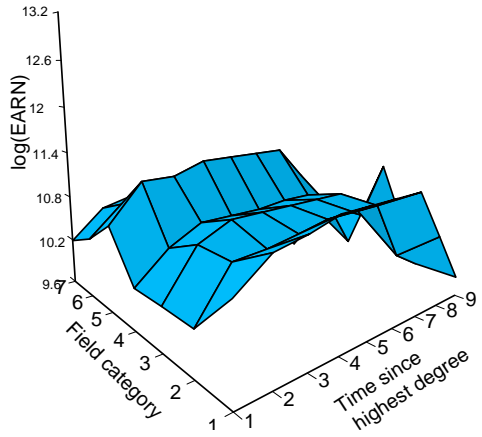
(a) Supervise=YES (unconstrained).



(b) Supervise=YES (constrained).

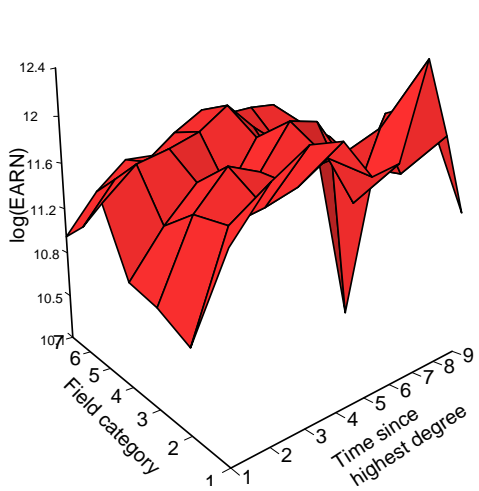


(c) Supervise=NO (unconstrained).

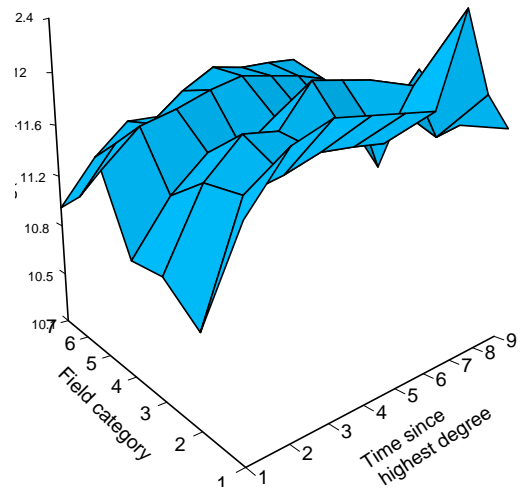


(d) Supervise=NO (constrained).

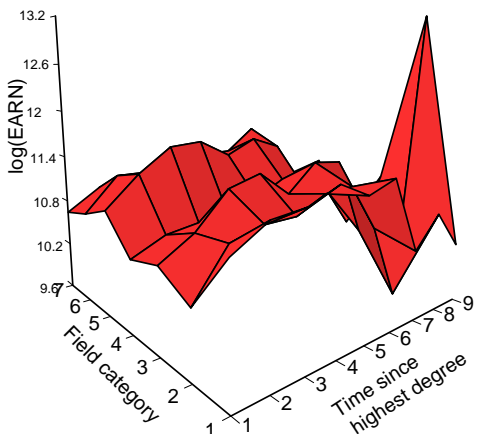
Figure 3.11: Unconstrained (left) and constrained (right) domain mean estimates for the 2015 NSCG data, given that Postgrad=NO is fixed.



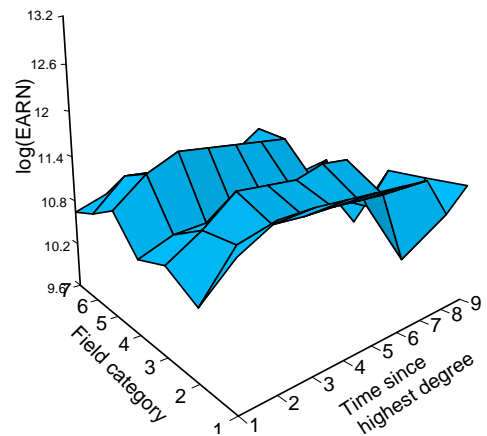
(a) Supervise=YES (unconstrained).



(b) Supervise=YES (constrained).



(c) Supervise=NO (unconstrained).



(d) Supervise=NO (constrained).

Figure 3.12: Unconstrained (left) and constrained (right) domain mean estimates for the 2015 NSCG data, given that Postgrad=YES is fixed.

by the Program Director of the Human Resources Statistics Program from the NCSES and are available upon request.

Figure 3.13 displays the ratio of these estimates for each of the 252 domains. Note that in the vast majority of cases, the standard error estimates of the proposed estimator are lower than those for the unconstrained estimator, with improvements of as much as 7 times smaller. However, there are some cases where the opposite behavior occurs. These are explored in Figure 3.14, which shows plots of two different slices: one with respect to the Time since highest degree variable and other with respect to Field category. These plots include unconstrained and constrained estimates, Wald confidence intervals and sample sizes. Further, each of these two slices contain one of the two domains that can be easily identified in Figure 3.13 to have the smallest ratios. The first of these domains is displayed in Figure 3.14a, indexed by 5. Here, the confidence interval is narrower for unconstrained estimates, which is as a direct consequence of having smaller standard deviation estimates. Note that the unconstrained estimates for the domains indexed by 5 and 6 violate the monotonicity assumption, and thus, are being pooled to obtain the constrained estimates. In contrast, Figure 3.14c shows that the samples sizes on these domains are considerably large, meaning that the noticed violation might be in fact true. Therefore, as the imposed restrictions are enforcing these two domains to get pooled, then domain indexed by 5 ends up producing a larger standard deviation on its constrained estimate. The second domain where unconstrained estimates produce smaller standard deviation estimates is displayed in Figure 3.14b, indexed by 1. Here, this domain is being pooled with its consecutive domain to obtain the constrained estimate. However, as these two domains have very low sample sizes (Figure 3.14d), they produce a constrained estimate that is based on a very small ‘effective’ sample size. Therefore, both the unconstrained and constrained estimates might be considered as unreliable, given the small sample circumstances.

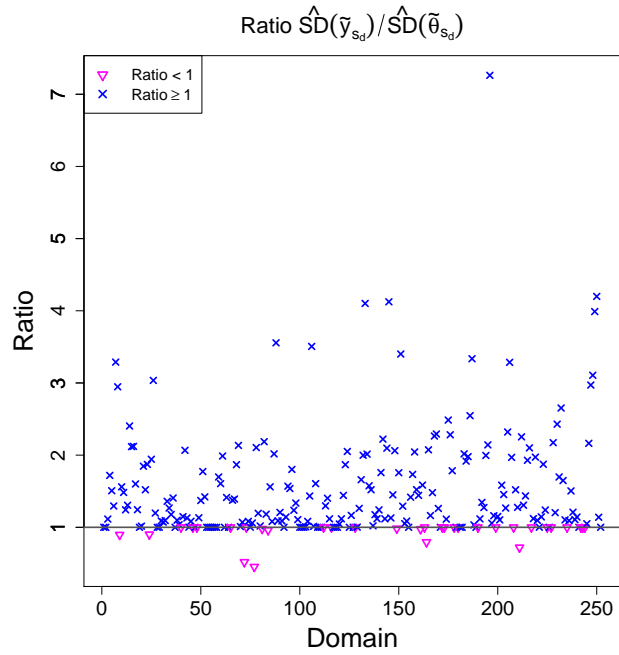


Figure 3.13: Ratio of the estimated standard errors of unconstrained estimates over those for constrained estimates for the 2015 NSCG data.

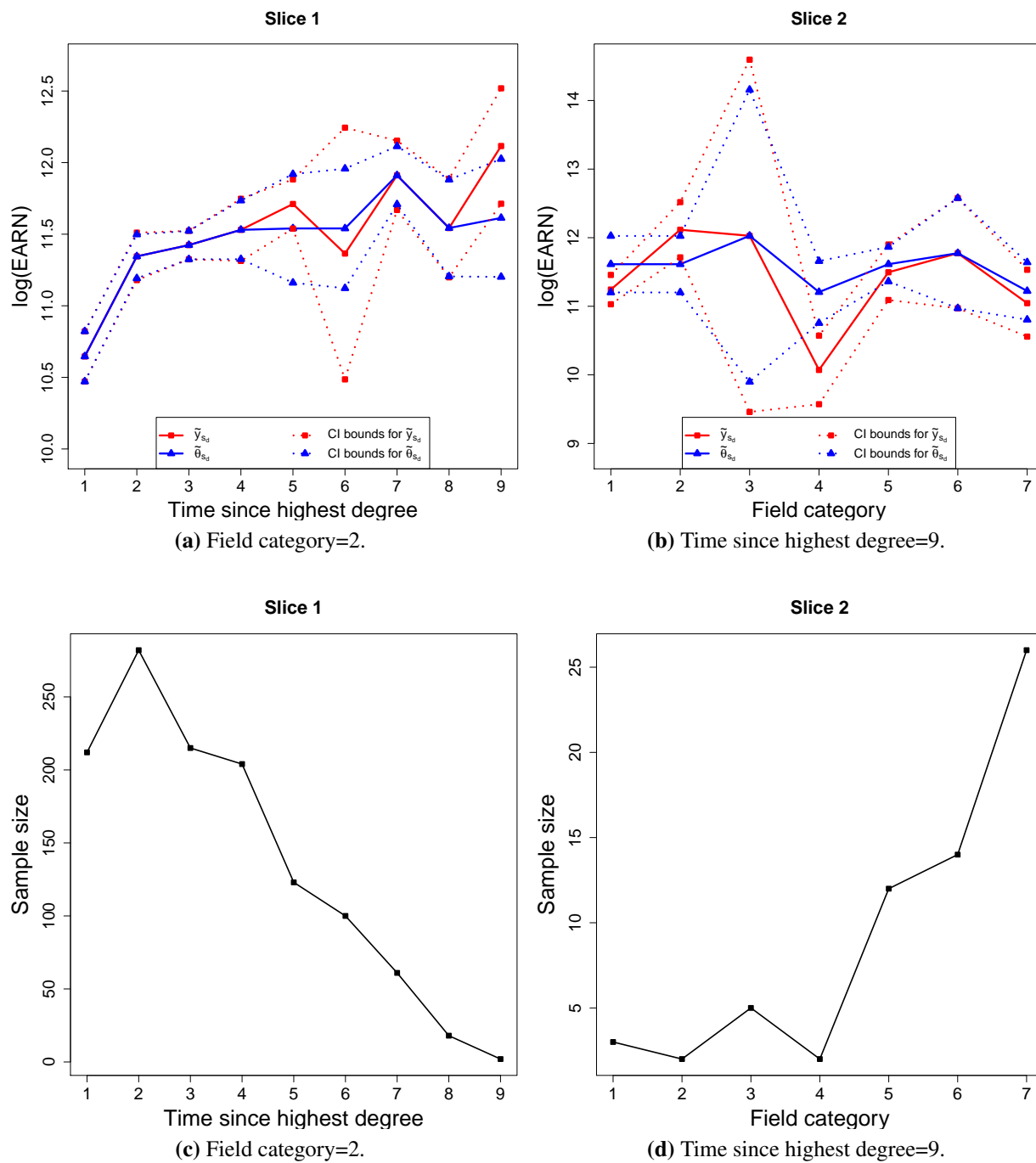


Figure 3.14: Slice plots of: unconstrained and constrained estimates with Wald confidence intervals (top) and sample sizes (bottom) for the 2015 NSCG data, given that Postgrad=YES and Supervise=YES.

Chapter 4

bcgam: An R package for Bayesian Constrained Generalised Additive Models

4.1 Introduction

A probability distribution is a member of the exponential family if it can be written

$$p(y|\theta, \phi) = \exp \left\{ \frac{y\theta - b(\theta)}{\phi} + c(y, \phi) \right\}. \quad (4.1)$$

where the parameter of interest θ depends on the expected value of y , ϕ is a scale parameter, and b and c are any arbitrary functions. Some of the most known members of the exponential family are: the *gaussian* distribution with $b(\theta) = \theta^2/2$ and $c(y, \phi) = -\{y^2\phi + \log(2\pi/\phi)\}/2$, the *binomial* distribution with $b(\theta) = \log(1 + e^\theta)$ and $c(y, \phi) = 0$, and the *Poisson* distribution with $b(\theta) = e^\theta$ and $c(y, \phi) = -\log(y!)$. Note that both the binomial and Poisson distributions do not require a scale parameter; i.e., $\phi = 1$.

Consider the class of generalised partial linear models with n independent observations from a distribution member of the exponential family described in Equation 4.1, where the mean value $E(y_i) = \mu_i$ is related to certain predictor variables through a link function $g(\mu_i) = \eta_i$. Following Meyer et al. (2011), assume the additive model for $\eta_i, i = 1, \dots, n$, given by

$$\eta_i = f_1(x_{1i}) + \dots + f_L(x_{Li}) + \boldsymbol{\gamma}^\top \mathbf{z}_i, \quad (4.2)$$

where x_{li} is the i -th observation of the l -th continuous predictor variable to be modelled non-parametrically, $\boldsymbol{\gamma}$ is a parameter vector, and \mathbf{z}_i is a vector of covariates to be modelled parametrically. The functions f_l are modelled nonparametrically, under smoothness assumptions and shape constraints such as monotonicity and/or convexity that are imposed through shape-restricted re-

gression splines. Meyer et al. (2011) considered two types of shape-restricted splines: quadratic I-splines (Ramsay, 1988) and cubic C-splines (Meyer, 2008). The former spline basis functions have the property that the space of smooth piecewise quadratic functions is spanned by the set formed by quadratic I-spline basis functions and the constant function. Further, any linear combination of such functions is non-decreasing if and only if the coefficients on the basis functions are non-negative. Similarly, the space of smooth of piecewise cubic basis functions is spanned by the set formed by cubic C-spline basis functions, the constant function, and the identity function. Also, any linear combination of such functions is convex if and only if the coefficients on the basis functions are non-negative. Figures 4.1a and 4.1b contain examples of quadratic I-splines and cubic C-splines, respectively; obtained using 5 equally spaced knots and $n = 50$ equally spaced observations in the unit interval. In addition, basis functions for monotonicity and convexity restrictions may also be constructed (Meyer, 2008). Figure 4.1c contains an example of basis functions that together with the constant function, span the space of piecewise cubic spline functions (with the given knots). Moreover, these basis functions have a similar property than I-splines and C-splines: any linear combination of them is decreasing and concave if and only if the coefficients on the basis functions are non-negative. Hence, each restricted function f_l can be expressed by a non-negative linear combination of one of the sets of spline basis functions described before.

Consider any shape-restricted function f_l . Given a set of k_l interior knots, let $s_{l1}(x), \dots, s_{lm_l}(x)$ be the spline basis functions that correspond to the assumed shape on f_l , where m_l is the total number of basis functions. Given the vector of data points $\mathbf{x}_l = (x_{l1}, \dots, x_{ln})^\top$, denote $\boldsymbol{\delta}_{l1}, \dots, \boldsymbol{\delta}_{lm_l}$ to be the spline basis vectors, where the i -th element of $\boldsymbol{\delta}_{lj}$ is $s_{lj}(x_{li})$, for $i = 1, \dots, n$ and $j = 1, \dots, m_l$. Meyer et al. (2011) proposed to approximate $\boldsymbol{\eta} = (\eta_1, \dots, \eta_n)^\top$ in Equation 4.2 by

$$\sum_{j=1}^{m_1} \beta_{1j} \boldsymbol{\delta}_{1j} + \dots + \sum_{j=1}^{m_L} \beta_{Lj} \boldsymbol{\delta}_{Lj} + \sum_{j=1}^p \alpha_j \boldsymbol{\nu}_j, \quad \text{where } \beta_{lj} \geq 0 \text{ for all } l, j; \quad (4.3)$$

where the $\boldsymbol{\nu}_j$ are the predictor variables to be parametrically modelled and the one vector. If there is any function f_l that is assumed to be either convex or concave, then the predictor variable x_l is also one of the $\boldsymbol{\nu}_j$.

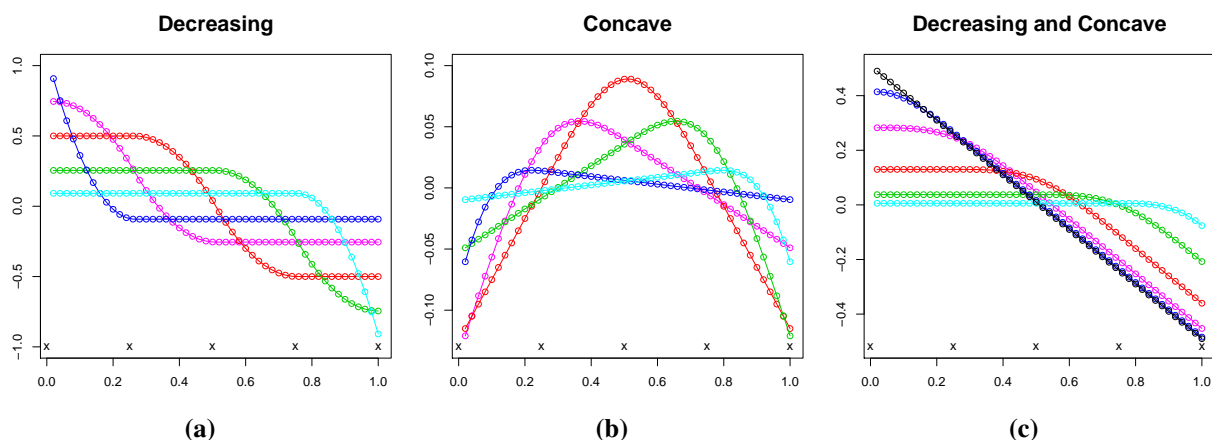


Figure 4.1: Shape-restricted regression splines. Knots are represented by the "X" marks, and dots represent the basis vectors. (a) Quadratic I-spline basis functions. (b) Cubic C-spline basis functions. (c) Spline basis functions for decreasing and concave restrictions.

Meyer (2013a) developed a frequentist methodology to fit the model in Equation 4.3 using a single cone projection. Such methodology has been implemented into the `cgam` package (Meyer and Liao, 2017) in R (R Core Team, 2018). Alternatively, a Bayesian framework for estimation and inference of the partial linear model in Equation 4.3 has been proposed by Meyer et al. (2011). Here, gamma prior distributions are assumed on the β coefficients with hyperparameters c_{l1} (shape) and c_{l2} (scale). These hyperparameters are chosen in such a way that the mean is small and the variance is large, making the prior distribution to be close to non-informative. In addition, normal priors with mean zero and a large variance M are assumed for the α coefficients.

The package `bcgam` (Oliva-Aviles and Meyer, 2018) in R implements the Bayesian approach mentioned above, and allows users to easily set up their models of interest and to select the type of shape constraints on each of the variables to be modelled non-parametrically. Also, it offers three options of generalised linear models: the gaussian model with constant variance σ^2 , the binomial model, and the Poisson model. The package `bcgam` is now available from the Comprehensive R Archive Network (CRAN) at <https://cran.r-project.org/package=bcgam>.

In Section 4.2, we explain the fundamental dependencies of the `bcgam` package and introduce its main functions. Further, Section 4.3 contains an illustrative analysis of the 'duncan' data set using these functions. The 'duncan' data is provided within the `bcgam` package.

4.2 Dependencies and main routines

4.2.1 NIMBLE dependency

As described in section 4.1, the `bcgam` package fits a Bayesian hierarchical generalised additive models. To set up such hierarchical Bayesian model and run Markov Chain Monte Carlo (MCMC) algorithms, the `bcgam` package depends on the NIMBLE system (NIMBLE Development Team, 2018). NIMBLE is a system for building and sharing analysis methods for statistical models, especially for hierarchical models and computationally-intensive methods. Although it is built in R, it gains speed by compiling models and algorithms in C++. NIMBLE also provides of a system for using models written in the BUGS model language as programmable objects in R. Hence, the `bcgam` package takes advantage of the convenient BUGS language to write hierarchical models and the efficient speed provided by C++, without actually requiring the user to neither know nor install these softwares. The only system requirement to appropriately install `bcgam` in R is the previous installation of `Rtools` for Windows or `Xcode` for Mac OS X. In fact, this is a system requirement for the correct installation of NIMBLE in R. The NIMBLE version 0.6-9 is available from CRAN, and is installed along with the package `bcgam`.

4.2.2 The primary function: `bcgam`

The function `bcgam` contains the primary routine in the `bcgam` package, which allows users to conveniently specify their generalised partial additive model of interest. The model specification syntax of this function is very similar to what is used in the `cgam` function of the `cgam` package. To fully specify a model, users might determine shape-restrictions on the non-parametrically modelled predictors, and also, add optional parametrically modelled covariates. In addition, the type of generalised additive model, the length of the MCMC, and the burn-in value of the MCMC might be also determined by the user through within this function.

To specify the shape constraint of a nonparametrically modelled predictor, any of the following auxiliary functions might be used: `sm.incr`, `sm.decr`, `sm.conv`, `sm.conc`,

`sm.incr.conv`, `sm.incr.conc`, `sm.decr.conv`, and `sm.decr.conc`. These functions do not actually create the splines basis vectors. Instead, they act as indicators of which knots and spline basis vectors will be considered for each nonparametrically modelled variable. For illustration, consider the simulated vectors $\mathbf{x}_1, \mathbf{x}_2, \mathbf{z}, \mathbf{y}$ obtained from the following code in R. Note that both \mathbf{z} and \mathbf{y} are binary variables.

```
R> n<-50
R> x1<-(1:n/n)^(1/3)
R> x2<-log(1:n/n)
R> z<-as.factor(rbinom(n, 1, 0.6))
R> eta<-x1+x2+0.2*as.numeric(z)+rnorm(n, sd=1.5)
R> mu<-exp(eta)/(1+exp(eta))
R> y<-(mu<0.6)
```

Suppose that \mathbf{y} is the response variable, so that fitting a binomial additive model is of interest. Also, suppose that the predictor variables \mathbf{x}_1 and \mathbf{x}_2 are assumed to be increasing and convex with respect to the systematic component η (log odds), respectively; and that \mathbf{z} wants to be included in the model as a parametrically modelled covariate. The following lines of code can be used to fit such a model using the `bcgam` function, and to save the output in an ‘bcgam’ class object named `bcgam.fit`.

```
R> bcgam.fit <- bcgam(y~sm.incr(x1, knots=c(0.4,0.6,0.8))+
R> sm.conv(x2,numknots=5)+z, family="binomial", nloop=10000)
```

Note the specification of the arguments `knots` and `numknots` inside the functions `sm.incr` and `sm.conv`. These indicate whether the exact knots or the number of knots are being specified by the user, respectively. When none of these commands are specified, then $4 + n^{1/7}$ equal quantile knots are created. In addition, note that the `family` argument determines the type of generalised model, and the `nloop` argument indicates the length of the MCMC.

4.2.3 Generic functions to summarize results

Five generic functions are provided in the `bcgam` package to summarize output from a `bcgam` class object. These are: `print.bcgam`, `summary.bcgam`, `predict.bcgam`, `plot.bcgam` and `persp.bcgam`.

`print.bcgam` shows the posterior means of the α coefficients. As it can be noticed in the output below, the posterior mean of predictor x_2 is also shown, even when it is being modelled nonparametrically. This happens since x_2 is being constrained to be convex with respect to η , so the identity function has to be included among the parametrically modelled variables.

```
R> print(bcgam.fit)
```

Call:

```
bcgam(formula = y ~ sm.incr(x1, knots = c(0.4, 0.6, 0.8)) +  
       sm.conv(x2, numknots = 5) + z, family = "binomial")
```

Coefficients:

```
(Intercept)          z1          x2  
-0.9884950   -0.2907676   -2.2308344
```

The `summary.bcgam` function compute and print summary statistics based on the posterior distributions of each of the α coefficients. Posterior means, standard errors, medians and 95% credible bounds are shown as part of the output of this generic function. The output below shows the summary obtained from the `bcgam.fit` object computed before.

```
R> summary(bcgam.fit)
```

Call:

```
bcgam(formula = y ~ sm.incr(x1, knots = c(0.4, 0.6, 0.8)) +  
       sm.conv(x2, numknots = 5) + z, family = "binomial")
```

Coefficients:

	Mean	Std. Error	2.5%	Median	97.5%
(Intercept)	-0.9884950	0.7186822	-2.429825	-0.9611992	0.3342667
z1	-0.2907676	0.6914935	-1.641616	-0.2632538	1.0199202
x2	-2.2308344	0.7839453	-3.906400	-2.1856031	-0.8717961

Prediction of new observations can be performed using the `predict.bcgam` function by providing a data frame with the observations of interest. For instance, suppose that we want to compute a prediction of the estimated probability at $x_1 = 0.5$, $x_2 = -1$ and $z = 0$. The following code shows an example of how to get such prediction using the generic function `predict.bcgam`. Note that the posterior standard error and credible interval bounds (95% by default) are also part of the output of this function.

```
R> predict(bcgam.fit , newdata=data.frame(x1=0.5 , x2=-1, z="0") ,  
  parameter="mu")  
$cred.mean  
[1] 0.6984425  
$cred.sd  
[1] 0.1256429  
$cred.lower  
[1] 0.43031  
$cred.upper  
[1] 0.9022911  
$y.lab  
[1] "Estimated probability"
```

The functions `plot.bcgam` and `persp.bcgam` create 2D and 3D plots of predicted values and interval estimates based on an object of the 'bcgam' class, respectively. To use these functions, nonparametric modelled predictors need to be specified (1 for a plot, 2 for a perspective). The rest of the continuous variables are evaluated at their largest value that is smaller than or equal to their median value. For the case of categorical covariates, these are evaluated at their mode. Figure 4.2 contains a plot and a perspective created by applying these two generic functions to the `bcgam.fit` object. The code is shown below.

```
R> plot(bcgam.fit , x2 , parameter="mu" , lwd=2)  
R> persp(bcgam.fit , x1 , x2 , theta=-60 , parameter="eta")
```

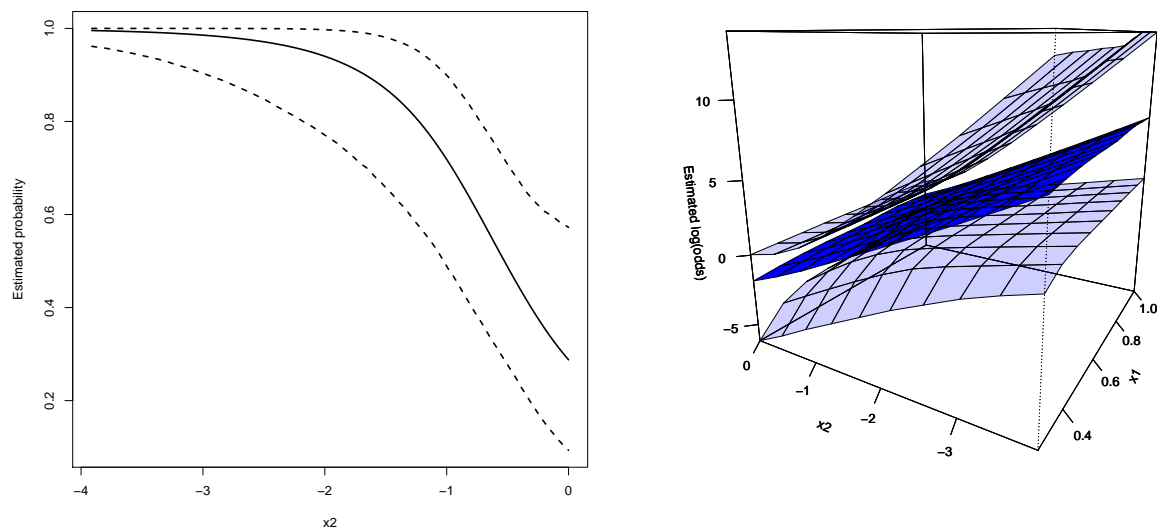


Figure 4.2: 2D and 3D plots created using the functions `plot.bcgam` and `persp.bcgam` with the `bcgam.fit` object, respectively.

4.3 Application to ‘duncan’ data

The ‘duncan’ data set provided within the `bcgam` package contains information about the prestige and other characteristics of 45 U.S. occupations in 1950 (Duncan, 1961, p. 119). The variables included in this data set are: *prestige*, percent of raters in NORC study (at the University of Chicago) rating occupation as excellent or good in prestige; *income*, percent of males in occupation earning \$3500 or more in 1950; *type*, a categorical variable for type of occupation (‘wc’, white-collar; ‘prof’, professional and managerial; ‘bc’, blue-collar); and *education*, percent of males in occupation in 1950 who were high-school graduates.

Suppose it is of interest to study the relationship between the variable *prestige* and the rest of them. Further, suppose that it is reasonable to assume that *prestige* tends to increase with *income*, given a type of occupation. Hence, we decide to constraint the variable *income* to be smooth and increasing with respect to *prestige*, and to include the categorical variable for type of occupation as a parametrically modelled covariate. Using the function `bcgam`, this is done using the following code:

```
R> duncan.fit<-bcgam(prestige~sm.incr(income)+type,
  data=duncan, nloop=100000)
```

As there is no specification on the number of knots to be used for the variable income, then 5 equal quantile knots are considered (by default) by the model. Furthermore, a MCMC algorithm of length 100,000 is specified, where the first 10,000 runs are burned-in (by default).

Before making any kind of conclusion from the fitted model, we would like to check whether the generated chains are mixing appropriately. For illustration, Figure 4.3 contains the trace plot of the chain that corresponds to the coefficient related to the ‘prof’ dummy variable (denoted by α_{prof}). Using the `bcgam` output, this can be done by accessing to the complete chains (after burn-in) of the coefficients on the parametrically modelled covariates, which are obtained using the command `duncan.fit$alpha.sims`. As this plot does not show evidence of lack of mixing, then we can proceed to make conclusions based on the fitted model.

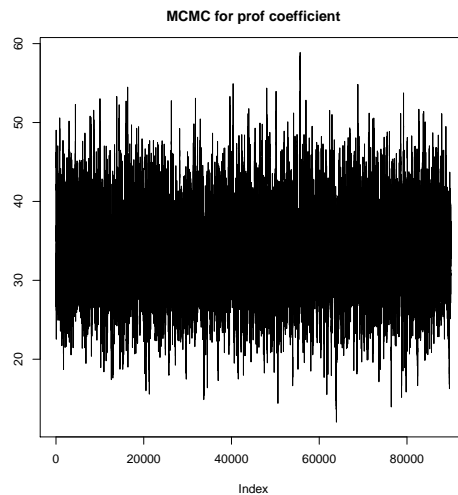


Figure 4.3: Trace plot of α_{prof} coefficient.

Table 4.1 contains the summary of results of the coefficients that correspond to the parametrically modelled covariates, based on the fitted model. In this model, the baseline type of occupation is ‘bc’, which implies that the intercept parameter explains the effect of such occupation category.

Figure 4.4 shows the fitted model for the blue-collar type of occupation along with its 95% credible interval. Moreover, Figure 4.5 contains the fitted models for each type of occupation. Note that these fitted models consist on parallel curves, which is expected given the design of our model. For illustration purposes, suppose that a follow-up question that arises from these fitted models is whether the effect of the ‘wc’ occupation type is different than the effect of the ‘bc’ occupation type, given a certain prestige value. This question is equivalent to whether the coefficient α_{wc} is expected to be different than zero or not. From Table 4.1, a 95% credible interval for this coefficient is given by $(-16.36, 6.89)$. Therefore, there is not enough evidence to conclude that the effect of the ‘wc’ occupation type is different than the effect of the ‘bc’ occupation type.

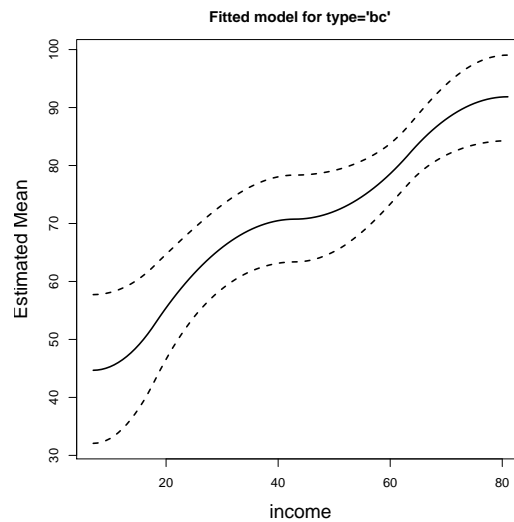


Figure 4.4: Fitted model and 95% credible bounds for blue-collar occupation.

Table 4.1: Results summary of α coefficients, based on the fitted model.

Coefficient	Mean	S.E.	2.5%	97.5%
Intercept	34.79	3.04	28.77	40.73
α_{prof}	33.87	5.08	24.03	43.93
α_{wc}	-4.90	5.89	-16.36	6.89

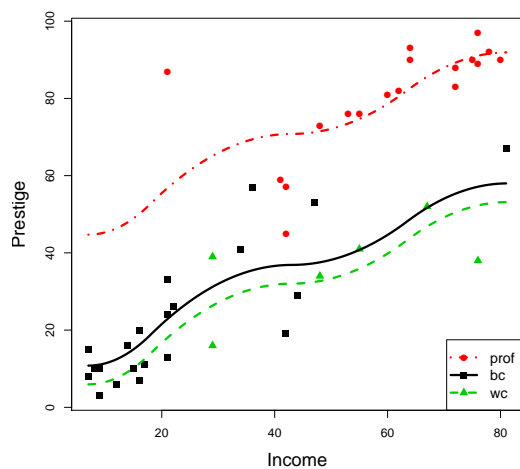


Figure 4.5: Fitted models for all types of occupation.

Chapter 5

Conclusion and Future Work

Merging shape-restricted regression techniques into survey estimation and inference has been shown to be a promising approach that aims to improve the quality of population estimates, in comparison with the most common used direct estimators. The paid price for these improvements is that they rely on prior shape constraints, such as qualitative or order assumptions, which arise often naturally on the survey data.

In this dissertation, we proposed the Cone Information Criterion for Survey data (CIC_s) as a data-driven criterion for choosing between the constrained and the unconstrained domain mean estimators. We showed that the CIC_s is consistently selecting the correct estimator based on the order of the limiting domain means μ . Also, the CIC_s also shares similar characteristics with other information criteria such as the AIC and the BIC, as it balances the deviation of the constrained estimator and its complexity. In addition, we proposed a methodology to estimate domain means that takes into account both design-based estimators and reasonable shape restrictions, and it was shown to largely improve their estimation and variability, especially on small domains. As this new methodology covers a broad range of shape restrictions beyond univariate monotonicity, it aims to jointly take advantage of several types of qualitative information that arises naturally for survey data. We also proposed a design-based variance estimation method of the estimator. However, as this estimation method depends solely on the half-space of the cone where the constrained estimator lands, then it tends to overestimate the variance. Replication-based methods are shown to behave similarly. Hence, further research might be carried out to develop variance estimation methods that do not ignore the randomness associated to the half-space where the constrained estimator could land. From the computational side, our proposed methodology is based on the Cone Projection Algorithm which is efficiently implemented in the package `coneproj`. Thus, we present this constrained methodology as an easy-to-implement attractive alternative for small area estimation. Finally, the package `bcgam` in R is developed to fit constrained generalised additive

models using a Bayesian approach, outside of the survey context. This package depends on the `nimble` system to efficiently run the MCMC algorithm that computes the posterior distribution. Further, the main routines of the `bcgam` package allow users to easily specify models, shape restrictions on nonparametrically modeled variables, and also, to obtain numerical and graphical output.

Our presented shape-constrained methodologies for survey data can be extended to other scenarios of interest. For instance, the trace term in the CIC_s could be multiplied by any positive constant C (instead of $C = 2$, as proposed) so that the consistency of the CIC_s remains true. The larger the value of C would imply a larger penalization of the constrained estimator complexity. Since we are able to control the amount of such penalization by changing the value of C , one question might be how to choose the optimum value C . In addition, the constrained estimator proposed in Chapter 3 might be used for missing data. Our methodology has the potential of ‘bounding’ domains with no observations, which will provide some knowledge (instead of none) regard those domain means.

Shape selection tools for survey data might also be developed from this dissertation. By combining both the proposed CIC_s and constrained estimator, the CIC_s might be extended to other shape constraints beyond monotonicity, so that it can be used to choose among many other types of shapes on the survey context. An immediate consequence of this would be the creation of a sample-based technique that chooses the most appropriate amount of relaxation when relaxed monotone assumptions are considered, such as the kernel bandwidth h shown in Section 3.2.

Methodologies for survey data that are analogous to partial additive linear models with shape restrictions might be also developed from this dissertation, such as model-assisted based estimators. Further, if population-level information is available, then a model-assisted based estimator that makes use of our proposed methodology can be developed. Under partial orderings, such estimator would be equivalent to a poststratified estimator (Särndal et al., 1992, Ch. 7.6) that uses the sample-selected pooling as the post strata. An R package that implements the proposed method-

ologies for survey data and have the capability of including future ones is of high priority, since it would allow practitioners to make use of these novel and useful techniques.

Bibliography

- Akaike, H. (1973). Information theory as an extension of the maximum likelihood principle. In Petrov, B. N. and Csaki, F., editors, *Second International Symposium on Information Theory*, pages 267–281. Akademiai Kiado, Budapest.
- Breidt, F. and Opsomer, J. (2000). Local polynomial regression estimators in survey sampling. *The Annals of Statistics*, 28(4):1026–1053.
- Brunk, H. D. (1955). Maximum likelihood estimates of monotone parameters. *The Annals of Mathematical Statistics*, 28:1026–1053.
- Brunk, H. D. (1958). Maximum likelihood estimates of monotone parameters. *The Annals of Mathematical Statistics*, 29(2):437–454.
- Duncan, O. D. (1961). A socioeconomic index for all occupations. In Reiss, A. J. Jr., editor, *Occupations and Social Status*. New York: Free Press [Table VI-1].
- Fay, R. E. and Herriot, R. A. (1979). Estimates of income for small places: an application of James-Stein procedures to census data. *Journal of the American Statistical Association*, 52:761–766.
- Fenchel, W. (1953). *Convex cones, sets, and functions*. Mimeographed notes by D. W. Blackett, Princeton Univ. Press, Princeton, New Jersey.
- Fuller, W. (1996). *Introduction to Statistical Time Series*. Wiley, New York, 2nd edition.
- Fuller, W. A. (1999). Environmental surveys over time. *Journal of the Agricultural, Biological and Environmental Statistics*, 4:331–345.
- Hájek, J. (1971). Comment on a paper by D. Basu. In Godambe, V. P. and Sprott, D. A., editors, *Foundations of Statistical Inference*, page 236. Holt, Rinehart and Winston, Toronto.
- Horvitz, D. G. and Thompson, D. J. (1952). A generalization of sampling without replacement from a finite universe. *Journal of the American Statistical Association*, 47:663–685.

- Kott, P. S. (2001). The delete-a-group jackknife. *Journal of Official Statistics*, 17:521–526.
- Liao, X. and Meyer, M. C. (2014). coneproj: an R package for the primal or dual cone projections with routines for constrained regression. *Journal of Statistical Software*, 61:1–22.
- Meyer, M. C. (1999). An extension of the mixed primal-dual bases algorithm to the case of more constraints than dimensions. *Journal of Statistical Planning and Inference*, 81:13–31.
- Meyer, M. C. (2008). Inference using shape-restricted regression splines. *Annals of Applied Statistics*, 2(3):1013–1033.
- Meyer, M. C. (2013a). Semi-parametric additive constrained regression. *Journal of Nonparametric Statistics*, 25:715–730.
- Meyer, M. C. (2013b). A simple new algorithm for quadratic programming with applications in statistics. *Communications in Statistics*, 42:1126–1139.
- Meyer, M. C., Hackstadt, A. J., and Hoeting, J. A. (2011). Bayesian estimation and inference for generalised partial linear models using shape-restricted splines. *Journal of Nonparametric Statistics*, 23(4):867–884.
- Meyer, M. C. and Liao, X. (2017). *cgam: Constrained Generalized Additive Model*. R package version 1.9, URL <https://CRAN.R-project.org/package=cgam>.
- NIMBLE Development Team (2018). Nimble: An R package for programming with BUGS models, version 0.6-9.
- Oliva-Aviles, C. and Meyer, M. C. (2018). *bcbgam: Bayesian Constrained Generalized Additive Model*. R package version 1.0, URL <https://CRAN.R-project.org/package=bcbgam>.
- Opsomer, J. D., Breidt, F. J., White, M., and Li, Y. (2016). Successive difference replication variance estimation in two-phase sampling. *Journal of Survey Statistical Methodology*, 4(1):43–70.

- Opsomer, J. D., Claeskens, G., Ranalli, M. G., Kauermann, G., and Breidt, F. J. (2008). Nonparametric small area estimation using penalized spline regression. *Journal of the Royal Statistical Society, series B*, 70:265–286.
- R Core Team (2018). *R: A Language and Environment for Statistical Computing*. R Foundation for Statistical Computing, Vienna, Austria.
- Ramsay, J. O. (1988). Monotone regression splines in action. *Statistical Science*, 3:425–461.
- Rao, J. N. K. (2003). *Small Area Estimation*. Wiley, Hoboken, New Jersey.
- Rao, J. N. K. (2008). Some methods for small area estimation. *Rivista Internazionale di Scienze Sociali*, 4:387–406.
- Rao, J. N. K. and Molina, I. (2015). *Small Area Estimation*. Wiley, Hoboken, New Jersey, 2nd edition.
- Robertson, T., Wright, F. T., and Dykstra, R. L. (1988). *Order Restricted Statistical Inference*. John Wiley & Sons, New York.
- Rockafellar, R. T. (1970). *Convex Analysis*. Princeton University Press, New Jersey.
- Särndal, C.-E., Swensson, B., and Wretman, J. (1992). *Model Assisted Survey Sampling*. Springer, New York.
- Schwarz, G. (1978). Estimating the dimension of a model. *Annals of Statistics*, 6:461–464.
- Silvapulle, M. J. and Sen, P. (2005). *Constrained Statistical Inference*. Wiley, Hoboken, New Jersey.
- VanEeden, C. (1956). Maximum likelihood estimation of ordered probabilities. *Indagationes Mathematicae*, 18:444–455.

Wollan, P. C. and Dykstra, R. L. (1986). Conditional tests with an order restriction as a null hypothesis. In Dykstra, R. L., Robertson, T., and Wright, F. T., editors, *Advances in Order Restricted Statistical Inference*, pages 279–295. Springer-Verlag, New York.

Wu, J., Meyer, M. C., and Opsomer, J. D. (2016). Survey estimation of domain means that respect natural orderings. *Canadian Journal of Statistics*, 44(4):431–444.

Appendix A

Supplemental materials for Chapter 2

The first part of this appendix contains all lemmas (with proofs) used to prove the theoretical results discussed in Chapter 2. Complete proofs of these results are included at the end of this appendix.

Lemma A.1. $\mathbb{E}[(\widehat{y}_{s_{i:j}} - \bar{y}_{U_{i:j}})^4] = o(n_N^{-1})$, for any $i \leq j$, $i, j = 1, 2, \dots, D$.

Proof of Lemma 1. For simplicity of notation and without loss of generality, we will use s instead of $s_{i:j}$ and U instead of $U_{i:j}$. Note that

$$\begin{aligned} n_N \mathbb{E}[(\widehat{y}_s - \bar{y}_U)^4] &= \frac{n_N}{N^4} \sum_{k \in U} \sum_{l \in U} \frac{y_k^2 y_l^2}{\pi_k^2 \pi_l^2} \mathbb{E}[(I_k - \pi_k)^2 (I_l - \pi_l)^2] \\ &+ \frac{n_N}{N^4} \sum_{k \in U} \sum_{p, q \in U: p \neq q} \frac{y_k^2 y_p y_q}{\pi_k^2 \pi_p \pi_q} \mathbb{E}[(I_k - \pi_k)^2 (I_p - \pi_p)(I_q - \pi_q)] \\ &+ \frac{n_N}{N^4} \sum_{k, l \in U: k \neq l} \sum_{p, q \in U: p \neq q} \frac{y_k y_l y_p y_q}{\pi_k \pi_l \pi_p \pi_q} \mathbb{E}[(I_k - \pi_k)(I_l - \pi_l)(I_p - \pi_p)(I_q - \pi_q)] \\ &= c_{1N} + c_{2N} + c_{3N}. \end{aligned}$$

We will now prove that c_{1N}, c_{2N}, c_{3N} converge to zero as N goes to infinity. For c_{1N} , we have that

$$\begin{aligned} |c_{1N}| &\leq \frac{n_N}{N^4} \sum_{k \in U} \frac{y_k^4}{\pi_k^4} \mathbb{E}[(I_k - \pi_k)^4] + \frac{n_N}{N^4} \sum_{(k, l) \in D_{2, N}} \frac{y_k^2 y_l^2}{\pi_k^2 \pi_l^2} \mathbb{E}[(I_k - \pi_k)^2 (I_l - \pi_l)^2] \\ &\leq \frac{n_N}{N \lambda^4} \frac{\sum_{k \in U} y_k^4}{N} \left(\frac{1}{N^2} + \frac{1}{N} \right), \end{aligned}$$

where the term to the right goes to zero from Assumptions (A2)-(A3). Further,

$$\begin{aligned}
|c_{2N}| &\leq \frac{2n_N}{N^4} \sum_{(k,p) \in D_{2,N}} \frac{y_k^3 y_p}{\pi_k^3 \pi_p} |\mathbb{E}[(I_k - \pi_k)^3 (I_p - \pi_p)]| \\
&+ \frac{n_N}{N^4} \sum_{(k,p,q) \in D_{3,N}} \frac{y_k^2 y_p y_q}{\pi_k^2 \pi_p \pi_q} |\mathbb{E}[(I_k - \pi_k)^2 (I_p - \pi_p) (I_q - \pi_q)]| \\
&\leq \frac{n_N}{N \lambda^4} \sum_{k \in U} \frac{y_k^4}{N} \left(\frac{2}{N} + \max_{(k,p,q) \in D_{3,N}} |\mathbb{E}[(I_k - \pi_k)^2 (I_p - \pi_p) (I_q - \pi_q)]| \right),
\end{aligned}$$

which converges to zero by Assumption (A7). Finally, note that

$$\begin{aligned}
|c_{3N}| &\leq \frac{2n_N}{N^4} \sum_{(k,l) \in D_{2,N}} \frac{y_k^2 y_l^2}{\pi_k^2 \pi_l^2} |\mathbb{E}[(I_k - \pi_k)^2 (I_l - \pi_l)^2]| \\
&+ \frac{2n_N}{N^4} \sum_{(k,l,p) \in D_{3,N}} \frac{y_k^2 y_l y_p}{\pi_k^2 \pi_l \pi_p} |\mathbb{E}[(I_k - \pi_k)^2 (I_l - \pi_l) (I_p - \pi_p)]| \\
&+ \frac{n_N}{N^4} \sum_{(k,l,p,q) \in D_{4,N}} \frac{y_k y_l y_p y_q}{\pi_k \pi_l \pi_p \pi_q} |\mathbb{E}[(I_k - \pi_k) (I_l - \pi_l) (I_p - \pi_p) (I_q - \pi_q)]| \\
&\leq \frac{1}{\lambda^4} \sum_{k \in U} \frac{y_k^4}{N} \left(\frac{2n_N}{N^2} + \frac{2n_N}{N} \max_{(k,p,q) \in D_{3,N}} |\mathbb{E}[(I_k - \pi_k)^2 (I_p - \pi_p) (I_q - \pi_q)]| \right. \\
&\left. + n_N \max_{(k,l,p,q) \in D_{4,N}} |\mathbb{E}[(I_k - \pi_k) (I_l - \pi_l) (I_p - \pi_p) (I_q - \pi_q)]| \right),
\end{aligned}$$

where the last term diminishes as $N \rightarrow \infty$ by Assumptions (A7)-(A8). This concludes the proof. \square

Lemma A.2. *Let $m \in \mathbb{N}$. Assume that $X_i - Y_i = O_p(a_n)$ for $i = 1, 2, \dots, m$. Then,*

$$f(X_1, X_2, \dots, X_m) - f(Y_1, Y_2, \dots, Y_m) = O_p(a_n)$$

where $f(\cdot)$ could be either $\min(\cdot)$ or $\max(\cdot)$ coordinate-wise function.

Proof of Lemma 2. We are going to prove this proposition by induction in m . The case $m = 1$ is clear since $f(X_1) - f(Y_1) = X_1 - Y_1 = O_p(a_n)$. Assume the result is true for $m = k$. That is,

$$f(X_1, X_2, \dots, X_k) - f(Y_1, Y_2, \dots, Y_k) = O_p(a_n).$$

We need to prove that the result is true for $m = k + 1$. Note that

$$f(X_1, \dots, X_k, X_{k+1}) = f(f(X_1, \dots, X_k), X_{k+1}),$$

which is also true for the sequence of Y 's.

Denote $u_k = f(X_1, \dots, X_k)$ and $v_k = f(Y_1, \dots, Y_k)$. By the induction assumption, $u_k - v_k = O_p(a_n)$. For the rest of the proof we are going to consider only the case when $f(\cdot) = \min(\cdot)$. Later we will note that the proof for $f(\cdot) = \max(\cdot)$ is analogous to what follows.

Note that we can write $\min(u_k, X_{k+1}) = \frac{1}{2}(u_k + X_{k+1} - |u_k - X_{k+1}|)$ and $\min(v_k, Y_{k+1}) = \frac{1}{2}(v_k + Y_{k+1} - |v_k - Y_{k+1}|)$. Hence,

$$\begin{aligned} & |\min(u_k, X_{k+1}) - \min(v_k, Y_{k+1})| \\ &= \frac{1}{2} |(u_k - v_k) + (X_{k+1} - Y_{k+1}) + (|v_k - Y_{k+1}| - |u_k - X_{k+1}|)| \\ &\leq \frac{1}{2} \{|u_k - v_k| + |X_{k+1} - Y_{k+1}| + ||v_k - Y_{k+1}| - |u_k - X_{k+1}||\} \\ &\leq \frac{1}{2} \{|u_k - v_k| + |X_{k+1} - Y_{k+1}| + |(v_k - u_k) - (X_{k+1} - Y_{k+1})|\} \\ &\leq \frac{1}{2} \{|u_k - v_k| + |X_{k+1} - Y_{k+1}| + |v_k - u_k| + |X_{k+1} - Y_{k+1}|\} \\ &= |u_k - v_k| + |X_{k+1} - Y_{k+1}|. \end{aligned}$$

Since both $u_k - v_k = O_p(a_n)$ and $X_{k+1} - Y_{k+1} = O_p(a_n)$, then for any $\epsilon > 0$ there exist $\delta_1 > 0$ and $\delta_2 > 0$ such that

$$P(a_n^{-1}|u_k - v_k| > \delta_1) < \frac{\epsilon}{2} \quad \text{and} \quad P(a_n^{-1}|X_{k+1} - Y_{k+1}| > \delta_2) < \frac{\epsilon}{2}.$$

Therefore,

$$\begin{aligned}
\epsilon &= \frac{\epsilon}{2} + \frac{\epsilon}{2} > P(a_n^{-1}|u_k - v_k| > \delta_1) + P(a_n^{-1}|X_{k+1} - Y_{k+1}| > \delta_2) \\
&\geq P(a_n^{-1}|u_k - v_k| + a_n^{-1}|X_{k+1} - Y_{k+1}| > \delta_1 + \delta_2) \\
&\geq P(a_n^{-1}|\min(u_k, X_{k+1}) - \min(v_k, Y_{k+1})| > \delta_1 + \delta_2).
\end{aligned}$$

Setting $\delta^* = \delta_1 + \delta_2$, then we can conclude that $\min(u_k, X_{k+1}) - \min(v_k, Y_{k+1}) = O_p(a_n)$. Thus, the result is true for $m = k + 1$. For the case when $f(\cdot) = \max(\cdot)$, we just need to use the fact that $\max(u_k, X_{k+1}) = \frac{1}{2}(u_k + X_{k+1} + |u_k - X_{k+1}|)$ and then follow an analogous proof as above. \square

Lemma A.3. Let $\theta_\mu = (\theta_{\mu_1}, \theta_{\mu_2}, \dots, \theta_{\mu_D})^\top$ be the weighted isotonic vector of the limiting domain means μ with weights $\gamma_1, \gamma_2, \dots, \gamma_D$. Then,

$$\tilde{\theta}_{s_d} - \theta_{\mu_d} = O_p(n_N^{-1/2}), \quad \text{for } d = 1, 2, \dots, D.$$

Proof of Lemma 3. Fix d . Following the proof of Lemma A.2, it can be proved that $\theta_{U_d} - \theta_{\mu_d} = O(N^{-1/2})$ from Assumption (A4). By Theorem 2.4, $\tilde{\theta}_{s_d} - \theta_{U_d} = O_p(n_N^{-1/2})$. Therefore, we can conclude that $\tilde{\theta}_{s_d} - \theta_{\mu_d} = O_p(n_N^{-1/2})$. \square

Lemma A.4. $(\tilde{\mathbf{y}}_s - \tilde{\boldsymbol{\theta}}_s)^\top \mathbf{W}_s(\tilde{\mathbf{y}}_s - \tilde{\boldsymbol{\theta}}_s) = (\boldsymbol{\mu} - \boldsymbol{\theta}_\mu)^\top \boldsymbol{\Gamma}(\boldsymbol{\mu} - \boldsymbol{\theta}_\mu) + O_p(n_N^{1/2})$, where $\boldsymbol{\Gamma}$ is the diagonal matrix with elements $\gamma_1, \gamma_2, \dots, \gamma_D$.

Proof of Lemma 4. From $\tilde{\mathbf{y}}_s - \bar{\mathbf{y}}_U = \mathbf{1}O_p(N^{-1/2})$ and $\bar{\mathbf{y}}_U - \boldsymbol{\mu} = \mathbf{1}O(N^{-1/2})$, we get that $\tilde{\mathbf{y}}_s - \boldsymbol{\mu} = \mathbf{1}O_p(n_N^{-1/2})$. Further, $\tilde{\boldsymbol{\theta}}_s - \boldsymbol{\theta}_\mu = \mathbf{1}O_p(n_N^{-1/2})$ by Lemma A.3. Therefore, $\tilde{\mathbf{y}}_s - \tilde{\boldsymbol{\theta}}_s = \boldsymbol{\mu} - \boldsymbol{\theta}_\mu + \mathbf{1}O_p(n_N^{-1/2})$. In addition, $\widehat{N}_d/\widehat{N} = \gamma_d + O_p(n_N^{-1/2})$ for $d = 1, \dots, D$. Thus, $(\tilde{\mathbf{y}}_s - \tilde{\boldsymbol{\theta}}_s)^\top \mathbf{W}_s(\tilde{\mathbf{y}}_s - \tilde{\boldsymbol{\theta}}_s) = (\boldsymbol{\mu} - \boldsymbol{\theta}_\mu)^\top \boldsymbol{\Gamma}(\boldsymbol{\mu} - \boldsymbol{\theta}_\mu) + O_p(n^{-1/2})$. \square

Lemma A.5. $\text{cov}(\widehat{\theta}_{s_i}, \widehat{\theta}_{s_j}) = O(n_N^{-1})$, for any $i, j = 1, 2, \dots, D$.

Proof of Lemma 5. Define \mathbb{F} to the set of representative elements F_i , and \mathbf{P}_{F_i} as it was done in the proof of Theorem 2.2. In addition, let \mathbb{F}_1 be the set of representative elements F_i of those poolings

that correspond to the disjoint sets J^0 and J^1 such that $J_\mu^0 \subseteq J^0$ and $J_\mu^1 \subseteq J^1$. That is, $F_i \in \mathbb{F}_1$ if and only if the pooling represented by F_i is allowed by μ to produce θ_μ . Further, let $\mathbb{F}_2 = \mathbb{F} \setminus \mathbb{F}_1$.

Suppose that there exist indexes $i \neq j$ such that $F_i, F_j \in \mathbb{F}_1$. First, note that both $\mathbf{P}_{F_i} \bar{\mathbf{y}}_U$ and $\mathbf{P}_{F_j} \bar{\mathbf{y}}_U$ converge to the vector θ_μ . From Assumption (A4), $\mathbf{P}_{F_i} \bar{\mathbf{y}}_U - \theta_\mu = \mathbf{1}O(N^{-1/2})$ and $\mathbf{P}_{F_j} \bar{\mathbf{y}}_U - \theta_\mu = \mathbf{1}O(N^{-1/2})$, which implies that $\mathbf{P}_{F_i} \bar{\mathbf{y}}_U - \mathbf{P}_{F_j} \bar{\mathbf{y}}_U = \mathbf{1}O(N^{-1/2})$.

Consider any index i such that $F_i \in \mathbb{F}_1$. Denote $p_{i,kl}$ to the (k, l) -element of \mathbf{P}_{F_i} . Fix d . From the fact that the function $\mathbb{E}[(\hat{\theta}_{s_d} - x)^2]$ is minimized by the constant $x = \mathbb{E}(\hat{\theta}_{s_d})$, then we have

$$\begin{aligned}
\text{var}(\widehat{\theta}_{s_d}) &= \mathbb{E} \left\{ \left[\widehat{\theta}_{s_d} - \mathbb{E}(\widehat{\theta}_{s_d}) \right]^2 \right\} \\
&\leq \mathbb{E} \left\{ \left[\widehat{\theta}_{s_d} - \left(\sum_{j=1}^D p_{i,dj} \bar{y}_{U_j} \right) \right]^2 \right\} \\
&= \mathbb{E} \left\{ \left[\left(\sum_{k=1}^{|\mathbb{F}|} \widehat{\theta}_{s_d} I\{\widehat{\mathbf{y}}_s \in F_k\} \right) - \sum_{k=1}^{|\mathbb{F}|} \left(\sum_{j=1}^D p_{i,dj} \bar{y}_{U_j} \right) I\{\widehat{\mathbf{y}}_s \in F_k\} \right]^2 \right\} \\
&= \mathbb{E} \left\{ \left[\sum_{k=1}^{|\mathbb{F}|} \left(\sum_{j=1}^D p_{k,dj} \widehat{y}_{s_j} - \sum_{j=1}^D p_{i,dj} \bar{y}_{U_j} \right) I\{\widehat{\mathbf{y}}_s \in F_k\} \right]^2 \right\} \\
&\leq |\mathbb{F}| \sum_{k=1}^{|\mathbb{F}|} \mathbb{E} \left[\left(\sum_{j=1}^D p_{k,dj} \widehat{y}_{s_j} - \sum_{j=1}^D p_{i,dj} \bar{y}_{U_j} \right)^2 I\{\widehat{\mathbf{y}}_s \in F_k\} \right] \\
&= |\mathbb{F}| \left\{ \sum_{F_k \in |\mathbb{F}_1|} \mathbb{E} \left[\left(\sum_{j=1}^D p_{k,dj} \widehat{y}_{s_j} - \sum_{j=1}^D p_{i,dj} \bar{y}_{U_j} \right)^2 I\{\widehat{\mathbf{y}}_s \in F_k\} \right] \right. \\
&\quad \left. + \sum_{F_k \in |\mathbb{F}_2|} \mathbb{E} \left[\left(\sum_{j=1}^D p_{k,dj} \widehat{y}_{s_j} - \sum_{j=1}^D p_{i,dj} \bar{y}_{U_j} \right)^2 I\{\widehat{\mathbf{y}}_s \in F_k\} \right] \right\} \\
&\leq |\mathbb{F}| \sum_{F_k \in |\mathbb{F}_1|} \mathbb{E} \left[\left(\sum_{j=1}^D p_{k,dj} \widehat{y}_{s_j} - \sum_{j=1}^D p_{i,dj} \bar{y}_{U_j} \right)^2 \right] + o(n_N^{-1}) \\
&= |\mathbb{F}| \sum_{F_k \in |\mathbb{F}_1|} \left[\text{var} \left(\sum_{j=1}^D p_{k,dj} \widehat{y}_{s_j} \right) + \left(\sum_{j=1}^D p_{k,dj} \bar{y}_{U_j} - \sum_{j=1}^D p_{i,dj} \bar{y}_{U_j} \right)^2 \right] + o(n_N^{-1}) \\
&= |\mathbb{F}| \left[\sum_{F_k \in |\mathbb{F}_1|} \text{var} \left(\sum_{j=1}^D p_{k,dj} \widehat{y}_{s_j} \right) + \sum_{F_k \in |\mathbb{F}_1|} \left(\sum_{j=1}^D p_{k,dj} \bar{y}_{U_j} - \sum_{j=1}^D p_{i,dj} \bar{y}_{U_j} \right)^2 \right] + o(n_N^{-1}) \\
&= O(n_N^{-1}) + O(N^{-1}) + o(n_N^{-1}),
\end{aligned}$$

which implies that $\text{var}(\widehat{\theta}_{s_d}) = O(n_N^{-1})$. Thus, by the Cauchy-Schwartz inequality, we conclude that $\text{cov}(\widehat{\theta}_{s_i}, \widehat{\theta}_{s_j}) = O(n_N^{-1})$ for $i, j = 1, 2, \dots, D$. \square

Proof of Proposition 1. Note that

$$\begin{aligned}
\text{PSE}(\widehat{\boldsymbol{\theta}}_s) &= \mathbb{E} \left[(\widehat{\boldsymbol{y}}_{s^*} - \widehat{\boldsymbol{\theta}}_s)^\top \mathbf{W}_U (\widehat{\boldsymbol{y}}_{s^*} - \widehat{\boldsymbol{\theta}}_s) \right] \\
&= \mathbb{E} \left[(\widehat{\boldsymbol{y}}_{s^*} - \bar{\boldsymbol{y}}_U)^\top \mathbf{W}_U (\widehat{\boldsymbol{y}}_{s^*} - \bar{\boldsymbol{y}}_U) \right] + 2\mathbb{E} \left[(\bar{\boldsymbol{y}}_{s^*} - \bar{\boldsymbol{y}}_U)^\top \mathbf{W}_U (\bar{\boldsymbol{y}}_U - \widehat{\boldsymbol{\theta}}_s) \right] \\
&\quad + \mathbb{E} \left[(\bar{\boldsymbol{y}}_U - \widehat{\boldsymbol{\theta}}_s)^\top \mathbf{W}_U (\bar{\boldsymbol{y}}_U - \widehat{\boldsymbol{\theta}}_s) \right] \\
&= \text{Tr} [\mathbf{W}_U \text{cov}(\widehat{\boldsymbol{y}}_{s^*}, \widehat{\boldsymbol{y}}_{s^*})] + \mathbb{E} \left[(\bar{\boldsymbol{y}}_U - \widehat{\boldsymbol{\theta}}_s)^\top \mathbf{W}_U (\bar{\boldsymbol{y}}_U - \widehat{\boldsymbol{\theta}}_s) \right].
\end{aligned}$$

By adding and subtracting $\widehat{\boldsymbol{y}}_s$ in the expectation term of the above equality, we have that

$$\begin{aligned}
\mathbb{E} \left[(\bar{\boldsymbol{y}}_U - \widehat{\boldsymbol{\theta}}_s)^\top \mathbf{W}_U (\bar{\boldsymbol{y}}_U - \widehat{\boldsymbol{\theta}}_s) \right] &= \text{Tr} [\mathbf{W}_U \text{cov}(\widehat{\boldsymbol{y}}_s, \widehat{\boldsymbol{y}}_s)] \\
&\quad + 2\mathbb{E} \left[(\bar{\boldsymbol{y}}_U - \widehat{\boldsymbol{y}}_s)^\top \mathbf{W}_U (\widehat{\boldsymbol{y}}_s - \widehat{\boldsymbol{\theta}}_s) \right] + \mathbb{E} [\text{SSE}(\widehat{\boldsymbol{\theta}}_s)].
\end{aligned}$$

Further,

$$\begin{aligned}
\mathbb{E} \left[(\bar{\boldsymbol{y}}_U - \widehat{\boldsymbol{y}}_s)^\top \mathbf{W}_U (\widehat{\boldsymbol{y}}_s - \widehat{\boldsymbol{\theta}}_s) \right] &= \mathbb{E} \left[(\bar{\boldsymbol{y}}_U - \widehat{\boldsymbol{y}}_s)^\top \mathbf{W}_U \widehat{\boldsymbol{y}}_s \right] + \mathbb{E} \left[(\widehat{\boldsymbol{y}}_s - \bar{\boldsymbol{y}}_U)^\top \mathbf{W}_U \widehat{\boldsymbol{\theta}}_s \right] \\
&= -\text{Tr} [\mathbf{W}_U \text{cov}(\widehat{\boldsymbol{y}}_s, \widehat{\boldsymbol{y}}_s)] + \text{Tr} [\mathbf{W}_U \text{cov}(\widehat{\boldsymbol{\theta}}_s, \widehat{\boldsymbol{y}}_s)].
\end{aligned}$$

$$\text{Hence, } \text{PSE}(\widehat{\boldsymbol{\theta}}_s) = \mathbb{E} [\text{SSE}(\widehat{\boldsymbol{\theta}}_s)] + 2 \text{Tr} [\mathbf{W}_U \text{cov}(\widehat{\boldsymbol{\theta}}_s, \widehat{\boldsymbol{y}}_s)]. \quad \square$$

Proof of Theorem 1. First, consider an index i such that $i \in J_\mu^0$ and assume that $i \notin J_s^0$. Define $L_\mu = J_\mu^1 \cup \{0, D\}$. Consider the largest index $l \in L_\mu$ that is less than i , and the smallest index $u \in L_\mu$ that is greater than i . Then, the slope from point $G_\mu(l)$ to $G_\mu(i)$ is greater than the slope from point $G_\mu(i)$ to $G_\mu(u)$. That is, $\mu_{l+1:i} > \mu_{i+1:u}$. Now, since $i \notin J_s^0$, then the slope from point $G_s(l)$ to $G_s(i)$ is at most equal to the slope from point $G_s(i)$ to $G_s(u)$. That implies $\widehat{y}_{s_{l+1:i}} \leq \widehat{y}_{s_{i+1:u}}$.

Therefore, we have

$$\begin{aligned}
P(i \notin J_s^0) &= P(\widehat{y}_{s_{i+1:u}} \geq \widehat{y}_{s_{l+1:i}}) \\
&= P((\widehat{y}_{s_{i+1:u}} - \mu_{i+1:u}) - (\widehat{y}_{s_{l+1:i}} - \mu_{l+1:i}) \geq \mu_{l+1:i} - \mu_{i+1:u}) \\
&\leq \frac{\mathbb{E} \left\{ [(\widehat{y}_{s_{i+1:u}} - \mu_{i+1:u}) - (\widehat{y}_{s_{l+1:i}} - \mu_{l+1:i})]^4 \right\}}{(\mu_{l+1:i} - \mu_{i+1:u})^4} = o(n_N^{-1}),
\end{aligned}$$

where the last equality comes from Lemma A.1 and Assumption (A4). Thus, $P(A_0^c) = o(n^{-1})$.

Now, consider an index i such that $i \in J_\mu^1$ but $i \notin J_s^1$. Let $L_s = J_s^1 \cup \{0, D\}$. Let $l, u \in L_s$ be the largest index less than i and the smallest index greater than i , respectively. Since i is not a corner point of G_s , then $G_s(i)$ is either on or above it, i.e. $\hat{y}_{s_{l+1:i}} \geq \hat{y}_{s_{i+1:u}}$. Moreover, $\mu_{l+1:i} < \mu_{i+1:u}$ because i is a corner point of G_μ . Hence,

$$\begin{aligned} P(i \notin J_s^1) &= P(\hat{y}_{s_{l+1:i}} \geq \hat{y}_{s_{i+1:u}}) \\ &= P((\hat{y}_{s_{l+1:i}} - \mu_{l+1:i}) - (\hat{y}_{s_{i+1:u}} - \mu_{i+1:u}) \geq \mu_{i+1:u} - \mu_{l+1:i}) \\ &\leq \frac{\mathbb{E}\{[(\hat{y}_{s_{l+1:i}} - \mu_{l+1:i}) - (\hat{y}_{s_{i+1:u}} - \mu_{i+1:u})]^4\}}{(\mu_{i+1:u} - \mu_{l+1:i})^4} = o(n_N^{-1}), \end{aligned}$$

which leads to the conclusion that $P(A_1^c) = o(n_N^{-1})$. \square

Proof of Theorem 2. Let $F_1, F_2, \dots, F_{2^D-1}$ be representative elements for each of the possible poolings (groupings) for a vector of length D . Also, define \mathbb{F} to the set of all of these representative elements. Since $J_\mu^0 \cup J_\mu^1 = \{1, 2, \dots, D-1\}$ and without loss of generality, let F_1 be the representative element of the unique pooling allowed by μ . Denote \mathbf{P}_{F_i} to be the weighted projection matrix that corresponds to the pooling represented by F_i with weights N_1, N_2, \dots, N_D . Also, define $P(\hat{\mathbf{y}}_s \in F_i)$ to the probability that the pooling represented by F_i is allowed by $\hat{\mathbf{y}}_s$ to obtain $\hat{\boldsymbol{\theta}}_s$. By Theorem 2.1,

$$P(\hat{\mathbf{y}}_s \in F_i) = \begin{cases} 1 + o(n_N^{-1}), & \text{if } i = 1; \\ o(n_N^{-1}), & \text{if } i \neq 1. \end{cases}$$

Also, since $|\hat{y}_{s_d}| \leq \lambda^{-1} N_d^{-1} \sum_{k \in U_d} |y_k|$ for $d = 1, \dots, D$, then for $i \neq 1$,

$$\begin{aligned} |\mathbb{E}(\hat{y}_{s_d} I\{\hat{\mathbf{y}}_s \in F_i\})| &\leq \mathbb{E}(|\hat{y}_{s_d}| I\{\hat{\mathbf{y}}_s \in F_i\}) \\ &\leq \left(\frac{1}{\lambda N_d} \sum_{k \in U_d} |y_k| \right) P(\hat{\mathbf{y}}_s \in F_i) \\ &\leq \lambda^{-1} \left(\frac{1}{N_d} \sum_{k \in U_d} y_k^4 \right)^{1/4} P(\hat{\mathbf{y}}_s \in F_i) = o(n_N^{-1}), \end{aligned}$$

which implies that $\mathbb{E}(\widehat{\mathbf{y}}_s I\{\widehat{\mathbf{y}}_s \in F_i\}) = \mathbf{1}o(n_N^{-1})$. Hence,

$$\mathbb{E}(\widehat{\mathbf{y}}_s) = \sum_{i=1}^{|\mathbb{F}|} \mathbb{E}(\widehat{\mathbf{y}}_s I\{\widehat{\mathbf{y}}_s \in F_i\}) = \mathbb{E}(\widehat{\mathbf{y}}_s I\{\widehat{\mathbf{y}}_s \in F_1\}) + \mathbf{1}o(n_N^{-1}).$$

Then, we obtain that

$$\begin{aligned} \mathbb{E}(\widehat{\boldsymbol{\theta}}_s) &= \sum_{i=1}^{|\mathbb{F}|} \mathbb{E}(\widehat{\boldsymbol{\theta}}_s I\{\widehat{\mathbf{y}}_s \in F_i\}) = \sum_{i=1}^{|\mathbb{F}|} \mathbb{E}(\mathbf{P}_{F_i} \widehat{\mathbf{y}}_s I\{\widehat{\mathbf{y}}_s \in F_i\}) \\ &= \mathbf{P}_{F_1} \mathbb{E}(\widehat{\mathbf{y}}_s I\{\widehat{\mathbf{y}}_s \in F_1\}) + \mathbf{1}o(n_N^{-1}) = \mathbf{P}_{F_1} \mathbb{E}(\widehat{\mathbf{y}}_s) + \mathbf{1}o(n_N^{-1}). \end{aligned}$$

Analogously, $\mathbb{E}(\widehat{\boldsymbol{\theta}}_s \widehat{\mathbf{y}}_s^\top) = \mathbf{P}_{F_1} \mathbb{E}(\widehat{\mathbf{y}}_s \widehat{\mathbf{y}}_s^\top) + \mathbf{J}o(n_N^{-1})$, where \mathbf{J} is the $D \times D$ matrix of ones. Therefore, we can conclude that

$$\begin{aligned} \text{cov}(\widehat{\boldsymbol{\theta}}_s, \widehat{\mathbf{y}}_s) &= \mathbb{E}(\widehat{\boldsymbol{\theta}}_s \widehat{\mathbf{y}}_s^\top) - \mathbb{E}(\widehat{\boldsymbol{\theta}}_s) \mathbb{E}(\widehat{\mathbf{y}}_s)^\top \\ &= \mathbf{P}_{F_1} \mathbb{E}(\widehat{\mathbf{y}}_s \widehat{\mathbf{y}}_s^\top) - \mathbf{P}_{F_1} \mathbb{E}(\widehat{\mathbf{y}}_s) \mathbb{E}(\widehat{\mathbf{y}}_s)^\top + \mathbf{J}o(n_N^{-1}) \\ &= \mathbf{P}_{F_1} [\mathbb{E}(\widehat{\mathbf{y}}_s \widehat{\mathbf{y}}_s^\top) - \mathbb{E}(\widehat{\mathbf{y}}_s) \mathbb{E}(\widehat{\mathbf{y}}_s)^\top] + \mathbf{J}o(n_N^{-1}) \\ &= \mathbf{P}_{F_1} \text{var}(\widehat{\mathbf{y}}_s) + \mathbf{J}o(n_N^{-1}). \end{aligned}$$

Now, note that

$$\left| \widehat{\Sigma}_{dd} \right| \leq \frac{1}{\lambda^2} \frac{\sum_{k \in U_d} y_k^2}{N_d} \left(\frac{1}{N_d} + 1 \right) \leq \frac{1}{\lambda^2} \left(\frac{\sum_{k \in U_d} y_k^4}{N_d} \right)^{1/2} \left(\frac{1}{N_d} + 1 \right),$$

which implies that $\mathbb{E}(\widehat{\Sigma}I\{\widehat{\mathbf{y}}_s \in F_i\}) = \mathbf{J}o(n_N^{-1})$ for $i \neq 1$. Moreover,

$$\mathbb{E}(\widehat{\Sigma}) = \sum_{i=1}^{|\mathbb{F}|} \mathbb{E}(\widehat{\Sigma}I\{\widehat{\mathbf{y}}_s \in F_i\}) = \mathbb{E}(\widehat{\Sigma}I\{\widehat{\mathbf{y}}_s \in F_1\}) + \mathbf{J}o(n_N^{-1}).$$

Then,

$$\begin{aligned} \mathbb{E}(\widehat{\mathbf{P}}_s \widehat{\Sigma}) &= \sum_{i=1}^{|\mathbb{F}|} \mathbb{E}(\mathbf{P}_{F_i} \widehat{\Sigma}I\{\widehat{\mathbf{y}}_s \in F_i\}) = \sum_{i=1}^{|\mathbb{F}|} \mathbf{P}_{F_i} \mathbb{E}(\widehat{\Sigma}I\{\widehat{\mathbf{y}}_s \in F_i\}) \\ &= \mathbf{P}_{F_1} \mathbb{E}(\widehat{\Sigma}I\{\widehat{\mathbf{y}}_s \in F_1\}) + \mathbf{J}o(n_N^{-1}) = \mathbf{P}_{F_1} \mathbb{E}(\widehat{\Sigma}) + \mathbf{J}o(n_N^{-1}) \\ &= \mathbf{P}_{F_1} \text{var}(\widehat{\mathbf{y}}_s) + \mathbf{J}o(n_N^{-1}). \end{aligned}$$

Thus, from Proposition 2.1,

$$\mathbb{E}[\text{CIC}_s(\widehat{\boldsymbol{\theta}}_s)] - \text{PSE}(\widehat{\boldsymbol{\theta}}_s) = 2 \text{Tr}\{\mathbf{W}_U [\mathbb{E}(\widehat{\mathbf{P}}_s \widehat{\Sigma}) - \text{cov}(\widehat{\boldsymbol{\theta}}_s, \widehat{\mathbf{y}}_s)]\} = o(n_N^{-1}).$$

□

Proof of Theorem 3. The $AC(\tilde{\mathbf{y}}_{s_{i_1:j_1}}, \tilde{\mathbf{y}}_{s_{i_2:j_2}})$ term can be broken into two sums: one with the common and one with the uncommon elements of $U_{i_1:j_1}$ and $U_{i_2:j_2}$. By doing that, we get

$$\begin{aligned}
n_N |AC(\tilde{y}_{s_{i_1:j_1}}, \tilde{y}_{s_{i_2:j_2}})| &= \frac{n_N}{N_{i_1:j_1} N_{i_2:j_2}} \left| \sum_{k \in U_{i_1:j_1}} \sum_{l \in U_{i_2:j_2}} \Delta_{kl} \left(\frac{y_k - \bar{y}_{U_{i_1:j_1}}}{\pi_k} \right) \left(\frac{y_l - \bar{y}_{U_{i_2:j_2}}}{\pi_l} \right) \right| \\
&\leq \frac{n_N}{N_{i_1:j_1} N_{i_2:j_2}} \left| \sum_{k \in U_{i_1:j_1} \cap U_{i_2:j_2}} \frac{1 - \pi_k}{\pi_k} (y_k - \bar{y}_{U_{i_1:j_1}}) (y_k - \bar{y}_{U_{i_2:j_2}}) \right| \\
&\quad + \frac{n_N}{N_{i_1:j_1} N_{i_2:j_2}} \left| \sum_{\substack{k \in U_{i_1:j_1} \\ l \in U_{i_2:j_2} \\ k \neq l}} \Delta_{kl} \left(\frac{y_k - \bar{y}_{U_{i_1:j_1}}}{\pi_k} \right) \left(\frac{y_l - \bar{y}_{U_{i_2:j_2}}}{\pi_l} \right) \right| \\
&\leq \frac{n_N}{N\lambda} \frac{N^2}{N_{i_1:j_1} N_{i_2:j_2}} \left(\frac{\sum_{k \in U_{i_1:j_1} \cap U_{i_2:j_2}} (y_k - \bar{y}_{U_{i_1:j_1}})^2}{N} \right. \\
&\quad \left. + \frac{\sum_{k \in U_{i_1:j_1} \cap U_{i_2:j_2}} (y_k - \bar{y}_{U_{i_2:j_2}})^2}{N} \right) \\
&\quad + \frac{n_N \max_{k,l \in U_N: k \neq l} |\Delta_{kl}|}{\lambda^2} \left(\frac{\sum_{k \in U_{i_1:j_1}} (y_k - \bar{y}_{U_{i_1:j_1}})^2}{N_{i_1:j_1}} + \frac{\sum_{l \in U_{i_2:j_2}} (y_l - \bar{y}_{U_{i_2:j_2}})^2}{N_{i_2:j_2}} \right)
\end{aligned}$$

where the last inequality is obtained from Assumption (A5). Given that each of the terms in the above upper bound is asymptotically bounded by Assumptions (A2)-(A5), then the first result is true.

To show the second result, note that

$$\begin{aligned}
& n_N \left| \frac{\widehat{N}_{i_1:j_1} \widehat{N}_{i_2:j_2}}{N_{i_1:j_1} N_{i_2:j_2}} \widehat{AC}(\tilde{y}_{s_{i_1:j_1}}, \tilde{y}_{s_{i_2:j_2}}) - AC(\tilde{y}_{s_{i_1:j_1}}, \tilde{y}_{s_{i_2:j_2}}) \right| \\
&= \frac{n_N}{N_{i_1:j_1} N_{i_2:j_2}} \left| \sum_{k \in U_{i_1:j_1}} \sum_{l \in U_{i_2:j_2}} \Delta_{kl} \left(\frac{y_k - \tilde{y}_{s_{i_1:j_1}}}{\pi_k} \right) \left(\frac{y_l - \tilde{y}_{s_{i_2:j_2}}}{\pi_l} \right) \frac{I_k I_l}{\pi_{kl}} \right. \\
&\quad \left. - \sum_{k \in U_{i_1:j_1}} \sum_{l \in U_{i_2:j_2}} \Delta_{kl} \left(\frac{y_k - \bar{y}_{U_{i_1:j_1}}}{\pi_k} \right) \left(\frac{y_l - \bar{y}_{U_{i_2:j_2}}}{\pi_l} \right) \right| \\
&\leq \frac{n_N}{N_{i_1:j_1} N_{i_2:j_2}} \left| \sum_{k \in U_{i_1:j_1}} \sum_{l \in U_{i_2:j_2}} \Delta_{kl} \left(\frac{y_k - \bar{y}_{U_{i_1:j_1}}}{\pi_k} \right) \left(\frac{y_l - \bar{y}_{U_{i_2:j_2}}}{\pi_l} \right) \left(\frac{I_k I_l - \pi_{kl}}{\pi_{kl}} \right) \right| \\
&\quad + \frac{n_N}{N_{i_1:j_1} N_{i_2:j_2}} \left| \sum_{k \in U_{i_1:j_1}} \sum_{l \in U_{i_2:j_2}} \Delta_{kl} \left(\frac{y_k - \bar{y}_{U_{i_1:j_1}}}{\pi_k} \right) \left(\frac{\bar{y}_{U_{i_2:j_2}} - \tilde{y}_{s_{i_2:j_2}}}{\pi_l} \right) \frac{I_k I_l}{\pi_{kl}} \right| \\
&\quad + \frac{n_N}{N_{i_1:j_1} N_{i_2:j_2}} \left| \sum_{k \in U_{i_1:j_1}} \sum_{l \in U_{i_2:j_2}} \Delta_{kl} \left(\frac{\bar{y}_{U_{i_1:j_1}} - \tilde{y}_{s_{i_1:j_1}}}{\pi_k} \right) \left(\frac{y_l - \bar{y}_{U_{i_2:j_2}}}{\pi_l} \right) \frac{I_k I_l}{\pi_{kl}} \right| \\
&\quad + \frac{n_N}{N_{i_1:j_1} N_{i_2:j_2}} \left| \sum_{k \in U_{i_1:j_1}} \sum_{l \in U_{i_2:j_2}} \Delta_{kl} \left(\frac{\bar{y}_{U_{i_1:j_1}} - \tilde{y}_{s_{i_1:j_1}}}{\pi_k} \right) \left(\frac{\bar{y}_{U_{i_2:j_2}} - \tilde{y}_{s_{i_2:j_2}}}{\pi_l} \right) \frac{I_k I_l}{\pi_{kl}} \right| \\
&= a_{1N} + a_{2N} + a_{3N} + a_{4N},
\end{aligned}$$

where we used the identities $y_k - \tilde{y}_{s_{i_1:j_1}} = (y_k - \bar{y}_{U_{i_1:j_1}}) + (\bar{y}_{U_{i_1:j_1}} - \tilde{y}_{s_{i_1:j_1}})$, and $y_l - \tilde{y}_{s_{i_2:j_2}} = (y_l - \bar{y}_{U_{i_2:j_2}}) + (\bar{y}_{U_{i_2:j_2}} - \tilde{y}_{s_{i_2:j_2}})$.

To conclude the proof, we just need to show that $a_{1N}, a_{2N}, a_{3N}, a_{4N}$ converge in probability to zero as $N \rightarrow \infty$. The Markov inequality guarantees that a_{1N} converges in probability to zero if its second moment does. Such moment can be written as

$$\begin{aligned}
& \mathbb{E}(a_{1N}^2) \\
&= \frac{n_N^2}{N_{i_1:j_1}^2 N_{i_2:j_2}^2} \sum_{p,k \in U_{i_1:j_1} \cap U_{i_2:j_2}} \frac{1-\pi_p}{\pi_p} \frac{1-\pi_k}{\pi_k} \left(y_p - \bar{y}_{U_{i_1:j_1}}\right)^2 \left(y_k - \bar{y}_{U_{i_2:j_2}}\right)^2 \frac{\Delta_{pk}}{\pi_p \pi_k} \\
&+ \frac{2n_N^2}{N_{i_1:j_1}^2 N_{i_2:j_2}^2} \sum_{p \in U_{i_1:j_1} \cap U_{i_2:j_2}} \sum_{\substack{k \in U_{i_1:j_1}, \\ k \neq l}} \sum_{l \in U_{i_2:j_2}} (y_p - \bar{y}_{U_{i_1:j_1}})(y_p - \bar{y}_{U_{i_2:j_2}})(y_k - \bar{y}_{U_{i_1:j_1}})(y_l - \bar{y}_{U_{i_2:j_2}}) \\
&\times \frac{1-\pi_p}{\pi_p} \frac{\Delta_{kl}}{\pi_k \pi_l} \mathbb{E} \left(\frac{I_p - \pi_p}{\pi_p} \frac{I_k I_l - \pi_{kl}}{\pi_{kl}} \right) + \frac{n_N^2}{N_{i_1:j_1}^2 N_{i_2:j_2}^2} \sum_{\substack{p \in U_{i_1:j_1}, \\ p \neq q}} \sum_{\substack{q \in U_{i_2:j_2} \\ k \in U_{i_1:j_1}, \\ k \neq l}} \sum_{l \in U_{i_2:j_2}} \frac{\Delta_{pq}}{\pi_p \pi_q} \frac{\Delta_{kl}}{\pi_k \pi_l} \\
&\times (y_p - \bar{y}_{U_{i_1:j_1}})(y_q - \bar{y}_{U_{i_2:j_2}})(y_k - \bar{y}_{U_{i_1:j_1}})(y_l - \bar{y}_{U_{i_2:j_2}}) \mathbb{E} \left(\frac{I_p I_q - \pi_{pq}}{\pi_{pq}} \frac{I_k I_l - \pi_{kl}}{\pi_{kl}} \right) \\
&= b_{1N} + b_{2N} + b_{3N}.
\end{aligned}$$

Furthermore,

$$\begin{aligned}
|b_{1N}| &\leq \frac{n_N^2}{N^3 \lambda^3} \frac{N^4}{N_{i_1:j_1}^2 N_{i_2:j_2}^2} \left(\frac{\sum_{k \in U_{i_1:j_1} \cap U_{i_2:j_2}} (y_k - \bar{y}_{U_{i_1:j_1}})^4}{N} + \frac{\sum_{k \in U_{i_1:j_1} \cap U_{i_2:j_2}} (y_k - \bar{y}_{U_{i_2:j_2}})^4}{N} \right) \\
&+ \frac{n_N^2 \max_{p,k \in U_N: p \neq k} |\Delta_{pk}|}{N^2 \lambda^4} \frac{N^4}{N_{i_1:j_1}^2 N_{i_2:j_2}^2} \\
&\times \left(\frac{\sum_{p \in U_{i_1:j_1} \cap U_{i_2:j_2}} (y_p - \bar{y}_{U_{i_1:j_1}})^4}{N} + \frac{\sum_{k \in U_{i_1:j_1} \cap U_{i_2:j_2}} (y_k - \bar{y}_{U_{i_2:j_2}})^4}{N} \right) \\
&\leq \frac{N^4}{N_{i_1:j_1}^2 N_{i_2:j_2}^2} \frac{n_N}{N \lambda^3} \left(\frac{n_N}{N^2} + \frac{n_N \max_{p,k \in U_N: p \neq k} |\Delta_{pk}|}{N \lambda} \right) \\
&\times \left(\frac{\sum_{p \in U_{i_1:j_1} \cap U_{i_2:j_2}} (y_p - \bar{y}_{U_{i_1:j_1}})^4}{N} + \frac{\sum_{k \in U_{i_1:j_1} \cap U_{i_2:j_2}} (y_k - \bar{y}_{U_{i_2:j_2}})^4}{N} \right)
\end{aligned}$$

which converges to zero as $N \rightarrow \infty$ by Assumptions (A2)-(A5). Also, after separating the double sum in b_{3N} into two sums where $(p, q) = (k, l)$ and $(p, q) \neq (k, l)$, we get that

$$|b_{3N}| \leq O\left(\frac{1}{N}\right) + \frac{(n_N \max_{p,q \in U_N: p \neq q} |\Delta_{pq}|)^2}{\lambda^4 \lambda^{*2}} \frac{N^4}{N_{i_1:j_1}^2 N_{i_2:j_2}^2} \max_{(p,q,k,l) \in D_{4,N}} |E[(I_p I_q - \pi_{pq})(I_k I_l - \pi_{kl})]|$$

$$\times \left(\frac{\sum_{p \in U_{i_1:j_1}} (y_p - \bar{y}_{U_{i_1:j_1}})^4}{N} + \frac{\sum_{q \in U_{i_2:j_2}} (y_q - \bar{y}_{U_{i_2:j_2}})^4}{N} \right)$$

where the last term goes to zero by Assumptions (A2)-(A6). In addition, an application of the Cauchy-Schwarz inequality along with the fact that both b_{1N}, b_{3N} tend to zero, shows that b_{2N} converges to zero. Therefore, the Markov-inequality let us conclude that $a_{1N} = o_p(1)$.

Now, note that

$$a_{4N} \leq \frac{N^2}{N_{i_1:j_1} N_{i_2:j_2}} |\tilde{y}_{s_{i_1:j_1}} - \bar{y}_{U_{i_1:j_1}}| |\tilde{y}_{s_{i_2:j_2}} - \bar{y}_{U_{i_2:j_2}}| \left(\frac{n_N}{N\lambda} + \frac{n_N \max_{k,l \in U_N: k \neq l} |\Delta_{kl}|}{\lambda^2 \lambda^*} \right).$$

Then, $a_{4n} = o_p(1)$ since $\tilde{y}_{s_{i_1:j_1}} - \bar{y}_{U_{i_1:j_1}} = O_p(n^{-1/2})$ and $\tilde{y}_{s_{i_2:j_2}} - \bar{y}_{U_{i_2:j_2}} = O_p(n^{-1/2})$. Analogously, $a_{2N} = o_p(1)$ and $a_{3N} = o_p(1)$. Thus,

$$n_N \left(\frac{\hat{N}_{i_1:j_1} \hat{N}_{i_2:j_2}}{N_{i_1:j_1} N_{i_2:j_2}} \widehat{AC}(\tilde{y}_{s_{i_1:j_1}}, \tilde{y}_{s_{i_2:j_2}}) - AC(\tilde{y}_{s_{i_1:j_1}}, \tilde{y}_{s_{i_2:j_2}}) \right) = o_p(1).$$

Finally, we have that $\frac{\hat{N}_{i_1:j_1} \hat{N}_{i_2:j_2}}{N_{i_1:j_1} N_{i_2:j_2}} - 1 = O_p(n^{-1/2})$ since $\frac{\hat{N}_{i_1:j_1}}{N_{i_1:j_1}} - 1 = O_p(n^{-1/2})$ and $\frac{\hat{N}_{i_2:j_2}}{N_{i_2:j_2}} - 1 = O_p(n^{-1/2})$. Therefore,

$$n_N \left(\widehat{AC}(\tilde{y}_{s_{i_1:j_1}}, \tilde{y}_{s_{i_2:j_2}}) - \frac{\hat{N}_{i_1:j_1} \hat{N}_{i_2:j_2}}{N_{i_1:j_1} N_{i_2:j_2}} \widehat{AC}(\tilde{y}_{s_{i_1:j_1}}, \tilde{y}_{s_{i_2:j_2}}) \right) = o_p(1),$$

which concludes the proof. □

Proof of Theorem 4. Fix d . First, recall that

$$\tilde{\theta}_{s_d} = \max_{i \leq d} \min_{d \leq j} \tilde{y}_{s_{i:j}} \quad \text{and} \quad \theta_{U_d} = \max_{i \leq d} \min_{d \leq j} \bar{y}_{U_{i:j}}.$$

By linearization arguments, it is true that $\tilde{y}_{s_{i:j}} - \bar{y}_{U_{i:j}} = O_p(n_N^{-1/2})$.

Define $v_{s_i} = (\tilde{y}_{s_{i:d}}, \tilde{y}_{s_{i:d+1}}, \dots, \tilde{y}_{s_{i:D}})^\top$ and $v_{U_i} = (\bar{y}_{U_{i:d}}, \bar{y}_{U_{i:d+1}}, \dots, \bar{y}_{U_{i:D}})^\top$ for $i = 1, 2, \dots, d$.

Hence, we have that

$$v_{s_i} - v_{U_i} = \mathbf{1} O_p(n_N^{-1/2}).$$

By Lemma A.2, it is true that

$$\min(v_{s_i}) - \min(v_{U_i}) = O_p(n_N^{-1/2})$$

Now, define $L_s = (\min(v_{s_1}), \dots, \min(v_{s_d}))^\top$ and $L_U = (\min(v_{U_1}), \dots, \min(v_{U_d}))^\top$. Therefore,

$$L_s - L_U = \mathbf{1} O_p(n_N^{-1/2}).$$

Finally, applying again Lemma A.2 let us conclude that

$$\max L_s - \max L_U = O_p(n_N^{-1/2}),$$

which concludes the proof. □

Proof of Theorem 5. The CIC_s difference between the constrained and the unconstrained estimator can be expressed as

$$\begin{aligned} \text{CIC}_s(\tilde{\theta}_s) - \text{CIC}_s(\tilde{\mathbf{y}}_s) &= (\tilde{\mathbf{y}}_s - \tilde{\theta}_s)^\top \mathbf{W}_s (\tilde{\mathbf{y}}_s - \tilde{\theta}_s) \\ &\quad - 2 \text{Tr} \left[\mathbf{W}_s \left(\widehat{\text{cov}}(\tilde{\mathbf{y}}_s, \tilde{\mathbf{y}}_s) - \widehat{\text{cov}}(\tilde{\theta}_s, \tilde{\mathbf{y}}_s) \right) \right] \\ &= \delta_{1N} - 2\delta_{2N}. \end{aligned}$$

First, assume that $\mu_1 < \mu_2 < \dots < \mu_D$. Define A to the event where $\tilde{y}_{s_1} < \tilde{y}_{s_2} < \dots < \tilde{y}_{s_D}$, that is, $J_s^0 = \emptyset$ and $J_s^1 = \{1, 2, \dots, D-1\}$. Then, from Theorem 2.1, we can conclude that

$P(A^c) = o(1)$. Moreover, note that the CIC_s difference is zero when A holds. Hence,

$$P\left(\text{CIC}_s(\tilde{\mathbf{y}}_s) < \text{CIC}_s(\tilde{\boldsymbol{\theta}}_s)\right) \leq P(A^c) = o(1).$$

Now, suppose that $\mu_1, \mu_2, \dots, \mu_D$ are not monotone. From Theorem 2.1 and Lemma A.3, $\delta_{1N} - 2\delta_{2N} = (\boldsymbol{\mu} - \boldsymbol{\theta}_\mu)^\top \boldsymbol{\Gamma} (\boldsymbol{\mu} - \boldsymbol{\theta}_\mu) + O_p(n_N^{-1/2})$. Further, $(\boldsymbol{\mu} - \boldsymbol{\theta}_\mu)^\top \boldsymbol{\Gamma} (\boldsymbol{\mu} - \boldsymbol{\theta}_\mu) > 0$, since the μ_d are not monotone. Thus,

$$P\left(\text{CIC}_s(\tilde{\mathbf{y}}_s) \geq \text{CIC}_s(\tilde{\boldsymbol{\theta}}_s)\right) = P(2\delta_{2N} \geq \delta_{1N}) = o(1)$$

which concludes the proof. □

Proof of Theorem 6. We can write the PSE difference as

$$\begin{aligned} \text{PSE}(\hat{\boldsymbol{\theta}}_s) - \text{PSE}(\hat{\mathbf{y}}_s) &= [\mathbb{E}(\hat{\mathbf{y}}_s) - \mathbb{E}(\hat{\boldsymbol{\theta}}_s)]^\top \mathbf{W}_U [\mathbb{E}(\hat{\mathbf{y}}_s) - \mathbb{E}(\hat{\boldsymbol{\theta}}_s)] + 2 \text{Tr}\{\mathbf{W}_U [\text{var}(\hat{\mathbf{y}}_s) - \text{var}(\hat{\boldsymbol{\theta}}_s)]\} \\ &= A_N + B_N. \end{aligned}$$

Assume first that $\mu_1 < \mu_2 < \dots < \mu_D$. This implies that $J_\mu^0 = \emptyset$ and $J_\mu^1 = \{1, 2, \dots, D-1\}$ i.e. all points of the GCM are corner points. Based on the proof of Theorem 2.2 (with $\mathbf{P}_{F_1} = \mathbf{I}_D$), we have that $\mathbb{E}(\hat{\boldsymbol{\theta}}_s) = \mathbb{E}(\hat{\mathbf{y}}_s) + \mathbf{1}o(n_N^{-1})$ and $\text{var}(\hat{\boldsymbol{\theta}}_s) = \text{var}(\hat{\mathbf{y}}_s) + \mathbf{J}o(n_N^{-1})$. Therefore, $A_N = o(n_N^{-1})$ and $B_N = o(n_N^{-1})$, which concludes the first part of the proof.

Assume now that $\mu_1, \mu_2, \dots, \mu_D$ are not monotone. Lemma A.5 and a direct application of Chebyshev's inequality imply that $\hat{\boldsymbol{\theta}}_s - \mathbb{E}(\hat{\boldsymbol{\theta}}_s) = \mathbf{1}O_p(n_N^{-1/2})$. Moreover, since $\hat{\boldsymbol{\theta}}_s - \boldsymbol{\theta}_\mu = O_p(n_N^{-1/2})$, then $\mathbb{E}(\hat{\boldsymbol{\theta}}_s) - \boldsymbol{\theta}_\mu = \mathbf{1}O(n_N^{-1/2})$. Hence, $A_N = (\boldsymbol{\mu} - \boldsymbol{\theta}_\mu)^\top \boldsymbol{\Gamma} (\boldsymbol{\mu} - \boldsymbol{\theta}_\mu) + o(1)$, where the quadratic form is strictly greater than zero by the non-monotone assumption on the μ 's. On the other hand, since both $\text{var}(\hat{\mathbf{y}}_s)$ and $\text{var}(\hat{\boldsymbol{\theta}}_s)$ are of the order $O(n_N^{-1/2})$, then $B_N = O(n_N^{-1})$. This concludes the proof. □

Appendix B

Supplemental materials for Chapter 3

The first part of this appendix contains all lemmas (with proofs) used to prove the theoretical results discussed in Chapter 3. Complete proofs of these results are included at the end of this appendix. The proof of Lemma B.1 can be also found in Fenchel (1953, Ch. 1).

Lemma B.1. *If a non-zero vector can be written as the positive linear combination of linearly dependent vectors, then it can be expressed as the positive linear combination of a linearly independent subset of these.*

Proof. Let \mathbf{v} be a non-zero vector such that it can be written as $\mathbf{v} = \sum_{i=1}^k a_i \boldsymbol{\ell}_i$; where $a_i > 0$ for $i = 1, 2, \dots, k$, and $\{\boldsymbol{\ell}_1, \boldsymbol{\ell}_2, \dots, \boldsymbol{\ell}_k\}$ is a set of linearly dependent vectors. Since this set of vectors is not linearly independent, then there exists constants b_i (not all different than zero) such that $\sum_{i=1}^k b_i \boldsymbol{\ell}_i = \mathbf{0}$. Without loss of generality, assume that there is at least one b_i that is positive. Now, let I_0 be the set of indexes given by

$$I_0 = \arg \min_{i: b_i > 0} \frac{a_i}{b_i}.$$

Note that I_0 cannot contain all indexes $\{1, 2, \dots, k\}$ because \mathbf{v} is a non-zero vector. Hence, for any index $i_0 \in I_0$,

$$\mathbf{v} = \sum_{i=1}^k \left(a_i - \frac{a_{i_0}}{b_{i_0}} b_i \right) \boldsymbol{\ell}_i = \sum_{i \notin I_0} \left(a_i - \frac{a_{i_0}}{b_{i_0}} b_i \right) \boldsymbol{\ell}_i$$

which means that the vector \mathbf{v} can be also written as a positive linear combination of a proper subset of $\{\boldsymbol{\ell}_1, \boldsymbol{\ell}_2, \dots, \boldsymbol{\ell}_k\}$. Finally, note that we can repeat the above argument until it is not possible to find constants $b_i \neq 0$ such that $\sum_i b_i \boldsymbol{\ell}_i = \mathbf{0}$. Thus, the resulting subset of vectors of $\{\boldsymbol{\ell}_1, \boldsymbol{\ell}_2, \dots, \boldsymbol{\ell}_k\}$ has to be linearly independent, and \mathbf{v} can be written as a positive linear combination of them. \square

Lemma B.2. *If \mathbf{A} is a $m \times D$ irreducible matrix and \mathbf{S} is a $D \times D$ diagonal matrix, then \mathbf{AS} is also irreducible.*

Proof. This is an immediate result derived from the fact that \mathbf{S} is non-singular. \square

Lemma B.3. Let \mathbf{A} be a $m \times D$ matrix. Also, let \mathbf{S}_1 and \mathbf{S}_2 be $D \times D$ diagonal matrices. For any set $J \subseteq \{1, 2, \dots, m\}$, denote $V_{i,J}$ to be the set of vectors in rows J of $\mathbf{A}_i = \mathbf{A}\mathbf{S}_i$, $i = 1, 2$. Then, for any $J^* \subseteq J$,

$$\mathcal{L}(V_{1,J^*}) = \mathcal{L}(V_{1,J}) \iff \mathcal{L}(V_{2,J^*}) = \mathcal{L}(V_{2,J}).$$

Proof. Let $\mathbf{A}_{i,J} = \mathbf{A}_J\mathbf{S}_i$, $i = 1, 2$; where \mathbf{A}_J denotes the submatrix of \mathbf{A} that contains the rows in positions J . First, assume that $\mathcal{L}(V_{1,J^*}) = \mathcal{L}(V_{1,J})$. Since $J^* \subseteq J$, it is straightforward that $\mathcal{L}(V_{2,J^*}) \subseteq \mathcal{L}(V_{2,J})$. Now, consider any $\mathbf{v} \in \mathcal{L}(V_{2,J})$. Hence, $\mathbf{v} = \mathbf{A}_{2,J}^\top \mathbf{a} = \mathbf{S}_2 \mathbf{A}_J^\top \mathbf{a}$ for some vector \mathbf{a} . Then, we have $\mathbf{S}_1 \mathbf{S}_2^{-1} \mathbf{v} = \mathbf{S}_1 \mathbf{A}_J^\top \mathbf{a} \in \mathcal{L}(V_{1,J})$. By assumption, there exists a vector \mathbf{b} such that $\mathbf{S}_1 \mathbf{S}_2^{-1} \mathbf{v} = \mathbf{S}_1 \mathbf{A}_{J^*}^\top \mathbf{b}$. Therefore, $\mathbf{v} = \mathbf{S}_2 \mathbf{A}_{J^*}^\top \mathbf{b} \in \mathcal{L}(V_{2,J^*})$. Thus, $\mathcal{L}(V_{2,J}) \subseteq \mathcal{L}(V_{2,J^*})$. Analogously, we can prove that $\mathcal{L}(V_{2,J^*}) = \mathcal{L}(V_{2,J})$ implies $\mathcal{L}(V_{1,J^*}) = \mathcal{L}(V_{1,J})$. \square

Lemma B.4. Under Assumptions A1-A5, then:

1. The $N^{-1} \widehat{t}_d$ are uniformly bounded in s_N .
2. The $N^{-1} \widehat{N}_d$ are uniformly bounded above and uniformly bounded away from zero in s_N .
3. $\text{var}(N^{-1} \widehat{t}_d) = O(n_N^{-1})$ and $\text{var}(N^{-1} \widehat{N}_d) = O(n_N^{-1})$
4. $\mathbb{E}[(N^{-1} \widehat{t}_d - r_d \mu_d)^2] = O(n_N^{-1})$ and $\mathbb{E}[(N^{-1} \widehat{N}_d - r_d)^2] = O(n_N^{-1})$.

Proof. 1. Note that

$$\frac{|\widehat{t}_d|}{N} = \left| \frac{\sum_{k \in s_d} y_k / \pi_k}{N} \right| \leq \frac{\sum_{k \in U} |y_k|}{\lambda N}$$

which does not depend on s_N , and is bounded independently of N by Assumption A2.

2. From Assumptions A4 and A5, note that

$$\frac{\epsilon n_N}{DN} \leq \frac{n_d}{N} \leq \frac{\widehat{N}_d}{N} = N^{-1} \sum_{k \in s_d} 1/\pi_k \leq \lambda^{-1} N^{-1} N_d \leq \lambda^{-1},$$

where both lower and upper bounds do not depend on s_N , and are bounded for all N by Assumptions A1, A2 and A4.

3. Note that

$$n_N \text{var}(N^{-1}\widehat{t}_d) = n_N \text{var}\left(N^{-1} \sum_{k \in s_d} y_k / \pi_k\right) \leq \frac{\sum_{k \in U_d} y_k^2}{\lambda^2 N} \left(\frac{n_N}{N} + n_N \max_{k, l \in U_d: k \neq l} |\Delta_{kl}|\right)$$

which is bounded by Assumptions A2, A4 and A5. Setting $y_k \equiv 1$ and following an analogous argument, it can be shown that $n_N \text{var}(N^{-1}\widehat{q}_d) = O(1)$.

4. Since

$$\mathbb{E} \left[(N^{-1}\widehat{t}_d - r_d \mu_d)^2 \right] = \text{var}(N^{-1}\widehat{t}_d) + \left(\frac{N_d}{N} \bar{y}_{U_d} - r_d \mu_d \right)^2,$$

then Assumption A3 and (iii) lead to the desired conclusion. Analogously, it can be proved that $\mathbb{E} \left[(N^{-1}\widehat{q}_d - r_d)^2 \right] = O(n_N^{-1})$.

□

Proof of Theorem 3.1. First, suppose that $\Pi(\mathbf{z}|\Omega^0) = \Pi(\mathbf{z}|\mathcal{L}(V_J)) = \mathbf{0}$. In that case, any subset $J^* \subset J$ such that V_{J^*} is linearly independent will satisfy $\Pi(\mathbf{z}|\mathcal{L}(V_{J^*})) = \mathbf{0} \in \overline{\mathcal{F}}_{J^*}$. Hence, it is enough to choose $J^* \subset J$ such that V_{J^*} is linearly independent and spans $\mathcal{L}(V_J)$. Now, suppose that $\Pi(\mathbf{z}|\Omega^0) \neq \mathbf{0}$. Since $\Pi(\mathbf{z}|\Omega^0) = \Pi(\mathbf{z}|\mathcal{L}(V_J)) \in \overline{\mathcal{F}}_J$, then $\Pi(\mathbf{z}|\mathcal{L}(V_J))$ can be written as the positive linear combination of vectors $\gamma_j, j \in J$. Moreover, $\langle \mathbf{z} - \Pi(\mathbf{z}|\mathcal{L}(V_J)), \gamma_j \rangle = 0$ for $j \in J$, and $\langle \mathbf{z} - \Pi(\mathbf{z}|\mathcal{L}(V_J)), \gamma_j \rangle \leq 0$, for $j \notin J$. From Lemma B.1, there exists $J_0 \subset J$ such that V_{J_0} is linearly independent and $\Pi(\mathbf{z}|\mathcal{L}(V_J))$ can be written as a positive linear combination of the vectors in V_{J_0} , which implies that $\Pi(\mathbf{z}|\mathcal{L}(V_J)) \in \overline{\mathcal{F}}_{J_0}$. In addition, since $\langle \mathbf{z} - \Pi(\mathbf{z}|\mathcal{L}(V_J)), \gamma_j \rangle = 0$ for $j \in J_0$, then $\Pi(\mathbf{z}|\mathcal{L}(V_{J_0})) = \Pi(\mathbf{z}|\mathcal{L}(V_J))$. Thus, $\Pi(\mathbf{z}|\Omega^0) = \Pi(\mathbf{z}|\mathcal{L}(V_{J_0}))$. If $\mathcal{L}(V_{J_0}) = \mathcal{L}(V_J)$ then $J^* = J_0$ satisfies all required conditions. Now, assume that $\mathcal{L}(V_{J_0}) \subset \mathcal{L}(V_J)$. The fact that $\Pi(\mathbf{z}|\mathcal{L}(V_{J_0})) = \Pi(\mathbf{z}|\mathcal{L}(V_J))$ implies that $\Pi(\mathbf{z}|\mathcal{L}(V_{J_1})) = \Pi(\mathbf{z}|\mathcal{L}(V_{J_0}))$ for any set J_1 such that $J_0 \subseteq J_1 \subseteq J$. Further, since $\Pi(\mathbf{z}|\mathcal{L}(V_{J_0})) \in \overline{\mathcal{F}}_{J_0}$ then $\Pi(\mathbf{z}|\mathcal{L}(V_{J_1})) \in \overline{\mathcal{F}}_{J_1}$. Thus, it is enough to

choose the set J^* such that $J_0 \subset J^* \subset J$ and V_{J^*} is a linearly independent set that spans $\mathcal{L}(V_J)$. This concludes the proof. \square

Proof of Theorem 3.2. Let \mathbf{A}_μ , $\mathbf{A}_{\mu,J}$ and γ_{μ_d} be the analogous versions of \mathbf{A}_s , $\mathbf{A}_{s,J}$ and γ_{s_d} obtained by substituting $\tilde{\mathbf{y}}_s$ and \mathbf{W}_s by $\boldsymbol{\mu}$ and \mathbf{W}_μ , respectively. Further, note that Lemma B.2 assures that both \mathbf{A}_s and \mathbf{A}_μ are irreducible since \mathbf{A} is.

First, suppose $\emptyset \notin \mathcal{G}_\mu$ and let $J = \emptyset$. Then, from conditions in Equation 3.9, $\emptyset \in \tilde{\mathcal{G}}_s$ if and only if $\langle \tilde{\mathbf{z}}_s, \boldsymbol{\gamma}_{s_j} \rangle \leq 0$ for $j = 1, 2, \dots, m$. In contrast, suppose that $\langle \mathbf{z}_\mu, \boldsymbol{\gamma}_{\mu_j} \rangle \leq 0$ for $j = 1, 2, \dots, m$. Hence, $\emptyset \in \mathcal{G}_\mu$, which contradicts our choice of J . Therefore, there exists j_0 such that $\langle \mathbf{z}_\mu, \boldsymbol{\gamma}_{\mu_{j_0}} \rangle > 0$. Then, we have

$$\begin{aligned} P\left(\emptyset \in \tilde{\mathcal{G}}_s\right) &\leq P\left(0 \geq \langle \tilde{\mathbf{z}}_s, \boldsymbol{\gamma}_{s_{j_0}} \rangle\right) \\ &= P\left(\langle \mathbf{z}_\mu, \boldsymbol{\gamma}_{\mu_{j_0}} \rangle - \langle \tilde{\mathbf{z}}_s, \boldsymbol{\gamma}_{s_{j_0}} \rangle \geq \langle \mathbf{z}_\mu, \boldsymbol{\gamma}_{\mu_{j_0}} \rangle\right) \\ &\leq \frac{1}{\langle \mathbf{z}_\mu, \boldsymbol{\gamma}_{\mu_{j_0}} \rangle^2} \mathbb{E}\left[\left(\langle \tilde{\mathbf{z}}_s, \boldsymbol{\gamma}_{s_{j_0}} \rangle - \langle \mathbf{z}_\mu, \boldsymbol{\gamma}_{\mu_{j_0}} \rangle\right)^2\right] \end{aligned}$$

where the last inequality is obtained by an application of Chebyshev's inequality. We show now that the expected value in the last term is $O(n_N^{-1})$. Note that $\langle \tilde{\mathbf{z}}_s, \boldsymbol{\gamma}_{s_{j_0}} \rangle$ is a function of the $N^{-1}\hat{t}_d$ and the $N^{-1}\hat{N}_d$. Let $f_1(N^{-1}\hat{t}_1, \dots, N^{-1}\hat{t}_D, N^{-1}\hat{N}_1, \dots, N^{-1}\hat{N}_D)$ be such a function. An application of the Mean Value Theorem to the continuous function $f_1(\cdot)$ (and to its first and second derivative functions) along with Lemma B.4 (i)-(ii), lead to the conclusion that $|f_1(\cdot)|$ and its first and second derivative functions are uniformly bounded for all N . Moreover, $f_1(N^{-1}\hat{t}_1, \dots, N^{-1}\hat{t}_D, N^{-1}\hat{N}_1, \dots, N^{-1}\hat{N}_D)$ and its first and second derivative functions, evaluated at $N^{-1}\hat{t}_d = r_d\mu_d$ and $N^{-1}\hat{N}_d = r_d$, are uniformly bounded for all N . By defining $g_1(\cdot)$ to the function $g_1(\cdot) = [f_1(\cdot) - f_1(r_1\mu_1, \dots, r_D\mu_D, r_1, \dots, r_D)]^2 = [f_1(\cdot) - \langle \mathbf{z}_\mu, \boldsymbol{\gamma}_{\mu_{j_0}} \rangle]^2$, we can make use of Lemma B.4 (iv) to fulfill the assumptions of Theorem 5.4.3 in Fuller (1996) with $\alpha = 1$, $s = 2$, and $a_N = O(N^{-1/2})$. Therefore, $\mathbb{E}\left[\left(\langle \tilde{\mathbf{z}}_s, \boldsymbol{\gamma}_{s_{j_0}} \rangle - \langle \mathbf{z}_\mu, \boldsymbol{\gamma}_{\mu_{j_0}} \rangle\right)^2\right] = O(n_N^{-1})$, since $g_1(\cdot)$ and its first derivative with respect to the $N^{-1}\hat{t}_d$ and the $N^{-1}\hat{N}_d$ evaluate to zero when $N^{-1}\hat{t}_d = r_d\mu_d$, $N^{-1}\hat{N}_d = r_d$.

Now, take $J \neq \emptyset$ where $J \notin \mathcal{G}_\mu$. Assume that $J \in \tilde{\mathcal{G}}_s$. Theorem 3.1 guarantees that we can always choose a subset $J^* \subseteq J$ such that $J^* \in \tilde{\mathcal{G}}_s$, V_{s,J^*} is linearly independent, and $\mathcal{L}(V_{s,J^*}) = \mathcal{L}(V_{s,J})$. Note that $\Pi(\tilde{\mathbf{z}}_s | \mathcal{L}(V_{s,J^*})) = \mathbf{A}_{s,J^*}^\top (\mathbf{A}_{s,J^*} \mathbf{A}_{s,J^*}^\top)^{-1} \mathbf{A}_{s,J^*} \tilde{\mathbf{z}}_s$. Let $\tilde{\mathbf{b}}_{s,J^*} = (\mathbf{A}_{s,J^*} \mathbf{A}_{s,J^*}^\top)^{-1} \mathbf{A}_{s,J^*} \tilde{\mathbf{z}}_s$. Hence, from conditions in Equation 3.9, we have that $J \in \tilde{\mathcal{G}}_s$ implies both $\tilde{\mathbf{b}}_{s,J^*} \geq \mathbf{0}$, and $\langle \tilde{\mathbf{z}}_s - \mathbf{A}_{s,J^*}^\top \tilde{\mathbf{b}}_{s,J^*}, \boldsymbol{\gamma}_{s_j} \rangle \leq 0$ for $j = 1, 2, \dots, m$. Now, assume that $\mathbf{b}_{\mu,J^*} = (\mathbf{A}_{\mu,J^*} \mathbf{A}_{\mu,J^*}^\top)^{-1} \mathbf{A}_{\mu,J^*} \mathbf{z}_\mu \geq \mathbf{0}$, and $\langle \mathbf{z}_\mu - \mathbf{A}_{\mu,J^*}^\top \mathbf{b}_{\mu,J^*}, \boldsymbol{\gamma}_{\mu_{j_0}} \rangle \leq 0$ for $j = 1, 2, \dots, m$. These conditions imply that $J^* \in \mathcal{G}_\mu$ which contradicts the original assumption that $J \notin \mathcal{G}_\mu$, since $\mathcal{L}(V_{\mu,J^*}) = \mathcal{L}(V_{\mu,J})$ by Lemma B.3. Therefore, either there is an element of \mathbf{b}_{μ,J^*} that is strictly negative or there exists j_0 such that $\langle \mathbf{z}_\mu - \mathbf{A}_{\mu,J^*}^\top \mathbf{b}_{\mu,J^*}, \boldsymbol{\gamma}_{\mu_{j_0}} \rangle > 0$. Hence, proving that $P(J_t \in \tilde{\mathcal{G}}_s) = O(n_N^{-1})$ in any case will conclude the proof.

First, suppose the j_0 -th element of \mathbf{b}_{μ,J^*} is strictly negative. That is, $\mathbf{e}_{j_0}^\top \mathbf{b}_{\mu,J^*} < 0$, where \mathbf{e}_j denotes the indicator vector that is 1 for entry j and 0 otherwise. Then, we have

$$\begin{aligned} P(J \in \tilde{\mathcal{G}}_s) &\leq P(\mathbf{e}_{j_0}^\top \tilde{\mathbf{b}}_{s,J^*} \geq 0) \\ &= P(\mathbf{e}_{j_0}^\top \tilde{\mathbf{b}}_{s,J^*} - \mathbf{e}_{j_0}^\top \mathbf{b}_{\mu,J^*} \geq -\mathbf{e}_{j_0}^\top \mathbf{b}_{\mu,J^*}) \\ &\leq \frac{1}{(\mathbf{e}_{j_0}^\top \mathbf{b}_{\mu,J^*})^2} \mathbb{E}[(\mathbf{e}_{j_0}^\top \tilde{\mathbf{b}}_{s,J^*} - \mathbf{e}_{j_0}^\top \mathbf{b}_{\mu,J^*})^2] \end{aligned}$$

where the last inequality is obtained by an application of Chebyshev's inequality. Let $f_2(N^{-1}\hat{t}_1, \dots, N^{-1}\hat{t}_D, N^{-1}\hat{N}_1, \dots, N^{-1}\hat{N}_D) = \mathbf{e}_{j_0}^\top \tilde{\mathbf{b}}_{s,J^*}$ and $g_2(\cdot) = [f_2(\cdot) - \mathbf{e}_{j_0}^\top \mathbf{b}_{\mu,J^*}]^2$. An analogous argument than the one used before to the smooth functions f_1 and g_1 can be applied to the smooth functions f_2 and g_2 , to conclude that the expected value of the last term of the inequality is $O(n_N^{-1})$.

Lastly, suppose that there exists j_0 such that $\kappa_{\mathbf{z}_\mu, j_0} = \langle \mathbf{z}_\mu - \mathbf{A}_{\mu, J_{j_0}^*}^\top \mathbf{b}_{\mu, J_{j_0}^*}, \boldsymbol{\gamma}_{\mu_{j_0}} \rangle > 0$. Also, denote $\kappa_{\tilde{\mathbf{z}}_s, j_0} = \langle \tilde{\mathbf{z}}_s - \mathbf{A}_{s, J_{j_0}^*}^\top \tilde{\mathbf{b}}_{s, J_{j_0}^*}, \boldsymbol{\gamma}_{s_{j_0}} \rangle$. Then, we have

$$\begin{aligned}
P\left(J \in \tilde{\mathcal{G}}_s\right) &\leq P\left(0 \geq \kappa_{\tilde{\mathbf{z}}_s, j_0}\right) \\
&= P\left(\kappa_{\mathbf{z}_\mu, j_0} - \kappa_{\tilde{\mathbf{z}}_s, j_0} \geq \kappa_{\mathbf{z}_\mu, j_0}\right) \\
&\leq \frac{1}{\kappa_{\mathbf{z}_\mu, j_0}^2} \mathbb{E}\left[\left(\kappa_{\tilde{\mathbf{z}}_s, j_0} - \kappa_{\mathbf{z}_\mu, j_0}\right)^2\right]
\end{aligned}$$

where the last inequality is an application of the Chebyshev's inequality. By applying an analogous argument than before to the smooth functions $f_3(N^{-1}\hat{t}_1, \dots, N^{-1}\hat{t}_D, N^{-1}\hat{N}_1, \dots, N^{-1}\hat{N}_D) = \kappa_{\tilde{\mathbf{z}}_s, j_0}$ and $g_3(\cdot) = [f_3(\cdot) - \kappa_{\mathbf{z}_\mu, j_0}]^2$, we conclude that $\mathbb{E}\left[(\kappa_{\tilde{\mathbf{z}}_s, j_0} - \kappa_{\mathbf{z}_\mu, j_0})^2\right] = O(n_N^{-1})$. \square

Proof of Theorem 3.3. Take any $J \in \tilde{\mathcal{G}}_s$ and any domain d . Note that the condition $\mathbf{A}\boldsymbol{\mu} \geq \mathbf{0}$ implies that $\emptyset \in \mathcal{G}_\mu$. Then, we can write $\tilde{\theta}_{s_d} - \bar{y}_{U_d}$ as

$$\tilde{\theta}_{s_d} - \bar{y}_{U_d} = (\tilde{y}_{s_d} - \bar{y}_{U_d})1_{J=\emptyset} + \sum_{J_G \in \mathcal{G}_\mu \setminus \emptyset} (\tilde{\theta}_{s_d, J_G} - \bar{y}_{U_d})1_{J_G=J} + \sum_{J_G \in \mathcal{G}_\mu^c} (\tilde{\theta}_{s_d, J_G} - \bar{y}_{U_d})1_{J_G=J},$$

where we used that $\tilde{\theta}_{s_d, \emptyset} = \tilde{y}_{s_d}$. Now, note that the unfeasible variance estimator $AV(\tilde{\theta}_{s_d, J})$ can be written as

$$AV(\tilde{\theta}_{s_d, J}) = AV(\tilde{y}_{s_d})1_{J=\emptyset} + \sum_{J_G \in \mathcal{G}_\mu \setminus \emptyset} AV(\tilde{\theta}_{s_d, J_G})1_{J=J_G} + \sum_{J_G \in \mathcal{G}_\mu^c} AV(\tilde{\theta}_{s_d, J_G})1_{J=J_G}.$$

Hence,

$$\begin{aligned}
& AV(\tilde{\theta}_{s_d, J})^{-1/2}(\tilde{\theta}_{s_d} - \bar{y}_{U_d}) = AV(\tilde{y}_{s_d})^{-1/2}(\tilde{y}_s - \bar{y}_{U_d})1_{J=\emptyset} \\
& + \sum_{J_G \in \mathcal{G}_\mu \setminus \emptyset} AV(\tilde{\theta}_{s_d, J_G})^{-1/2}(\tilde{\theta}_{s_d, J_G} - \bar{y}_{U_d})1_{J=J_G} + \sum_{J_G \in \mathcal{G}_\mu^c} AV(\tilde{\theta}_{s_d, J_G})^{-1/2}(\tilde{\theta}_{s_d, J_G} - \bar{y}_{U_d})1_{J=J_G} \\
& = \left[AV(\tilde{y}_{s_d})^{-1/2}(\tilde{y}_s - \bar{y}_{U_d})1_{J=\emptyset} + \sum_{J_G \in \mathcal{G}_\mu \setminus \emptyset} AV(\tilde{\theta}_{s_d, J_G})^{-1/2}(\tilde{\theta}_{s_d, J_G} - \theta_{U_d, J_G})1_{J=J_G} \right. \\
& \left. + \sum_{J_G \in \mathcal{G}_\mu^c} AV(\tilde{\theta}_{s_d, J_G})^{-1/2}(\tilde{\theta}_{s_d, J_G} - \theta_{U_d, J_G})1_{J=J_G} \right] \\
& + \left[\sum_{J_G \in \mathcal{G}_\mu \setminus \emptyset} AV(\tilde{\theta}_{s_d, J_G})^{-1/2}(\theta_{U_d, J_G} - \bar{y}_{U_d})1_{J=J_G} \right] \\
& + \left[\sum_{J_G \in \mathcal{G}_\mu^c} AV(\tilde{\theta}_{s_d, J_G})^{-1/2}(\theta_{U_d, J_G} - \bar{y}_{U_d})1_{J=J_G} \right] \\
& = c_{1N} + c_{2N} + c_{3N},
\end{aligned}$$

where θ_{U_d, J_G} is the population version of $\tilde{\theta}_{s_d, J_G}$. Note that, for any J_G , the term of the form $AV(\tilde{\theta}_{s_d, J_G})^{-1/2}(\tilde{\theta}_{s_d, J_G} - \theta_{U_d, J_G})$ converges in distribution to a standard normal distribution by Assumption A6. Thus, c_{1N} converges in distribution to a standard normal distribution. Now, note that for each $J_G \in \mathcal{G}_\mu^c$, then

$$AV(\tilde{\theta}_{s_d, J_G})^{-1/2}(\theta_{U_d, J_G} - \bar{y}_{U_d}) = [n_N AV(\tilde{\theta}_{s_d, J_G})]^{-1/2} [n_N^{1/2}(\theta_{U_d, J_G} - \bar{y}_{U_d})] = O(n_N^{1/2}).$$

In contrast, for $J_G \in \mathcal{G}_\mu^c$, we have that $1_{J=J_G} = O_p(n_N^{-1})$ by Theorem 3.2 (since $J \in \tilde{\mathcal{G}}_s$). Thus, $c_{3N} = O_p(n_N^{-1/2})$. Now, note that $\theta_{U_d, J_G} - \bar{y}_{U_d} = O(N^{-1/2})$ when $J_G \in \mathcal{G}_\mu \setminus \emptyset$ by Assumption A3. Hence, for any $J_G \in \mathcal{G}_\mu \setminus \emptyset$,

$$AV(\tilde{\theta}_{s_d, J_G})^{-1/2}(\theta_{U_d, J_G} - \bar{y}_{U_d}) = [n_N AV(\tilde{\theta}_{s_d, J_G})]^{-1/2} [n_N^{1/2}(\theta_{U_d, J_G} - \bar{y}_{U_d})] = O\left(\sqrt{\frac{n_N}{N}}\right),$$

which implies that $c_{2N} = O\left(\sqrt{\frac{n_N}{N}}\right)$ (bias term). Thus, by combining these properties of c_{1N} , c_{2N} and c_{3N} , we conclude that

$$AV(\tilde{\theta}_{s_d,J})^{-1/2}(\tilde{\theta}_{s_d} - \bar{y}_{U_d}) \xrightarrow{\mathcal{L}} \mathcal{N}(B, 1),$$

where $B = O(\sqrt{\frac{nN}{N}})$.

Now, write the feasible variance estimator $\widehat{V}(\tilde{\theta}_{s_d,J})$ as

$$\widehat{V}(\tilde{\theta}_{s_d,J}) = \widehat{V}(\tilde{y}_{s_d})1_{J=\emptyset} + \sum_{J_G \in \mathcal{G}_\mu \setminus \emptyset} \widehat{V}(\tilde{\theta}_{s_d,J_G})1_{J=J_G} + \sum_{J_G \in \mathcal{G}_\mu^c} \widehat{V}(\tilde{\theta}_{s_d,J_G})1_{J=J_G}.$$

By Assumption A6, we have that $\widehat{V}(\tilde{\theta}_{s_d,J_G}) - AV(\tilde{\theta}_{s_d,J_G}) = O(n_N^{-1})$ for any J_G . The latter implies that $\widehat{V}(\tilde{\theta}_{s_d,J})^{1/2} - AV(\tilde{\theta}_{s_d,J})^{1/2} = O(n_N^{-1/2})$. Hence, an application of Slutsky's theorem allows to replace $AV(\tilde{\theta}_{s_d,J})^{-1/2}$ by $\widehat{V}(\tilde{\theta}_{s_d,J})^{-1/2}$.

To prove the last part of this theorem, just note that $\mathbf{A}\boldsymbol{\mu} > \mathbf{0}$ implies $\mathcal{G}_\mu = \{\emptyset\}$. Thus, the term c_{2N} does not exist, so the bias term vanishes. \square